An Optimization Method for Matched Abundance-Ratio Cascades by Varying the Key Weight

A Dissertation Presented for the

Doctor of Philosophy

Degree

The University of Tennessee, Knoxville

Richard Dale Harvey

May 2017

Copyright © 2017 by Richard Dale Harvey
All rights reserved.

DEDICATION

For my family who have provided unlimited love and support.

ACKNOWLEDGEMENTS

I would like to express my sincerest gratitude to all those who have helped me with this endeavor. Thanks to Professor Howard Hall, my advisor, and the remainder of my dissertation committee; Professors Robert Counce, Jamie Coble, and Alan Icenhour. My committee's support and guidance were instrumental to my successful completion. I will be forever grateful for your utmost patience and flexibility.

I'd like to give a special thanks to the late Ed von Halle with whom I had the honor to work for a short period. Ed was a pioneer in this field and an American treasure. Ed personally encouraged the topic of my dissertation and provided much theoretical insight before his passing in 2013.

I'd like to thank several scientists and engineers at Oak Ridge National Laboratory. Bill Strunk contributed much of the funding to this research and provided tremendous support, flexibility, and encouragement. Tom Slankas, David Sulfredge, Duane Starr, Elwood Gift, and Richard Cox were all extremely knowledgeable and approachable resources for the cascade theory, mathematics, and calculations. Each of these dedicated professionals contributed hours of discussion, insight, and mentorship on this complex topic.

Finally, thanks to Patrick Williams, who provided extensive help with the intricacies of the computer programming. Patrick provided considerable help overcoming obstacles encountered, and he was a limitless resource for new approaches and the art of the possible within MATLAB®.

ABSTRACT

The theory of multicomponent isotope separation in matched abundance-ratio cascades (MARC) has been well established by Cohen, de la Garza, von Halle, and others. Because separation factors of different isotopes vary in the same separator, isotopic weight fractions cannot be matched in the same sense as in a two-component ideal system. Therefore, the abundance ratios of the desired isotope and a selected key isotope are matched, hence the name. These ratios are matched by choosing a key weight between the two selected components of separation.

Desirable stable isotopes for separation can exist as minor components of a natural, multicomponent isotope system. Behaviors of these isotopes vary within the cascade depending on the relative weight, relative fractions, and relative location in the sequence of isotopes. Various theoretical methods have been developed to simplify analysis and to optimize isotopic separation within a cascade. The possibility of varying key weights within a cascade for optimization was first proposed as future work by de la Garza in 1963, but only a few results have been published showing that varying the key weights can improve efficiency in a theoretical cascade.

This dissertation will review the theory of matched abundance-ratio cascades; examine the behavior of individual isotopes within the cascade; and propose concepts and a methodology for optimizing a cascade by varying the key weight within the cascade.

TABLE OF CONTENTS

CHAPTER 1: BACKGROUND AND INTRODUCTION 1

Background 1

Stable Isotopes *1*

Matched Abundance-Ratio Cascade Theory *4*

Introduction 8

CHAPTER 2: LITERATURE REVIEW 10

Stable Isotopes 10

Theoretical Cascade Studies 11

Matched Abundance-Ratio Cascades *12*

Q-Cascades *15*

Considerations for Optimization 17

CHAPTER 3: METHODOLOGY 20

Assumptions 20

Verification of Code Results 21

Parametric Study 26

CHAPTER 4: RESULTS AND DISCUSSION 29

Validation of Optimization Criterion 29

The Case for an End Component 33

Single Cascade with Constant Key Weight *33*

The Number of Stages in a Single Cascade *41*

Feed Parametric *44*

Cascade of Cascades 44

Cascade of Cascades without Recycle *46*

Cascade of Cascades with Recycle *48*

The Case for a Middle Component 59

Second Component *61*

Third Component *61*

Fourth Component *61*

Fifth Component *65*

CHAPTER 5: CONCLUSIONS AND RECOMMENDATIONS 67

Optimization Methodology 67

Single Optimized Cascade for an End Component with Constant Key Weight *67*

Single Optimized Cascade for a Middle Component with Constant Key Weight *68*

Cascade of Cascades *69*

Future Work 70

BIBLIOGRAPHY 71

APPENDICES 78

APPENDIX A-CODE VERIFICATION SAMPLES *79*

APPENDIX B-OPTIMUM CONSTANT KEY WEIGHTS IN A CASCADE *86*

APPENDIX C-OPTIMUM KEY WEIGHTS IN A CASCADE OF CASCADES WITHOUT RECYCLE 94

APPENDIX D-OPTIMUM KEY WEIGHTS IN A CASCADE OF CASCADES WITH RECYCLE 97

VITA 100

LIST OF TABLES

Table 1. Stable Isotopes with Known Applications 2
Table 2. Comparison of Cascade Performance by Configuration. 53
Table 3. Comparison of Optimized Cascade-of-Cascades Results to the Single Optimized Cascade. 56
Table 4. Comparison of Calculated Results 79
Table 5. Previously Published Results for Comparison 80
Table 6. Calculated Results for Comparison 82
Table 7. Differences in Calculated and Published Results 84

LIST OF FIGURES

Figure 1. Relative mass flows and weight fractions in the top stages of a MARC 5
Figure 2. Reproduction of de la Garza figure where key weight is 300.5 amu 22
Figure 3. Reproduction of de la Garza figure where key weight is 300.0 amu 23
Figure 4. Reproduction of de la Garza figure where key weight is 299.5 amu 24
Figure 5. Comparison of separative work calculation methods. 31
Figure 6. End component weight fraction in a cascade with a fixed number of stages versus continuous key weights. 34
Figure 7. End component optimization case for $x_P = 0$ .3, $\alpha = 1.3$, and NS = 0. 36
Figure 8. End component optimization case for $x_P = 0.3$, $\alpha = 1.3$, and NS = 3. 37
Figure 9. Optimum constant key weights for different separation factors and average optimum key weights versus single cascade target weight fractions. 40
Figure 10. Determination of optimum waste weight fraction 43
Figure 11. Optimum key weight versus product weight fraction and feed distribution for the $\alpha = 1.3$ case. 45
Figure 12. Cascade of cascades without waste recycle. 47
Figure 13. Cascade of cascades with waste recycle. 49
Figure 14. Optimum key weight versus product weight fraction by cascade in an optimized cascade of cascades with recycle. 58
Figure 15. Optimum key weights for the second component. 62
Figure 16. Optimum key weights for the third component. 63
Figure 17. Optimum key weights for the fourth component. 64
Figure 18. Optimum key weights for the fifth component. 66
Figure 19. Optimum key weights for $x_P = 0.4$, $\alpha = 1.1$. 86
Figure 20. Optimum key weights for $x_P = 0.4$, $\alpha = 1.2$. 86
Figure 21. Optimum key weights for $x_P = 0.4$, $\alpha = 1.3$. 87

Figure 22. Optimum key weights for $x_P = 0.4$, $\alpha = 1.4$. 87
Figure 23. Optimum key weights for $x_P = 0.4$, $\alpha = 1.5$. 88
Figure 24. Optimum key weights for $x_P = 0.7$, $\alpha = 1.1$. 88
Figure 25. Optimum key weights for $x_P = 0.7$, $\alpha = 1.2$. 89
Figure 26. Optimum key weights for $x_P = 0.7$, $\alpha = 1.3$. 89
Figure 27. Optimum key weights for $x_P = 0.7$, $\alpha = 1.4$. 90
Figure 28. Optimum key weights for $x_P = 0.7$, $\alpha = 1.5$. 90
Figure 29. Optimum key weights for $x_P = 0.9$, $\alpha = 1.1$. 91
Figure 30. Optimum key weights for $x_P = 0.9$, $\alpha = 1.2$. 91
Figure 31. Optimum key weights for $x_P = 0.9$, $\alpha = 1.3$. 92
Figure 32. Optimum key weights for $x_P = 0.9$, $\alpha = 1.4$. 92
Figure 33. Optimum key weights for $x_P = 0.9$, $\alpha = 1.5$ 93
Figure 34. Optimum key weight versus cascade product weight fraction for cascade of six cascades with no recycle and $\alpha = 1.1$. 94
Figure 35. Optimum key weight versus cascade product weight fraction for cascade of eight cascades with no recycle and $\alpha = 1.2$. 94
Figure 36. Optimum key weight versus cascade product weight fraction for cascade of eight cascades with no recycle and $\alpha = 1.3$. 95
Figure 37. Optimum key weight versus cascade product weight fraction for cascade of eight cascades with no recycle and $\alpha = 1.4$. 95
Figure 38. Optimum key weight versus cascade product weight fraction for cascade of nine cascades with no recycle and $\alpha = 1.5$. 96
Figure 39. Optimum key weight versus cascade product weight fraction for cascade of cascades with recycle for $x_P = 0.7$ and $\alpha = 1.1$. 97
Figure 40. Optimum key weight versus cascade product weight fraction for cascade of cascades with recycle for $x_P = 0.9$ and $\alpha = 1.2$. 97
Figure 41. Optimum key weight versus cascade product weight fraction for cascade of cascades with recycle for $x_P = 0.9$ and $\alpha = 1.3$. 98

Figure 42. Optimum key weight versus cascade product weight fraction for cascade of cascades with recycle for $x_P = 0.9$ and $\alpha = 1.4$. 98
Figure 43. Optimum key weight versus cascade product weight fraction for cascade of cascades with recycle for $x_P = 0.9$ and $\alpha = 1.5$. 99

NOMENCLATURE

Symbol – Meaning	Symbol – Meaning
α – separation factor	α_i^* – isotopic separation factor
α_o – separation factor per amu	θ – stage cut
ψ – enrichment factor	γ – feed-to-waste separation factor
β – product-to-feed separation factor	ψ_o – enrichment factor per amu
L_n – flow for stage n	ε – enrichment factor in the Q-cascade construct
R – abundance ratio	i – specific isotopic (i^{th}) component
R_n' – R for stage n upflow	R_n'' – R for stage n downflow
$x_{i,n}$ – isotope weight fraction at stage n	M – molecular weight
F – cascade feed flow	x_F – feed weight fraction
P – cascade product flow	x_P – product weight fraction
W – cascade waste flow	x_W – waste weight fraction
k – key component	J – total number of components
j – reference component	M^* – key weight
ΔU – total separative power	v – value function
N – number of stages/length of cascade	n – stage number
NS – number of stripper stages	NE – number of enricher stages
H – number of cascades	h – cascade number
C – total cost	C_F – unit cost of feed
C_U – unit cost of separative work	

ABBREVIATIONS & ACRONYMS

amu – atomic mass unit

C-of-C – cascade of cascades

g – gram

kg – kilogram

MARC – matched abundance-ratio cascade

MCCP – model cascades of continuous profile

ppm – parts per million

RTF – relative total flow

SWU – separative work unit

CHAPTER 1: BACKGROUND AND INTRODUCTION

Background

Stable Isotopes

Since the 1980s, a specialized market for high-purity isotopic species has evolved. Because of the desirable properties, the need for highly pure isotopic materials has risen in nuclear medicine and other highly technical fields. For example, when stable isotopes are used to manufacture radioisotopes in an accelerator or a nuclear reactor, high-purity isotopes are required to minimize adverse effects of undesirable activation by-products. Likewise, stable isotopes are commonly used for materials inside a nuclear reactor environment to prevent the undesirable activation by-products. Common levels of isotopic purity need to exceed 99-percent.

Because of the relative utility of gas centrifuges, the use of these isotope separators in the stable isotope industry has gradually become the preferred method for many isotopes. Centrifuge technology itself is highly guarded due to nuclear proliferation concerns and intellectual property rights. Only a handful of companies worldwide can produce stable isotopes by gas centrifuge.

As of 2008, none of the 220 stable non-gaseous isotopes are produced in the United States (U.S.) [1]. Current U.S. supply is mainly imported from Russia and the Netherlands [2]. There are several reasons, but most isotopic candidates for separation require electromagnetic or gas centrifuge separation technology. These technologies have limited availability in the U.S. Recent efforts have expanded to ensure adequate supply of these isotopes in the U.S. allowing the potential for gas centrifugation of stable isotopes in the future [3]. In 2013, Egle at al. reported that Oak Ridge National Laboratory had begun investigating the potential benefits of combining the two separating technologies [4]. In the report, Egle identifies approximately 29 elements consisting of 145 isotopes that have been demonstrated or proposed as gas centrifuge separation candidates. Table 1 lists many of the stable isotopes that have been reported by

Table 1. Stable Isotopes with Known Applications [5, 6, 7, 8].

Isotope	**Desired Product***	**Commercial Use**
Si-28	Si-28	Physics research and semiconductor.
Depleted Ti-46	Depleted Ti-46	Irradiation capsules. Minimizes production of Sc-46.
Fe-54,57,58	Co-57, Fe-59	Medical applications.
Ni-58,60,61,62,64	Ni-63	Nuclear batteries and detectors.
Ni-64	Cu-64	Medical imaging and treatments.
Zn-66,68,70	Cu-67	Medical treatments.
Depleted Zn-64	Depleted Zn-64	Coolant additive in nuclear plants.
Zn-67, 68	Ga-67	Medical imaging.
Se-74,76,77	Se-75	Non-destructive testing.
Sr-82	Rb-82	Medical imaging.
Kr-80	Rb-81	Medical diagnostics.
Rb-87	Rb-87	High precision instruments.
Sr-88, Y-89	Sr-89, Y-90	Medical treatments.
Depleted Mo-95	Depleted Mo-95	Nuclear fuel.
Mo-98, 100	Mo-99/Tc-99^{m}	Medical diagnostic imaging.
Ag-107, 109	Cd-109	Calibration source.
Cd-110,111,112	In-110, In-111	Laser applications, medical diagnostics.
Ge-68,72,73,74	As-73, 74	Non-radioactive tracers. non-destructive testing.
Pd-102, Rh-103	Pd-103	Medical treatments.
Xe-124	I-123, 125	Medical treatments.
Xe-129, 133	Xe-129, 133	Magnetic diagnostics and imaging.
Te-130	I-131	Medical treatments.
Sm-152	Sm-153	Medical treatments.
Dy-165, Ho-165	Dy-166, Ho-166	Medical treatments.
Yb-176, Lu-176	Lu-177	Medical treatments.
W-180	W-181	Medical treatments.
Re-185,187	Re-186, 188	Medical diagnostics and treatments.
W-186,188	Re-188	Medical diagnostics and treatments.
Ir-191	Ir-192	Radiography source.
Tl-203	Tl-201, Tl-204	Medical diagnostics, fine measurements.

*Desired product can be produced by irradiation of stable isotope in an accelerator or nuclear reactor.

multiple sources (including companies that market them) as currently being used in medicine, research, and industry.

Table 1 also lists some of the product radioisotopes and their uses. Many of the radioisotopes are used in life-saving medical diagnostics and treatments. The known applications are due to the relative availability of the current isotopes and available separation processes. Many of the stable elements that need to be separated are made up of several isotopic components in nature. The number of stable components for each element range from two components to as many as nine components, in the case of xenon (Xe). Tellurium (Te), tin (Sn), and cadmium (Cd) each contain eight components. Many of the minor components, those with low relative abundance, have not been concentrated in sufficient quantities to be considered in research. As separations technology improves and larger quantities of high-purity stable isotopes become available, more applications for the non-targeted components will likely be discovered.

When separating or enriching isotopes, an enrichment cascade is most often necessary because the capability of the individual isotope separator is limited. Individual separators are linked together in parallel to form a stage. In turn, individual stages are linked together in series to form a cascade. The number of separators in parallel determines the cascade throughput, while the number of stages in series determines the weight fractions of isotopes in the product stream at the "top" of the cascade and the waste stream at the "bottom." Unfortunately, a larger number of isotopes and the distribution of their relative abundances complicates the design of an enrichment cascade.

For the separations case of a natural feed stream with only two isotopes, the design of the cascade strives to minimize loss of separative capacity. The theory employed for a two-component system is called "ideal cascade theory." This theory was well-established during the Cold War while designing enrichment cascades to separate uranium isotopes. One primary tenet of the theory is to prohibit the mixing of cascade streams with differing isotopic weight fractions. This effectively prevents inefficiencies due to the loss of separative work that has already been

performed. The ideal cascade is a theoretical design limit, but a real cascade necessitates approximations resulting in reduced efficiency, as will be further discussed.

Matched Abundance-Ratio Cascade Theory

When extending the ideal two-component case to a system of several isotopic components, commonly referred to as multicomponent, the ability to match component weight fractions breaks down. While matching the weight fraction of one component, the weight fractions of the other components cannot be matched because of the inherent physical limitations of the individual separator. In 1963, de la Garza developed the theory for multicomponent systems with small separation factors[1] in which two components are chosen such that their abundance ratios are matched, very much like the two-component ideal system. The matched abundance-ratio cascade (MARC) theory has proven to be successful for modeling enrichment cascades. In 1987, von Halle extended the theory to cascades with large separation factors [9], and his paper is the basis for the following explanation.

In the MARC, the weight fraction (x) of each component (i) in a system of a number of total components (J) is compared to the weight fraction of a key component (k). The abundance ratio (R) of the component (i) is given by

$$R_i = \frac{x_i}{x_k} \tag{1}$$

The stage separation factor (α) is defined by the ratio of the abundance ratios of the stage upflow (R') to the stage downflow (R'') and is given by

$$\alpha_i = \frac{R_i'}{R_i''} \tag{2}$$

[1] A small separation factor is one that approximates unity such that the natural log approaches zero.

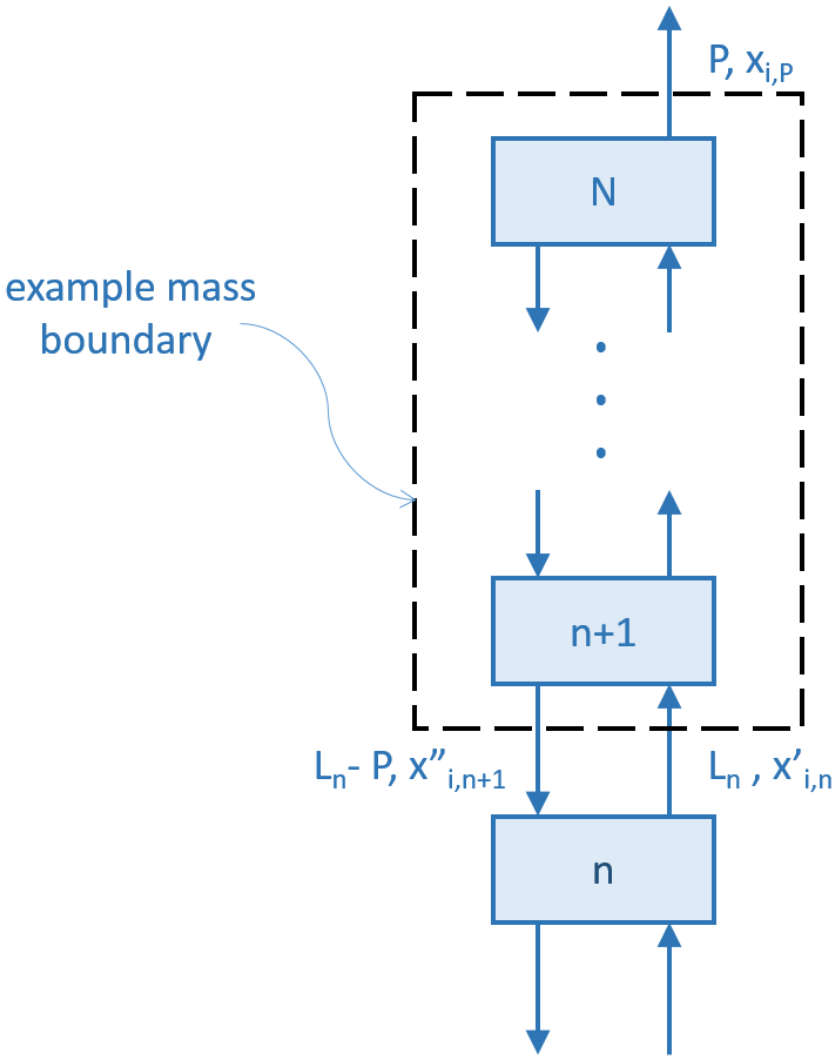

Figure 1. Relative mass flows and weight fractions in the top stages of a MARC [10]. In a one-up, one-down cascade, the stage (*n*) product stream is directed to the next stage (*n+1*) in the cascade, and the stage waste stream is directed to the previous stage. The mass flows (*L*) are conserved until the cascade product stream (*P*) is removed across the mass boundary from the top of the cascade.

The stage separation factor quantifies the isotopic weight fraction change from one cascade stage to the next. Figure 1 shows the relationship of quantities from one stage (*n*) to the next stage (*n+1*). The mass flows (*L*) are conserved throughout the cascade until the enriched product stream (*P*) is removed from the top of the cascade. Likewise, the other mass flows across the cascade system boundaries consist of the feed stream (*F*) and the depleted waste stream (*W*). The analysis here will be limited to these three streams unless otherwise noted. By convention, the product is considered to be the light isotopic stream. Cascades designed to concentrate heavy isotopes as the target components will still be considered to be in the waste stream. As this topic is considered later, reminders will be included for disambiguation. From Figure 1, a material balance at the top of the cascade across a mass boundary yields [9]

$$L_n x'_{i,n} = (L_n - P) x''_{i,n+1} + P x_{i,P} \tag{3}$$

After considerable derivation, von Halle [9] shows that the weight fraction from the down flowing (waste) stream of any stage in the enriching section is given by

$$x''_{i,n} = \frac{\frac{x_{i,P}}{\alpha_i^* - 1}\{1 - (\alpha_i^*)^{n-N-1}\}}{\sum_{i=1}^{J} \frac{x_{i,P}}{\alpha_i^* - 1}\{1 - (\alpha_i^*)^{n-N-1}\}} \tag{4}$$

In equation 4, *N* is the total number of stages in the enricher, and α_i^* is the effective separation factor for the isotope being considered. The summation in the denominator is the sum over all the isotopic components (*J*). The isotopic separation factor is given by

$$\alpha_i^* = \alpha_o^{(M^* - M_i)} \tag{5}$$

where α_o is the separation factor per atomic mass unit (amu) [9, 11, 12, 13]. Note the separation factor differs for each isotopic component based on the difference in mass as compared to the

key weight (M^*). Equation 5 shows how the isotopic separation factor varies exponentially with the mass difference of the specific isotope and the key weight. The key weight, which is the focus of this study, is the arithmetic average of the molecular weight of the key isotope (the isotope selected for separation) and a reference isotope (M_j) and is given by

$$M^* = \frac{M_k + M_j}{2} \tag{6}$$

Interestingly, the selection of the reference isotope is considered to be arbitrary. The choice of the reference isotope results in considerable latitude in cascade performance and results in numerous calculation anomalies. From a practical standpoint, the selection of the key weight implies that any isotope in the feed material weighing less than the key weight will be concentrated in the product stream. Likewise, any isotope weighing more than the key weight will be concentrated in the waste stream. For an infinitely long[2] cascade, this concentration is absolute (i.e., all isotopes lighter than the key weight will exist in the product stream but will not exist in the waste stream).

Based on the definition of the key weight, it might appear that the key weight would be limited to a small set of discrete values approximately equal to an arithmetic series of the number of isotopes in the feed material. However, the key weight can be treated as having continuous values and can be any real number. The only subset of real numbers that are meaningful from a separations standpoint are those real numbers ranging from the molecular weight[3] of the lightest isotope to the molecular weight of the heaviest isotope in the feed material. The selection of a key weight that does not coincide with the mass of a real reference isotope in the feed material,

[2] The dimensions of a cascade refer to the length and the width of the cascade. The length of the cascade refers to the total number of stages. A long cascade has many stages. The width implies the number of separators in parallel in a stage, which is proportional to cascade throughput or production capacity. In this work, two cascades with equal dimensions implies the cascades contain equal numbers of enricher and stripper stages.

[3] In this work, the term molecular weight is used generically to cover the terms molecular weight and atomic weight, in the cases where a pure elemental gas form exists for separation, such as Xe and Kr.

suggests the selection of a notional reference isotope with a weight fraction equal to zero [14, 15, 16]. This technique has been shown to be practicable for both calculation purposes and real cascade design. This paper will focus on the selection of the reference isotope (thus, the key weight), and how this affects the efficiency and design of the MARC. The MARC theory for large separation factors as presented by von Halle provides a closed-form solution [9]. The resulting explicit solution allows relative ease in the application of extensive numerical treatment for optimization. The extension to large separation factors is also pertinent to the gas centrifuge. Previously, the multicomponent isotope separation theory development had been limited to the condition of a small separation factor. The condition was valid for gaseous diffusion technology; however, gas centrifuges commonly exceed a separation factor of 1.1 making the condition of near unity no longer valid.

Introduction

Several methods of optimizing cascades for multicomponent isotope separation have been considered. Some of these methods provide rigorous mathematical treatment to a generalized case that may or may not be applicable to real cascades, as will be discussed later. The MARC model provides discrete stage-wise calculations, which are directly applicable to real world applications and provide a closed-form solution. By varying the key weight within the cascade, an applicable optimization methodology may be defined. Recent publications have considered varying the key weight within the cascade as an optimization tool in other cascade models.[4] These previous works will be considered with the analysis here.

This work will define a general optimization methodology for cascade design by varying the key weight in a MARC. This work is mainly interested in the centrifugal separation of stable isotopes in the gaseous state. Although it is intended to treat the most general cases of separator technology, real decisions in the development of the calculations and subsequent analysis had to be limited to a logical subset of cases. When these decisions were made, the default range of

[4] See Q-cascade below in literature review.

parameters were intended to capture the range suitable for centrifuge operation. For instance, the separation factors and assumptions considered here reflect those comparable to centrifuge cascades as presented in the literature. Real centrifuge cascades have a fixed, integer number of stages, integer number of machines in each stage, and rely on stage-wise modelling instead of a continuous calculation. Continuous models, as will be discussed, are likely more general, but may be limited in their ability to accurately model stage-wise cascades with large separation factors, e.g. gas centrifuge cascades. Going forward, the term centrifuge and the term separator will be used interchangeably.

CHAPTER 2: LITERATURE REVIEW

Stable Isotopes

Many papers have been written discussing the prospect and some considerations of separating stable isotopes by gas centrifuge. Shubin et al. discussed limitations of centrifugal stable isotope enrichment, as well as various isotopes of utility [5]. Roberts published examples of stable isotope enrichment by centrifugation in 1989 providing expected separations for several Xe and krypton (Kr) isotopes [17]. Russian authors from the Kurchatov Institute, which markets stable isotopes around the world, have published a series of papers discussing the specific enrichment of a number of isotopes [7, 18, 19, 20, 21]. These papers, summarized here, include results of several different isotopes in actual separations tests.

In 1999, Sosnin and Tcheltsov shared results of Te enrichment in a laboratory-scale columnar[5] cascade [19]. A series of batch operations were used to prepare adequate feed for a non-steady-state cascade. The result was high purity Te-123 by operating the cascade with waste recycle and periodic product withdrawal.

In 2006, Cheltsov and Sosnin provided results for lead (Pb), nickel (Ni), and molybdenum (Mo) separations by operating in batch-mode for as many as five batches [18]. Future work may provide an opportunity to compare the experimental results with the optimization methodology developed here. However, these comparisons may prove difficult as cascade specifics, such as the number of stages and separation factors, are not provided by the literature. Also, a square cascade is likely valuable from an experimental results standpoint, but would almost certainly yield less efficient results than the optimized calculation results.

[5] A *square* cascade implies that the individual stages have the same width, as opposed to a *tapered* cascade. A tapered cascade gets narrower as the flow approaches the top and the bottom of the cascade. The tapered cascade is a direct result of optimization (i.e., matching abundance ratios). *Rectangular* cascade is a term used interchangeably with square cascade. A *columnar* cascade, however, implies that each stage consists of only one separator.

In 2014, Cheltsov et al. provided a more detailed description of cascade separations of Ni isotopes [7]. The rectangular cascades were operated in at least six batches with various multiple recycle operations. The process took well over a year and produced tens of grams of each stable Ni isotope by gas centrifuge. Again, in 2014, Cheltsov et al. published a similarly scoped paper with a detailed description of separating sulfur (S) isotopes [20].

Chinese authors have also published some studies regarding stable isotope separation by gas centrifuge. In 1996, Wu and Zhuge compared theoretical and experimental results from cascade enrichment of Xe [22]. The paper is not very detailed but appears to use a MARC model for the theoretical calculations. The comparison of the data supports a rough agreement between the calculated and experimental weight fractions. The paper falls short in the areas of cascade design specifics, conclusions about findings, and future application of the results.

In 2006, Zhou et al. examined the separation of stable isotopes in a short, four-centrifuge cascade [11]. The cascade could be configured in a three- or four-stage configuration. The paper provides good data on the separation factors and cascade weight fractions for several isotopes, including those of tungsten (W), silicon (Si), and Te. In 2008, Li et al. published an analytic study for separating Si-28 in a short cascade by operating in batch mode for a sequence of five iterations [23]. This is comparable to the cascade-of-cascades cases that will be examined here. Li et al. did not publish considerations of optimizing the key weight.

Theoretical Cascade Studies

Originally, de la Garza first developed the theory of multicomponent isotope separation in 1961 and generalized the MARC theory in 1963 [10, 24]. In his 1963 paper, de la Garza himself proposed varying key weights within the cascade.

Over time, more theoretical models have been considered for optimization. The theories for optimizing multicomponent cascades vary in their assumptions regarding several different

cascade parameters. In 2014, Zeng et al. developed and compared several cascade models, based on existing theories, with the goal of obtaining useful numerical methods for each model [13]. The analysis stopped short of comparing the properties and performance of each of the models. Although an interesting mathematical pursuit, some of the models appear to develop arbitrary constraints as a matter of practice without any grounding in a physical separations basis. For instance, the matched X-cascade fails to address some theoretical inconsistencies on the development of the assumptions. Without the accompanying theoretical development, it remains unclear how the model represents a viable cascade.

The MARC model uses a theoretical approach that considers a cascade gradient, or a stage-wise calculation.[6] These types of models have been termed model cascades of continuous profile (MCCP), defined as "cascades with uninterruptible distribution of the stage feed flow over the feed stages" [25]. Another MCCP that has been extensively researched and well-accepted for cascade modeling is the Q-cascade. Because of the extent of the research and the similarity in the approaches, the literature on the MARC and the Q-cascade are reviewed more in depth here.

Matched Abundance-Ratio Cascades

The MARC theory is similar to the ideal cascade for two-component isotope systems that considers each stage as a unit. The stage width is not constrained to an integer number of separators. The analysis is a theoretical calculation, because a real cascade must employ an integer number of separators in each stage [26]. However, the approach has shown validity. The theory approximates the separative capacity of a real cascade with only small losses of efficiency when "squaring off" the stages (i.e., expanding the stage width to correspond to an integer number of separators). Unlike the Q-cascade model discussed later, the MARC model uses a discrete number of separation stages comparable to a real centrifuge cascade.

[6] Occasionally, the MARC is referred to as a matched-R cascade [13].

In 1965, de la Garza considered two cases of separating a middle isotope by configuring two cascades in series [27]. The two cases considered the order in which the target isotope was enriched. In one cascade, the heavier isotopes were removed as product. In the other cascade, the lighter isotopes were removed as product. The first case considered removal of the heavier isotopes first, while the second case removed the lighter isotopes first. For the same mass of the target isotope at the desired weight fraction, the sums of the cascade internal flows in the two methods differed by 6-percent. In other words, the sequence of the cascades in which the lighter isotopes were removed first resulted in a 6-percent efficiency improvement over the sequence where the heavier isotopes were removed first. This result sums up the basis for the analysis here. The optimum configuration is that which minimizes the total cascade internal flows while producing the same quantity and weight fraction of the target isotope. The basis for this optimization criterion will be discussed later.

In his 1965 paper [27], de la Garza developed the form of a small enrichment factor given by

$$\psi_{i,M^*} = \psi_o (M^* - M_i) \tag{7}$$

The enrichment factor is related to the separation factor by

$$\psi = \alpha - 1 \tag{8}$$

The enrichment factor will recur later when methods of optimization are considered. As mentioned previously, von Halle extended de la Garza's work to cascades with large separation factors [9]. The benefit of von Halle's approach is that it provides a closed-form approach with an explicit solution that allows for effective parametric study. Multiple papers have been written on optimizing cascades through a variety of techniques using the MARC model [28, 29, 30, 31].

Olander considered optimizing a cascade by varying the separation factor [32]. Although the analysis is interesting from a theoretical point of view, the findings considered designing and operating individual stages by changing operating parameters of each individual stage. This

strategy implies deviating from the optimum parameters of the centrifuges or changing centrifuge technology by stage. Because centrifuge technology is difficult to master, the intentional deviation from optimum parameters may be self-defeating. Another issue with this strategy is that a real, one-up, one-down cascade configuration requires matching the product-to-feed separation factor[7] of one stage to the feed-to-waste separation factor[8] of the next stage. This may be beneficial for one stage but necessitates the next stage having different parameters in order to avoid mixing. Having different stage parameters at alternating stages practically ensures the inability to optimize the individual stage parameters.

Palkin published a series of papers considering a variety of methods for optimizing cascades by minimizing the total internal flows. Palkin considers allowing mixing in a fixed cascade with the only condition being the target weight fraction [33]. Also, Palkin considers the effects of shifting the relative feed stage in the cascade [34]; optimizing for an arbitrary number of feed streams and withdrawal streams [29]; specifying different separation factors by stage [28]; and varying the stage width in a fixed cascade [35]. Palkin seems to have developed a numerical technique specifically for optimizing a fixed cascade. He discusses the differences in an optimum cascade versus a MARC, and discusses the differences in efficiency somewhat vaguely. The papers give some numbers for interstage weight fractions and cascade flows, but overall, the level of detail would make reproduction of the results difficult. In conclusion, the papers seem to be more suited for optimizing an existing fixed cascade to a specific set of conditions. It is possible the intent of the series is to use the same cascade for separating various types of feeds.

[7] Also referred to as the enrichment factor (β) and not to be confused with the enrichment factor (ψ) referenced in the MARC theory.

[8] Also referred to as the depletion factor (γ).

Q-Cascades

The Q-cascade is another MCCP first developed in the 1960s. The mathematical model is derived from cascades with stages of "weak enrichment." In other words, the theory is applicable when separation factors approach unity [25]. The development is similar to the theoretical development by de la Garza, and claims to be applicable to large separation factors. The model generalizes an approach to cascade analysis which treats the length of the cascade as continuous. In other words, the stages are not discretized but are considered continuous. A transformation allows for the finite-difference equations in MARC to be approximated with differential equations. The generalization seems to lend itself to more flexible cascade analysis. Although more generalized, it is unclear how the approximation applies to a real cascade that uses discrete stages. Using the MARC model, the stage flows can be "squared off" to correspond to discrete numbers of separators per stage with only marginal losses in efficiency. The Q-cascade calculations require the squaring-off approximation in the cascade width (number of separators per stage) as well as an additional approximation to a discrete length. It is unclear how squaring off the length affects the overall efficiency of a cascade when compounded with the effects of squaring off the width. But more importantly, the discrete nature of a real cascade suggests that not only will the entire length of the cascade need to be squared off, but the individual stages will require squaring off, as well. For a centrifuge cascade with large separation factors, the number of stages is a relatively small number when compared to those with small separation factors. The effect of squaring off the small number of stages will likely introduce significant inefficiencies. Furthermore, it remains unclear how the expansion to a large separation factor remains valid in an open form solution. The assumption that the stage-wise calculation is a smooth function breaks down when considering the discrete nature of large separation factors [13]. The lack of smoothness in large separation factors is apparent when considering the MARC, as will be shown later.

In 2010, A.Y. Smirnov et al. showed varying the value of a constant cascade key weight resulted in changes in flows and component weight fractions within the cascade length [36].

Smirnov postulated removing an intermediate isotope by adding an additional product "side stream" at the location of that isotope's maximum weight fraction in order to improve efficiency.

A series of fairly recent papers have varied the key weight in a method to optimize the Q-cascade calculation [13, 37, 38]. In 2011, Borisevich et al. showed that the optimum key weight for a cascade depends on the cascade's target weight fraction in a Q-cascade [39]. Similar results from MARC calculations have been provided in the results section here for comparison.

In 2015, Zhang et al. considered the possibility of varying the key weight within a Q-cascade for optimization [15]. The authors' methodology divided a Q-cascade into four segments with each segment having a different assigned key weight. Zhang et al. also termed the ratio of the flows as relative total flow (RTF), which is defined by

$$RTF \equiv \frac{\sum_{stages} \varepsilon_o^2 L}{2P} \tag{9}$$

where ε_o is the corresponding enrichment factor per amu (ψ_o) for the Q-cascade construct. The sum of the internal stage flows is divided by twice the cascade product flow. RTF methodology will be covered more thoroughly later. For now, it suffices to say that minimizing RTF is a method of optimization. Zhang et al. showed that the optimum segmented Q-cascade had a lower RTF than a Q-cascade with constant key weight. The authors state their inference is that a cascade with a continuously changing key weight throughout would provide the optimum RTF. The results are compelling and parallel the goals set forth for this work applying the key weight variation to a MARC. A few issues with the analysis remain unclear. First, as mentioned earlier, the applicability of the Q-cascade with large separation factors and continuous length may not translate as well as the MARC to a real cascade. Next, the variation of the key weight continuously throughout a cascade most likely introduces inefficiencies at the segment boundaries. In the case of the MARC, the matched abundance-ratio criterion at the individual stage interfaces are not met, introducing some mixing losses. It remains unclear if these mixing losses are acceptable in comparison to the gains made be varying the key weight. However, the

losses are likely more acceptable in a long cascade while reducing the number of segment interfaces to a fraction of the overall number of stages. As the number of stages decreases with large separation factors and the number of segment interfaces increases, the more likely the mixing losses will overtake the modest gains made by varying the key weight. Furthermore, it is unclear how varying the key weight at every stage will affect the achievable separation factor and whether the assumption of a constant separation factor is valid.

In 2016, Zeng et al. considered optimizing Q-cascades by adjusting segment lengths to coincide with side stream withdrawals of the peak weight fraction of intermediate isotopic components. This method shows the potential of removing those intermediate components at the peak weight fraction for use while reducing the RTF and obtaining the desired product weight fraction. For multicomponent isotope separation, this is especially significant in the case of having multiple desirable product isotopes. The idea of multiple isotope products and the effect on optimization has been identified for possible future work.

Considerations for Optimization

Optimization in a two-component separation cascade has been well established. Cohen first developed the value function from Dirac in 1951 [40]. The development assumes that a stream has a value based on its weight fraction (x). The value function for a two-component system is given by

$$v = (2x-1)\ln\left(\frac{x}{1-x}\right) \tag{10}$$

The separative work performed in a cascade is determined by the differences in the values of the product and waste streams compared to the feed stream as shown by

$$\Delta U = Pv_P + Wv_W - Fv_F \tag{11}$$

Therefore, an optimized cascade minimizes the amount of separative work performed to produce the desirable outcome, presumably, an amount of product at a desired weight fraction.

Unfortunately, the value function has proven difficult to apply in a multicomponent system [41, 42]. The difficulty comes from the assumptions developed by Dirac and the validity of these assumptions and the Taylor series expansion in the multicomponent case. In 2008, Louvet published a summary paper explaining the various methods and the attempts to expand the value function to the general multicomponent case [43]. Benedict shared results of the value function expanded to a three-component case [44]. Until now, the value function has not been properly expanded to the *n*-component case [12, 43]. Smorodinskii and others proposed approaches as alternatives to the Dirac value function [45]. Several authors have proposed general methods of calculating an alternative to the value function for multicomponent isotope separation based on a set of assumptions and initial conditions [46, 47, 48]. Some of the most recent papers examining cascade models confirm the lack of a consensus method for calculating the value function for multicomponent isotope separation [13, 38].

Borisevich, Sulaberidze, and Wood reduced the previous general forms into an equation applicable to cascade analysis [49]. The approach extended a previous one described by Gadkari and Govind in minimizing cascade internal flows as a method of optimization [50]. The resulting equation was similar in form to de la Garza's original analysis that compared cascade flow and separation factors to the work, and is given by

$$\Delta U = \frac{\psi^2}{4} \sum L_n \tag{12}$$

Many studies have equated minimizing total internal cascade flow with optimization. Many authors, including de la Garza, Wood, and Smirnov, have proposed similar methods using flow ratios as valid optimization criteria [41, 51, 27]. Zeng et al. proposed minimizing total flow as the criterion for optimization in the Q-cascade [37]. Likewise, Borisevich considered flow

criteria as a method for optimization for different key weights for the Q-cascade [39]. These flow ratios are similar to the previously defined RTF. A total flow criterion will be compared with the generalized *n*-component value function in the methodology section for validation of the optimization criterion to be used here.

CHAPTER 3: METHODOLOGY

A code based on the theory presented in von Halle's 1987 paper was converted to MATLAB® to provide more flexibility and computational power [9]. Because of the numerous variables represented in the theory, a number of practical assumptions are made both for simplification and for practical application to real cascade.

Assumptions

1. Individual centrifuge performance characteristics are considered constant and uniform throughout the cascade. Because of the complexity in centrifuge development and operation, the assumption that a successful design will be chosen and used consistently in the cascade is pragmatic. Without this assumption, analysis of the number of combinations of varying centrifuge performance parameters would be counterproductive.

2. The separation factor, α, is considered constant within the cascade for the purposes of optimization. Separation factor is an individual centrifuge characteristic. Some previous analyses have considered varying separation factor within the same cascade as an optimization tool. Because of Assumption 1 and the reliance of the key weight on separation factor in MARC theory, the separation factor is held constant. Varied values of separation factors are examined across different cascade calculations to provide a parametric analysis, but are limited to values ranging from 1.10 to 1.50 to be consistent with literature [12, 13, 11, 52]. The results here will, in general, compare the cascade performance over the range of separation factors to show the considerable influence the value has on cascade calculations. On the occasion when a single separation factor or a subset of the range of separation factors is indicated here, the selection has been chosen either as adequate intermediate sample values or the value which best illustrates the effect to be shown.

3. A symmetric cascade is assumed based on Assumption 2. This assumption is also consistent with Assumption 1 and the application of the MARC model to real centrifuge cascade design. This assumption implies that β equals γ, and that the analysis here is limited to a one-up, one-down cascade configuration. This means that the product stream of any one stage will be directed to the next adjacent stage's feed stream flowing upward in the cascade. Also, the waste stream of any one stage will be directed to the adjacent stage's feed stream flowing downward in the cascade.

4. The cascade is assumed to be in steady-state operation.

5. Only the feed, product, and waste cross the cascade mass boundary. Conservation of mass is assumed on the feed, product, and waste.

Verification of Code Results

The MATLAB® code used here was verified by reproducing previously published results. First, the results from de la Garza's 1963 paper were recreated to ensure the code reproduces results consistent with MARC theory [10]. The flexibility of the code and the ability to plot figures allowed reproduction of the paper's figures. The de la Garza figures illustrate the isotopes' behaviors throughout the cascade as the key weight is varied. To provide an evenly distributed feed for an unbiased analysis, de la Garza uses a fictional material with one amu mass difference between five isotopes (298-302 amu) with equal initial weight fractions of 0.20. Figures 2-4 show the individual isotopic behavior within a cascade of nominally 50 stages, where the feed is directed into a stage near the middle of the cascade (stage number 25). The isotopes with molecular weights heavier than the key weight are concentrated in the stripper section (the left side of the figures), while those with molecular weights lighter than the key weight are concentrated in the enricher section (right side of the figures). In an infinitely long cascade, the product contains only those isotopes lighter than the key weight. The 50-stage

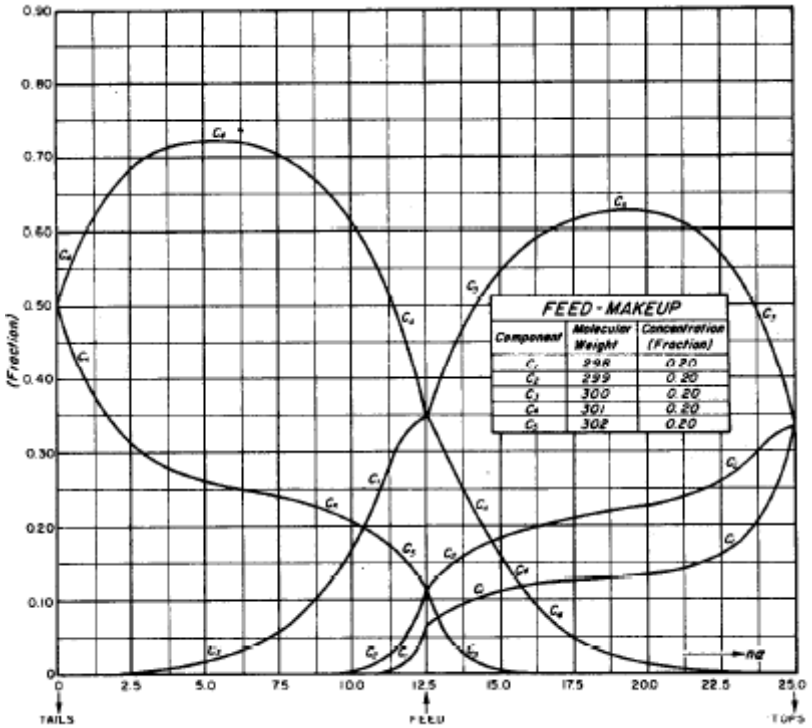

(a)

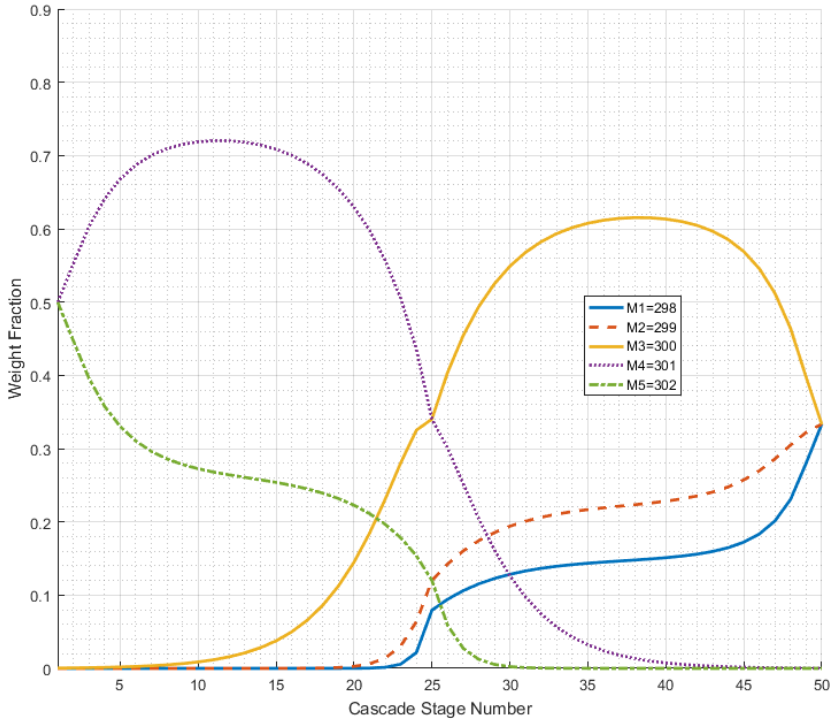

(b)

Figure 2. Reproduction of de la Garza figure where key weight is 300.5 amu[10]**.** (a) Original figure by de la Garza. (b) The recreated figure. The only isotopes with significant weight fractions in the product stream (the far right of the figure) are those with molecular weights less than 300.5 amu, namely M_1, M_2, and M_3. Because those three isotopes each have the same initial weight fraction in the feed material, each isotope has an equal weight fraction approximately equal to one third in the product stream.

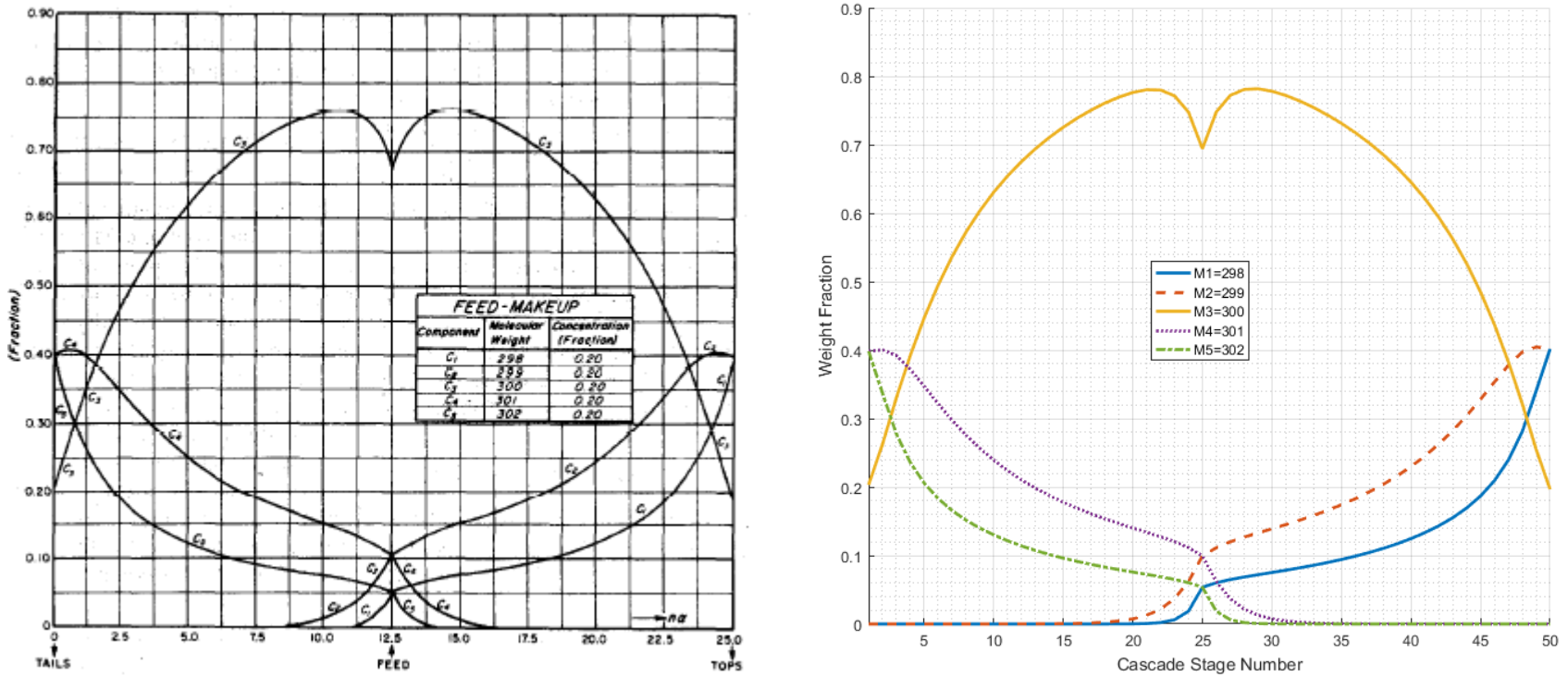

(a) (b)

Figure 3. Reproduction of de la Garza figure where key weight is 300.0 amu[10]. (a) Original figure by de la Garza. (b) The recreated figure. Because the key weight equals the molecular weight of M_3, that isotope is split equally into the product stream and the waste stream (the far left of the figure). Because all the isotopes have equal initial weight fractions, M_3 has only half of the weight fractions of the other isotopes in both the product and waste streams.

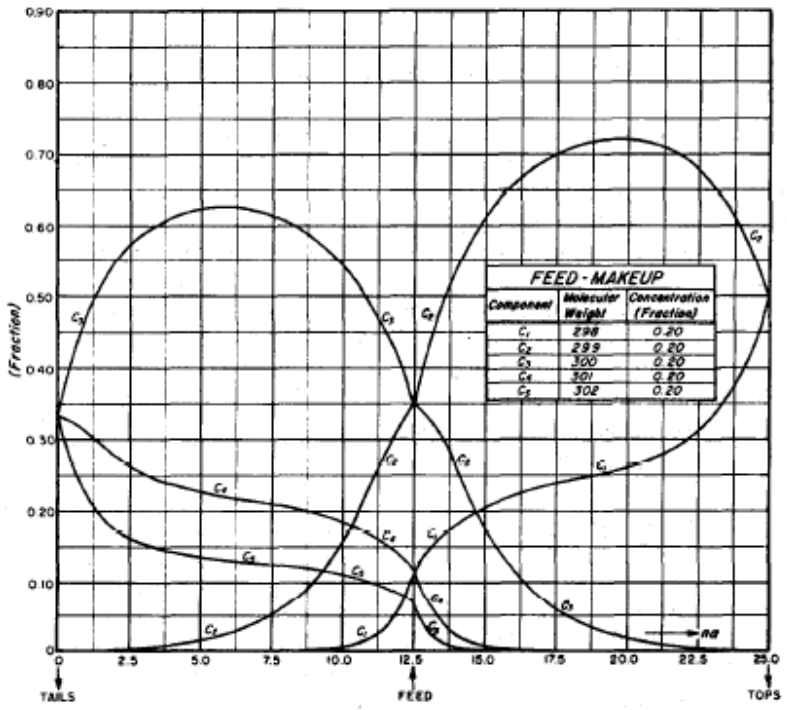

(a)

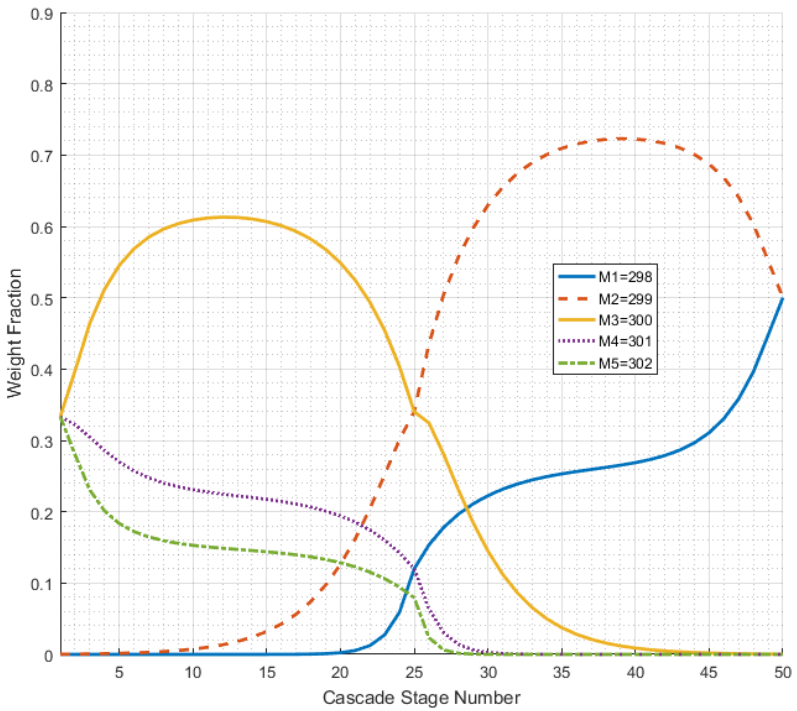

(b)

Figure 4. Reproduction of de la Garza figure where key weight is 299.5 amu[10]. (a) Original figure by de la Garza. (b) The recreated figure. The only isotopes with significant weight fractions in the product stream (the far right of the figure) are those with molecular weights less than 299.5 amu, namely M_1 and M_2. Each isotope has an equal weight fraction, approximately equal to one half, in the product stream.

cascade chosen by de la Garza is sufficiently long to show this effect. In Figure 2, the key weight is set equal to 300.5 amu, the only isotopes with significant weight fraction in the product stream are those lighter than 300.5 amu. This can be seen in the figure at stage number 50, where the product of the cascade is removed. The isotopes with molecular weights equal to 298 amu, 299 amu, and 300 amu are concentrated in the product stream to equal weight fractions of approximately one third.

Similarly, in Figure 3 the key weight is set to 300.0 amu. However, in this case, since the key weight matches the molecular weight of one of the isotopes, that isotope is split equally between the product and the waste streams. The other two components lighter than 300.0 amu, namely M_1=298 amu and M_2=299 amu are concentrated in their full quantity in the product stream. Since their weight fraction is double that of the split fraction of M_3=300 amu, they each account for a 0.4 weight fraction of the total product mass. M_3 accounts for only 0.2 weight fraction. Finally, in Figure 4, the key weight is set to 299.5 amu, thereby concentrating only the two lighter components in the product with a weight fraction each of approximately 0.5. Figures 2-4 appear to match precisely those presented by de la Garza with some common distinct features worth noting. First, the region of the figure near stage 25, the feed stage, shows a lack of smoothness in the function. This is indicative of the piecewise method the stripper sections and enricher sections are calculated independently.

Next, interestingly, one of the components reaches a maximum weight fraction in both the enricher and the stripper sections prior to the top and the bottom of the cascades. For instance, in Figure 4, the M_2=299 amu component reaches a peak weight fraction of approximately 0.72. These higher weight fractions illustrate a possible opportunity to remove another stream of material, or side stream, prior to the usual waste or product streams at the ends of the cascade. If the M_2=299 amu component were withdrawn at 0.72 weight fraction, the product weight fraction of M_1=298 amu would likely be much higher and require fewer stages. The notion of adding side product streams have been investigated by Sulaberidze and others [51, 53]. Theoretically, these side streams seem feasible but may be difficult to implement, or at least may only be applicable in very specific cases, especially when the optimization techniques

considered here are employed. Because of these practical problems, the use of side streams in this optimization study will be deferred to future work.

To ensure the robustness of the code, the code was further verified by reproducing results of other published papers. Appendix A shows the comparison of the current calculated results to examples of previously published results. Table 4 compares the data published by de la Garza in 1965 [27]. The published results are presented in the top section of the table. The calculated results from the code used here are presented in the middle section of the table. The difference in the two sets of results are presented in the bottom section of the table. The results are consistent to within four significant figures, matching the precision of the provided feed stream weight fractions.

Tables 5 and 6 compare the data published by von Halle in 1987 [9]. Table 5 provides von Halle's published data. Table 6 shows the calculated results from the code used here. Table 7 presents the calculated difference in the data from the previous two tables. Table 7 shows that the data matches to five significant figures except in just a few cases. In these few cases, the differences are in the last decimal place and are most likely due to minor rounding differences due to the precision of the input data. It is also possible that the current computing capabilites with MATLAB® on modern systems are more precise than the historical capabilities, although this speculation could not be confirmed. The difference in the results amounts to approximately 10 ppm. This difference is certainly within the purity requirements of the stable isotope product, and well within the typical measurement precison available using a gas chromatography-mass spectrometer.

Parametric Study

In order to consider more general multicomponent materials, the code was modified to accept an unspecified number of isotopes. For the study here, a fictitious feed material composed of ten components with equal weight fractions has been chosen to be a general case

for a cascade parametric study. The molecular weights[9] chosen for the feed material here range from 125.0-134.0 amu. Each isotope of the fictitious feed material has a one amu mass difference to its nearest neighbor in the isotopic sequence. This is the general limiting mass difference for isotope separation and should provide a convenient benchmark when evaluating a real feed material. The molecular weight range was chosen as a midrange value on the periodic table for future baselining considerations. This material considered has a molecular weight comparable to the atomic weight of the element Xe. The element Xe has nine stable isotopes, the largest number found of any element. The fictitious feed material used here, with ten isotopes, will bound all the cases found in nature. Again, equal weight fractions in the feed will provide a convenient benchmark when evaluating a real feed material.

Calculations will be performed for several cascade configurations. First, the separation of an end-component isotope, either the lightest or the heaviest in the isotopic sequence, will be analyzed. For the data and results presented here, the lightest isotope, M=125.0 amu, was chosen to illustrate the end-component behavior. The heaviest isotope will behave similarly in the waste stream with the optimization of the key weight chosen in a similar manner. A middle component will also be considered. The separation of a middle component is expected to be much the same as an end component, except that it will require the separation to be performed in two distinct steps. These distinct steps imply the consideration of two distinct cascades [53]. The first cascade to isolate the isotope with either the lighter isotopes or the heavier isotopes. The product stream of the first cascade will result in the middle isotope essentially becoming an end component at that point. Then a second separate cascade is required to isolate the isotope as an end component.

For the end component, the first cascade design problem considered will be to optimize a single cascade with a constant key weight. The result of the single cascade calculation is pertinent. Originally, de la Garza suggested the optimum key weight is the arithmetic mean of

[9] The term molecular weight (M) is used generically for consistent comparisons between different types of feed materials including atomic species of gaseous materials.

the two components to be separated, or in the multicomponent case, the mean of the two neighbor components where the separation is to occur [27]. More recently, Sulaberidze et al. [14] and Borisevich et al. [39] showed that the optimum key weight appears to vary continuously and is a function of the target product weight fraction. The results of this single cascade case will be used to develop a general methodology for choosing the optimum key weight.

Next, the single cascade case will be compared to cascades composed of multiple smaller cascades (a cascade of cascades), each with different key weights, to determine if varying the key weights by cascade will improve efficiency. These cascades of cascades will consider cases where the waste streams are recycled, meaning the waste streams for higher level cascades will be redirected back to the feed stages of lower level cascades. Also, the cascades of cascades will consider cases with no recycle. The efficiency criterion will be compared for each cascade with practical considerations for cascade application discussed. Finally, a method for optimizing a cascade by varying the key weight will be proposed.

CHAPTER 4: RESULTS AND DISCUSSION

Validation of Optimization Criterion

As previously discussed, the value function has been difficult to extend to the multicomponent case (i.e., greater than two components). Recently, the value function was generalized to a case of *n* components [54]. Recall that work performed in a cascade is given by

$$\Delta U = Pv_P + Wv_W - Fv_F \tag{13}$$

In the multicomponent case, *v* is now defined as

$$v_i = \left(2x_1 + \left(\frac{2b_2}{2b_2 - 1}\right)x_2 + \ldots + \left(\frac{2b_{n-1}}{2b_{n-1} - 1}\right)x_{n-1} - 1\right)\ln\left(\frac{x_1}{x_n}\right) \tag{14}$$

where *i=1* to *n, 1* is the key isotope, *n* is the reference isotope, and *b* is given by

$$b_i = \left(\frac{M_i - M_n}{M_1 - M_n}\right), \text{ when } b_i \neq \frac{1}{2} \tag{15}$$

otherwise

$$\left(\frac{2b_i}{2b_i - 1}\right) \text{ is replaced by } \frac{1}{2}\ln\left(\frac{x_i}{x_n}\right), \text{ when } b_i = \frac{1}{2} \tag{16}$$

It is still unclear how the calculated value of a given set of parameters changes solely with the selection of the key isotope and the reference isotope. Preliminary calculations seem to indicate that the answer is the same regardless of the choices of key and reference isotopes. If these results hold true, one significant result is that cascades can be compared without regard to the number of targeted product isotopes obtained. In other words, a scenario may be possible in a multicomponent case where multiple isotopes are desired in the product. The comparison of

cascade calculations would be simplified if the value functions were the same without regard to which of the two targeted isotopes were selected as the key isotope.

Another benefit of the generalized value function is that it allows a side-by-side comparison to the previously used method of minimizing internal cascade flows. Figure 5 shows the results of a comparison of the two different methods of calculating separative work in a cascade while varying the key weight through the discrete values available using equation (6) for chosen fictitious material used in the study. This comparison does not vary the key weight continuously using the notional isotope concept discussed previously, because defining the value function using the notional isotope concept would be cumbersome at best. The cascade parameters represented in Figure 5 are a separation factor equal to 1.3 with five enricher stages and four stripper stages.

The results shown in Figure 5 indicate that both methods of calculating separative work yield quite similarly shaped curves. Although the curves are not identical in magnitude, the main shapes are consistent and provide the same minimum value of separative work. In other words, the shapes of the curves are quadratic yielding a minimum value of separative work for the same value of key weight. Both methods of calculating separative work are valid. As long as the value of separative work is calculated consistently, the methodology chosen is inconsequential to determining the optimum key weight. Here forward, separative work calculations will be based on the sum total of cascade internal flows. The calculation of internal flows already exists in the MARC calculation as an integral part of determining the weight fractions throughout the cascade. The separative work calculation uses the value function in an additional calculation performed as a call function. This value function calculation includes exponentials and the potential for division by numbers approaching zero. Because of this consideration and the methods employed later in convergence calculations using many iterations, the separative work calculations based on the value function may introduce numerical errors, as an artifact, and possible instabilities in the computer code. Because of these possible errors and instabilities, the calculation based on total cascade flows is used from here forward as a matter of simplifying calculations.

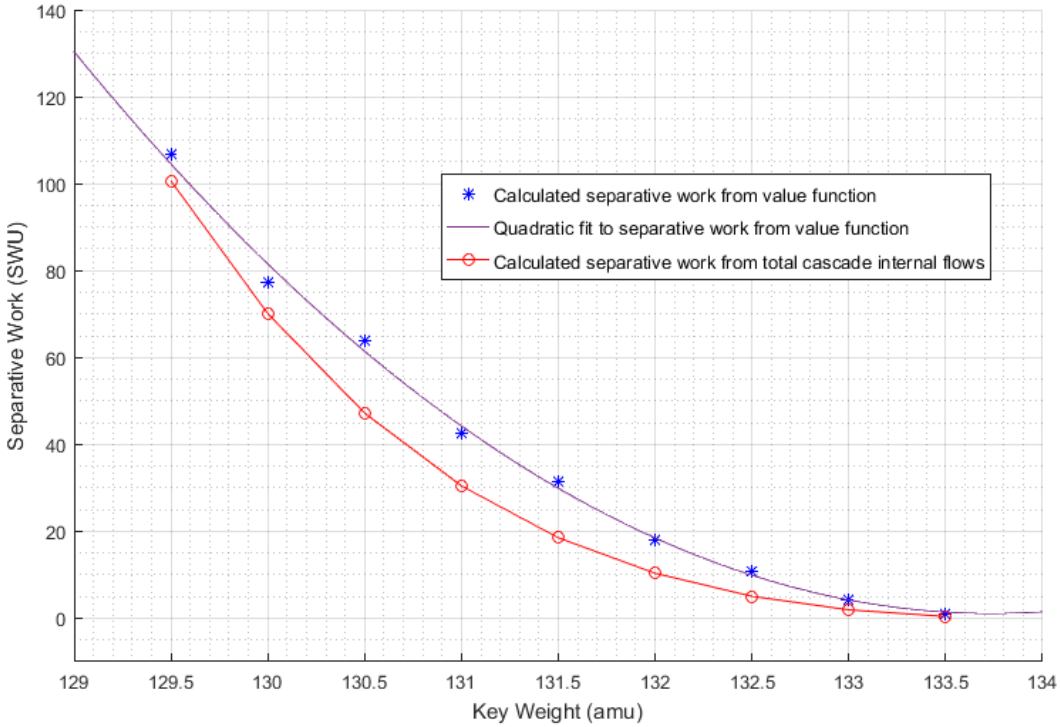

Figure 5. Comparison of separative work calculation methods. The red (o) markers represent the separative work calculation using total internal cascade flows. The blue (*) markers represent the separative work calculation using the value function. Although the discrete values do not match precisely, the values are approximately the same magnitude. The fitted curves have a similar shape, and the minimum value of the curves occur at the same key weight. This suggests that a cascade optimization would yield the same result for the key weight regardless of the method chosen.

The choice of minimizing total flow as the method of optimization seems to be logically consistent with minimizing the number of operating separators to achieve the same quantity and quality of product [49, 16, 51]. Real individual separators can only process an amount of a certain material per unit of time. Stage feed flows should be indicative of the number of real separators required per stage in a cascade. Assuming the choice of separator is determined without consideration of this methodology, the amount of power consumed in a cascade generally increases with the number of separators [38]. Similarly, the number of separators is likely proportional to the upfront capital costs in a cascade, as well as the cascade operating costs and maintenance costs. These optimization considerations are consistent with minimizing the total number of separators, which is consistent with minimizing the total internal cascade flow.

Minimizing total internal cascade flow is important, but the purpose of the cascade is to produce a product isotope at a threshold weight fraction. Arguably, producing the maximum amount of product could be a criterion for optimization while minimizing the total internal flows. Several authors, including de la Garza, have chosen to use the ratio of the of the total internal cascade flows to the product flow at the desired weight fraction as the optimization criterion [37, 43]. The relative total flow (RTF), as previously discussed, will be retained here for simplicity, but here RTF will be reduced simply to

$$RTF \equiv \frac{\sum_{stages} L}{P} \tag{17}$$

consistent with the historical literature [53, 27, 14]. The simplified version used here retains the desired properties sought; maximizing product flow while minimizing total internal cascade flow. The omitted enrichment factor term and the doubling of the product in the denominator cancel out when comparing cascades with same enrichment factors. As previously discussed, it is assumed the cascade will be constructed with a constant separation factor. So, the omitted terms will not affect the comparisons here. Minimizing the RTF in a cascade will be used as the optimization criterion from here forward.

Another term encountered when optimizing cascades is efficiency. Efficiency is generally calculated as a comparison to the optimum cascade, which is only useful when the optimum cascade is known. Efficiency will be used here for comparing two similar cascades, and it will be defined as

$$Efficiency \equiv \frac{\Delta RTF}{RTF} \times 100\% \tag{18}$$

Although not referred to as efficiency, Zhang et al. used this definition to describe the improvement in performance when comparing similar cascades [15]. For two cascades that produce the same amount of desired product, one cascade with less total internal cascade flow will be a percentage more efficient than the original.

The Case for an End Component

Single Cascade with Constant Key Weight

The first case considered is the case where the key isotope is an end component. Based on the previously defined key weight, it makes logical sense that any key weight chosen between the key isotope (assuming it is the lightest isotope) and the next component will result in the key isotope being concentrated in the product stream. The remainder of the components will be concentrated in the waste stream.

In this calculation, the key weight was allowed to vary continuously across the spectrum of isotopes for a fixed number of stages. First, the code was configured to determine the number of stages required to achieve a product weight fraction greater than 0.99. With the number of enrichers (*NE*) set equal to 25 and the number of strippers (*NS*) set equal to zero, the code varied the key weight through the spectrum of available values. The key weight was held fixed for each cascade calculation. Figure 6 shows the results with the product weight fraction, the RTF, and a relative product flow (the product flow normalized to fit on the same figure) plotted with respect to the key weight values. Figure 6 suggests that as the key weight approaches the isotopic mass

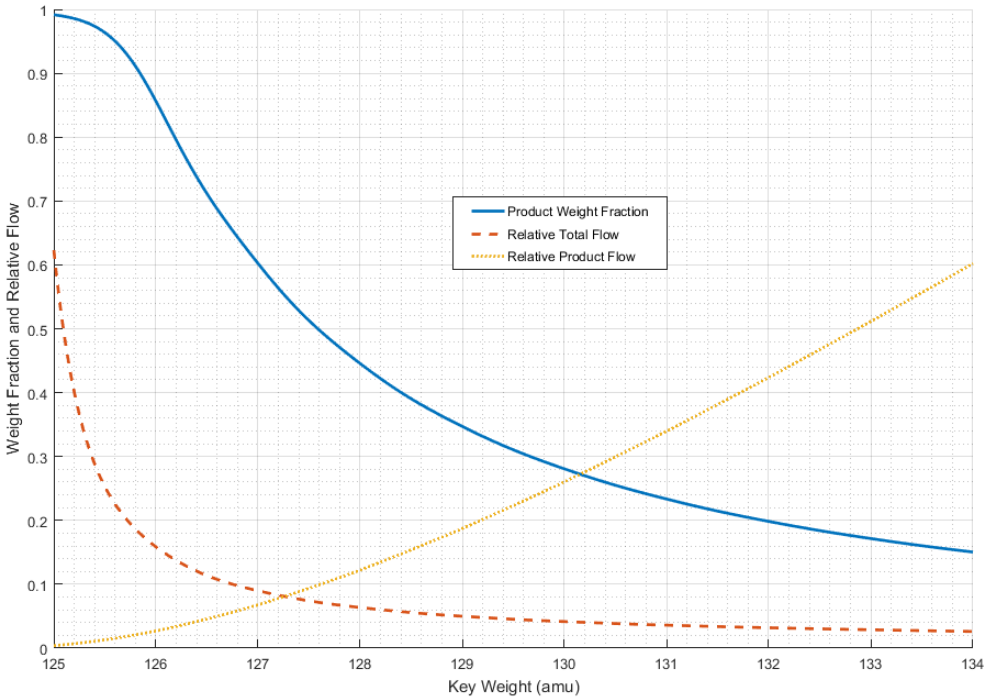

Figure 6. End component weight fraction in a cascade with a fixed number of stages versus continuous key weights. The figure shows that as the key weight approaches the isotopic mass of the end component, the product weight fraction continues to improve. Although other factors must be considered in the interpretation, the results suggest that key weights continuously approaching the molecular weight of the target component may be a valid tool for optimization.

of the end component, the product weight fraction continues to improve. Care must be taken to interpret this result. Although the key weight approaches the mass of the end component, the highest product weight fraction does not equate to an optimization. The criteria chosen for optimization, minimizing the RTF, cannot be interpreted from
Figure 6. The RTF is at a maximum value at the highest product weight fraction. The RTF decreases rather sharply with a smooth hyperbolic shape asymptotically approaching a low value. However, the product weight fraction also decreases rapidly, while the product flow increases. The one discernable inflection point occurs in the product weight fraction near the key weight value of 126 amu. This suggests a possible range of an optimum key weight value ranging from 125.0-126.0 amu. Although inconclusive, this range is consistent with the discrete value predicted by de la Garza et al. [27]. Additional consideration must be given to the quantity of product.

In order to gain better insight into the minimum RTF, the artificial constraint on the number of stages was removed. By setting a condition on the product weight fraction, the code was reconfigured to find both the optimum key weight and the number of stages needed to meet the conditional product weight fraction. Figures 7 and 8 show the results for two representative cases. For each of these cases, the product weight fraction condition was set to 0.30 and a separation factor equal to 1.3. In Figure 7, *NS* is set to zero. The scope of the figure makes it difficult to see exactly what is happening, but it is clear that when *NE* is equal to three, the optimum key weight corresponds to 127.6 amu. When *NE* is set to four, the next discrete value that is allowed in the MARC model, a discontinuity occurs in the plot. As more stages are added, similar discontinuities occur. There is one value of *NE* that results in a minimum RTF, and therefore, an optimum key weight for that particular cascade configuration. This is a characteristic of the MARC model, which imposes some difficulty in analysis. Figure 8 provides a better illustration of the effect. This case is the same as in Figure 7, except now *NS* is set to equal three. *NE* ranges from a minimum of two to a maximum of six for the range of key weights shown. For *NE* equal to two, the optimum key weight has a value of 125.9 amu.
For each increasing value of *NE*, there is a corresponding optimum key weight. However, as *NE* increases, the corresponding RTFs also increase. Therefore, the one optimum value of key

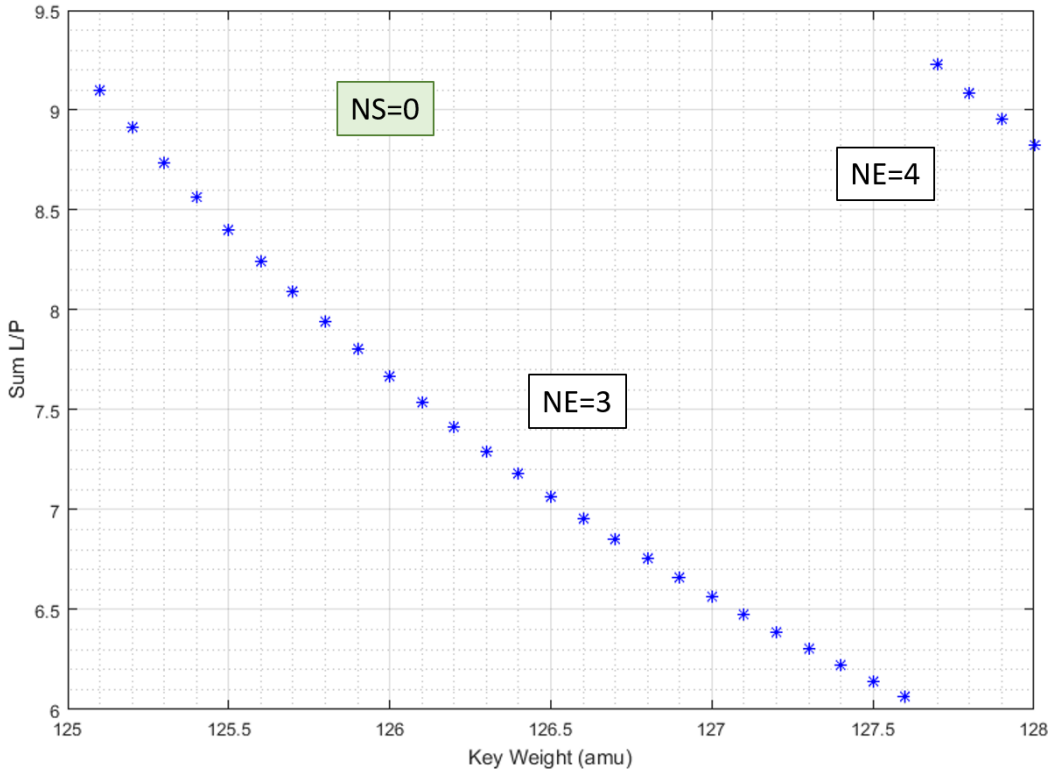

Figure 7. End component optimization case for x_P = 0 .3, α = 1.3, and *NS* = 0. When *NE* is equal to three, the optimum key weight corresponds to 127.6 amu. When *NE* is set to four, the next discrete value that is allowed in the MARC model, a discontinuity occurs in the plot.

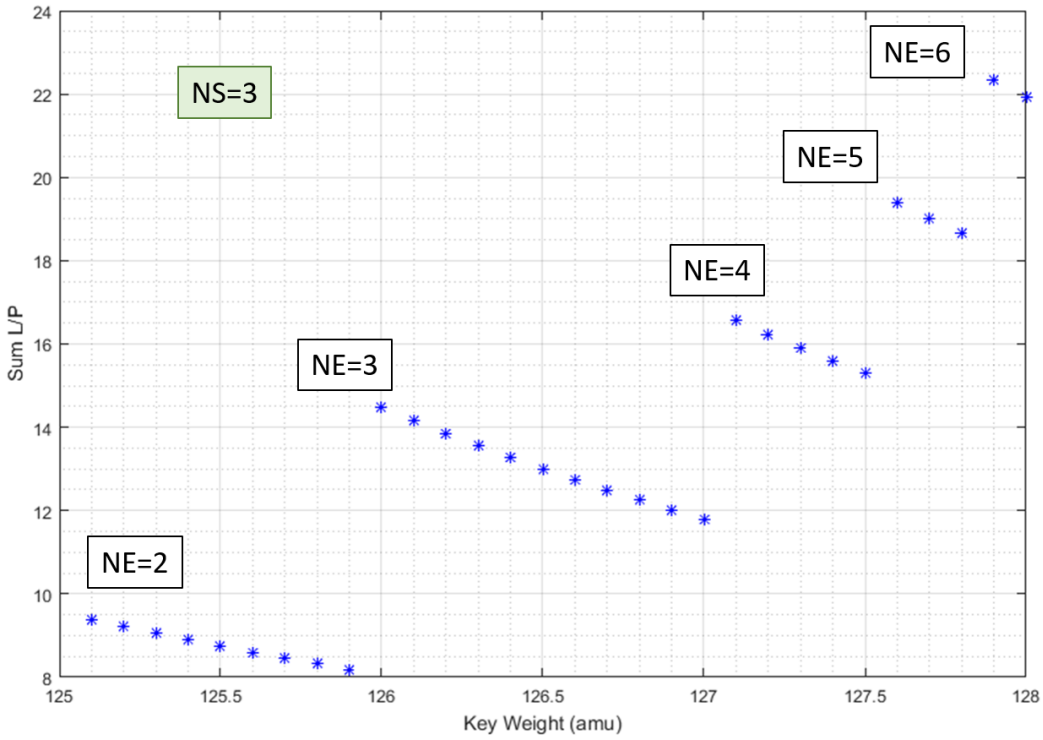

Figure 8. End component optimization case for x_P = 0.3, α = 1.3, and *NS* = 3. *NE* ranges from a minimum of two to a maximum of six for the range of key weights shown. For *NE* equal to two, the optimum key weight has a value of 125.9 amu. For each increasing value *NE*, there is a corresponding local optimum key weight. However, as *NE* increases, the corresponding RTFs also increase. Therefore, the one optimum value of key weight, in this case, corresponds to an *NE* equal to 2.

weight, in this case, corresponds to an *NE* equal to 2. The optimum values that correspond to each value of *NE*, when plotted separately together, form a smooth curve. This will be shown in the parametric calculations to follow. Song et al. previously showed the discontinuous nature of the MARC model compared to the smooth curve provided with the Q-cascade [55].

A series of parametric calculations were performed varying the conditional end-component weight fraction and the separation factor. The weight fractions ranged from the feed value of 0.10 to 0.90 in increments of 0.10. The separation factors ranged from 1.10 to 1.50 in increments of 0.10. In each case presented here, the targeted end component has a molecular weight equal to 125.0 amu. A sample of the results are provided in Figures 19-33 in Appendix B. One consistent finding from the calculations is that for a single cascade with constant key weight, adding stripper stages *always* increases the RTF. Therefore, the figures provided in Appendix B only consider the cases of *NS* equal to zero. The determination of whether to add stripper stages must be considered separately and is described further below.

The results in Appendix B show several interesting features. Only the smooth curve connecting the optimum key weights, indicated by the markers, for various *NE* is shown. (Note that the smooth curve is only a simple curve fit to the calculated optimum key weights to be used as a visual aid. The curves do not represent functions and should not be used for extrapolation purposes.) The smooth curves show that as the target product weight fraction increases, the optimum key weight (the curve minimum) generally approaches the molecular weight of the target end component isotope. The smooth curves are consistent with the findings presented by Borisevich et al. for the Q-cascade [39] and by Sulaberidze et al. for the MARC [14]. But unique to the MARC model, as separation factor increases, the number of markers corresponding to a discrete number of stages decreases. The result is that the minimum of the curve may not directly coincide with a discrete number of stages. Likewise, the optimum key weight may fluctuate as it corresponds to the integer number of stages. It is possible that two optimum key weights could exist as they fall upon the curve at the same RTF. These results complicate the goal of this paper to apply a method for optimization the key weight. Applying a catch-all rule to determine the optimum key weight based solely on the target weight fraction and separation

factor does not present a convenient function when considering the discrete nature of the number of stages. This effect will be a consistent recurrence in the results going forward.

In general, though, as the target weight fraction increases, the optimum key weight approaches the molecular weight of the target end component isotope. Figure 9 shows all the calculated optimum key weights with respect to target weight fractions for various separation factors. The plotted line in the figure shows the mean optimum key weight for all the separation factors plotted with respect to target weight fraction. From the figure, clearly, as target weight fraction increases, the optimum key weights converge as indicated by the smaller deviations from the mean. At the low target weight fraction of 0.20, the mean separation factor resides at approximately one-third the range of the isotopes (M=128.0 amu). The deviations in the individual optimum key weights at the low target weight fraction are quite large and are indicative of discrete nature of the MARC model and the large fluctuations imposed by the separation factors. At the target weight fraction of 0.30, the average optimum key weight shifts significantly to approximately one amu mass difference of the molecular weight of the target end component. The deviations in the individual optimum key weights are still quite large at the 0.30 target weight fraction. As the target weight fractions increase, the deviations continue to decrease. This convergence occurs due to a larger number of stages needed to reach the higher weight fractions. The large fluctuations imposed by the individual separation factors are averaged out over the relatively large number of stages. As the number of stages increases, the optimum key weight within the individual cascade also converges. The value for the convergence in a single cascade with constant key weight coincides to that predicted by de la Garza [27]. For an end component, de la Garza et al. showed the analytical optimum key weight approaches the mean of the end component and the next isotopic neighbor. This result and the theory from which it was derived, was applicable to a long cascade with a small separation factor. In this case, the mean of the molecular weights is 125.5 amu.

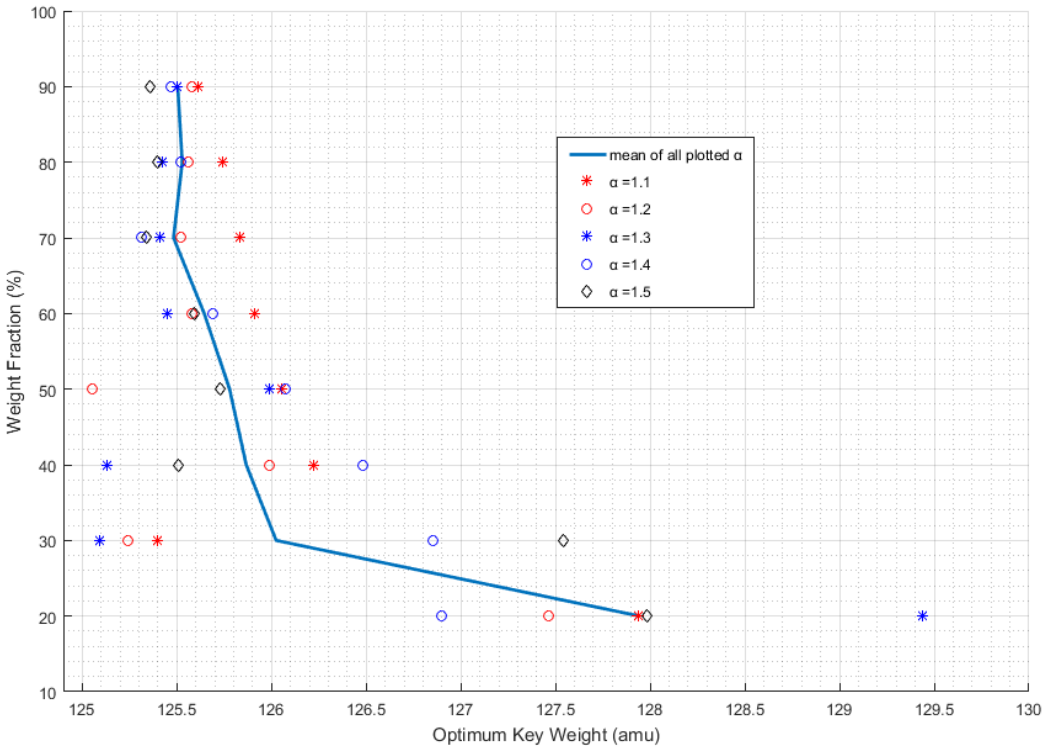

Figure 9. Optimum constant key weights for different separation factors and average optimum key weights versus single cascade target weight fractions. The plotted (blue) line in the figure shows the mean optimum key weight for all the separation factors plotted with respect to target weight fraction. From the figure, clearly, as target weight fraction increases, the optimum key weights converge as indicated by the smaller deviations from the mean.

However, the optimum key weight varies for a short cascade and is heavily influenced by the magnitude of the separation factor. The shapes of the smooth curves in Appendix B and the relationship of the optimum key weights to target weight fractions are consistent to those reported by Sulaberidze et al. [14] and Borisevich et al. [39]. The findings reported by Borisevich were for the Q-cascade and did not reflect the fluctuations due to the discrete nature of stage-wise enrichment. On the other hand, Sulaberidze reported findings for the MARC as not being optimal, likely referring to the discrete nature of the MARC. However, Sulaberidze states that the optimal key weight is not dependent upon the separation factor. Sulaberidze does not report the large dependence of the optimum key weight in the MARC on the separation factor.

The Number of Stages in a Single Cascade

The difficulty in the current analysis is largely complicated by the large number of both dependent and independent variables considered, some of which contribute to the discrete nature of the MARC model. The preliminary analysis seems to have eliminated a couple of variables from consideration based on the selected optimization criterion, at least in the case of the single cascade. The total number of stages is equal to the sum of enricher stages and stripper stages. However, the calculations have shown that adding stripper stages only increases the total internal cascade flows in all cases. Based on the method used here to determine the optimization by minimizing internal cascade flow, no strippers were considered to determine the methodology for finding the optimum key weight in a single cascade.

The determination of the number of stripper stages needed in a cascade is determined by the economic considerations of the feed material. Certainly, the number of stripper stages must be considered in a real cascade. However, the use of stripper stages mainly offsets the cost of the feed material. Preparing the feed material has some associated cost. The materials used in separations cascades must be chemically pure and non-reactive. Ensuring these characteristics can be quite expensive. Adding stripper stages serves to conserve feed material, but there is a

balance. The economic analysis for determining the number of stripper stages has been well established [44, 56]. In an effort to provide a comprehensive cascade analysis, the economic analysis is reviewed here. The total cost, *C*, of a cascade is determined by adding the cost due to separative work plus the cost due to feed [56], as shown by

$$C = C_U \Delta U + C_F F \tag{19}$$

where C_U is the cost per unit of separative work and C_F is the cost per unit of feed. The relationship for optimization is shown in Figure 10. Both the cost of the feed and the cost of separation contribute to the cost of the product. The optimum waste weight fraction is where the sum of the curves is minimized (i.e., the aforementioned balance). Once the target waste weight fraction is determined based on the economic model, the number of stripper stages will be determined by the MARC model and separation factor. After the desired number of stripper stages is found, then the cascade must be optimized. The number of stripper stages will ultimately affect the number of enricher stages required. Adding stripper stages will reduce the number of enriching stages required, but not one-for-one. The number of enricher stages conserved will depend on the overall length of the cascade prior to the stripper stages being added. Adding stripper stages in a single, constant key weight cascade will draw the optimum key weight toward the targeted end component molecular weight. As shown previously in Figures 7 and 8, adding three stripper stages eliminates the need for one of the enricher stages; and, causes the optimum key weight to shift closer to the end component molecular weight (M=125.0 amu), as would be expected in a longer cascade.

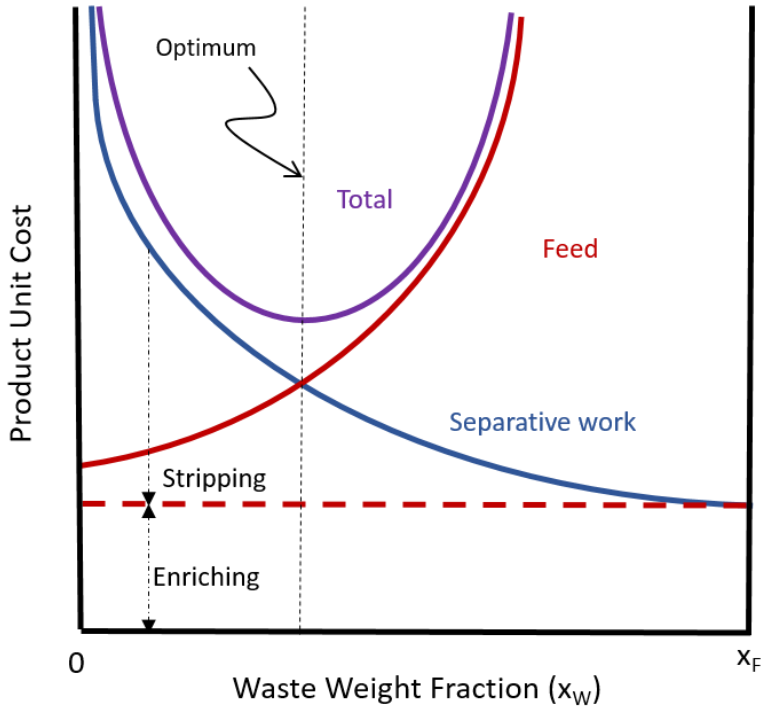

Figure 10. Determination of optimum waste weight fraction [56]. This notional figure shows that the cost of the feed and the cost of separation contribute to the cost of the product. The optimum waste weight fraction corresponds to where the sum of the curves is minimized.

Feed Parametric

The results shown in Figure 9 provide insight into how the optimum key weight varies with an evenly distributed feed. To better understand how the optimum key weight varies with the isotopic weight distribution of the feed, a series of feed parametric calculations were performed. Over 30 million calculations were performed to obtain roughly 9000 sets of optimized data for analysis. Figure 11 shows the results for one separation factor case ($\alpha = 1.3$). In the figure, the heat map shows warmer colors as the weighted cubic-mass difference[10] of the feed distribution increases away from the target component (the target component is not used in the calculation). As the feed distribution is more heavily weighted away from the target component, the optimum key weight increases as indicated by the yellow colors. Likewise, as the feed distribution is weighted toward the target component, the optimum key weight necessarily approaches the target component to allow separation to take place. In most of these cases, only a small amount of enrichment can occur as indicated by the deep blue colors.

Cascade of Cascades

As an alternative to separating an end component in a single long cascade, the idea of using several smaller cascades in series to achieve the desired product weight fraction is considered. The series of these cascades is referred to as a "cascade of cascades." Other terms are used to convey similar meanings, such as "tandem cascades." Batch-mode operation can also be treated as a cascade of cascades in which the cascade product is fed back into the same cascade. The concept of a cascade of cascades is a necessary engineering consideration for a real enrichment cascade. Enriching a highly-pure product in one cascade generally requires a relatively wide feed stage, and then gradually narrowing to the top of the cascade. The top

[10] The multicomponent feed distribution was represented as a scalar by taking the weighted cubic-mass difference. The mass difference of each isotope and the targeted end component was cubed and then weighted (multiplied) by that isotope's weight fraction. The sum of these values for each isotope were used to characterize the feed distribution as a scalar for a simplified data analysis.

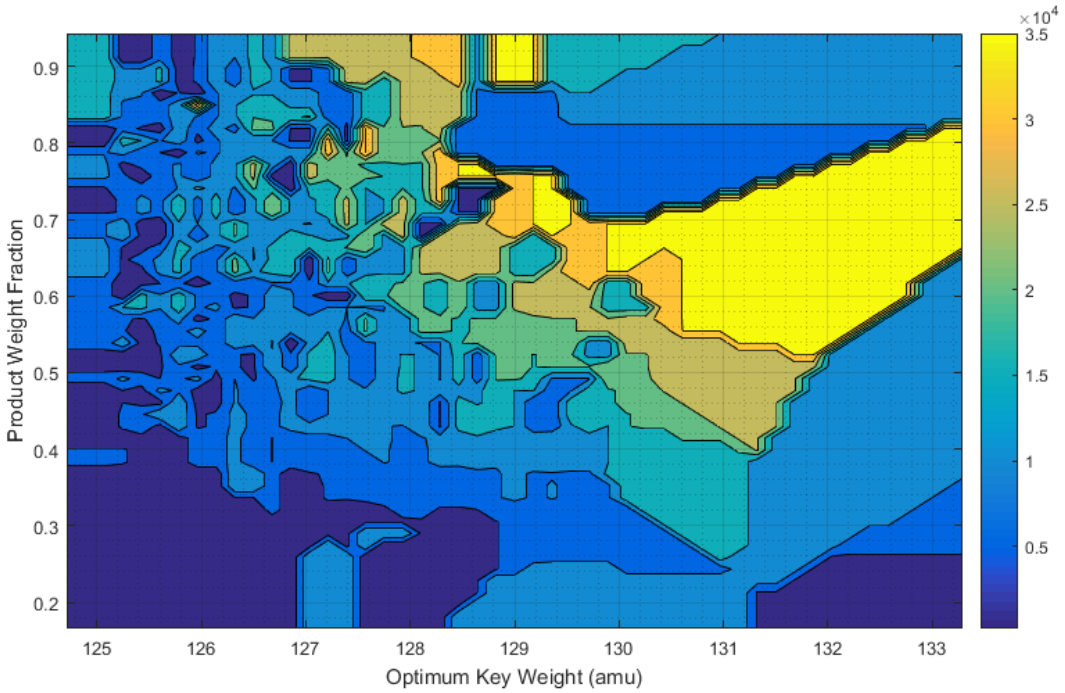

Figure 11. Optimum key weight versus product weight fraction and feed distribution for the α = 1.3 case. The figure shows how the optimum key weight is not only a function of product weight fraction, but also a function of the initial feed distribution. The heat map shows the feed distribution as a weighted function of the cubic-mass difference of the remaining components as compared to the target component. The higher the weighting of the feed distribution away from the target component, the warmer the colors on the heat map as indicated by the color scale (the dots depict actual data points). Predicting the optimum key weight is still complicated by the discrete nature of the MARC; however, the heat map indicates the importance of the initial feed distribution.

enricher stage is quite narrow and may consist of only a few separators. From an engineering standpoint, a failure of a single separator in the top enricher stage could be detrimental to the functioning of the entire cascade. Because of this, cascades are frequently designed to operate as a cascade of cascades or in batch operation.

Cascade of Cascades without Recycle

Figure 12 illustrates an example cascade of cascades without recycle. The product stream (or waste stream in the case of a heavy end component) from one cascade is directed to the feed of the next cascade. This is repeated until the desired product weight fraction is achieved in the top (or bottom for heavy end component) cascade. The waste streams (or product streams for heavy end components) are rejected. They may be used as feed in the cascades later, used in their current isotopic state for alternative product, or disposed of as process waste. Nevertheless, rejected streams are not considered in the optimization calculation.

In order to perform these calculations, individual cascade calculations were optimized for arbitrary target end-component weight fractions. The product was then used as the feed for the next cascade optimization. The process was completed until the final, target end-component weight fraction was achieved.

Figures 34-38 show the results of optimization calculations for cascade-of-cascades configurations with no recycle. These results are for a target, end-component weight fraction equal to 0.90. The individual cascades target end component was arbitrarily chosen to be in approximately 0.10 increments. (This methodology could be changed to ensure each of the cascades dimensions are the same length.) The methodology chosen here resulted in eight cascades needed to achieve the 0.90 weight fraction. The notable exception is in Figure 34 where the separation factor is equal to 1.1. In this case, the cascade configuration was unable to achieve the targeted 0.90 product weight fraction, and a targeted weight fraction of 0.70 was substituted for illustration.

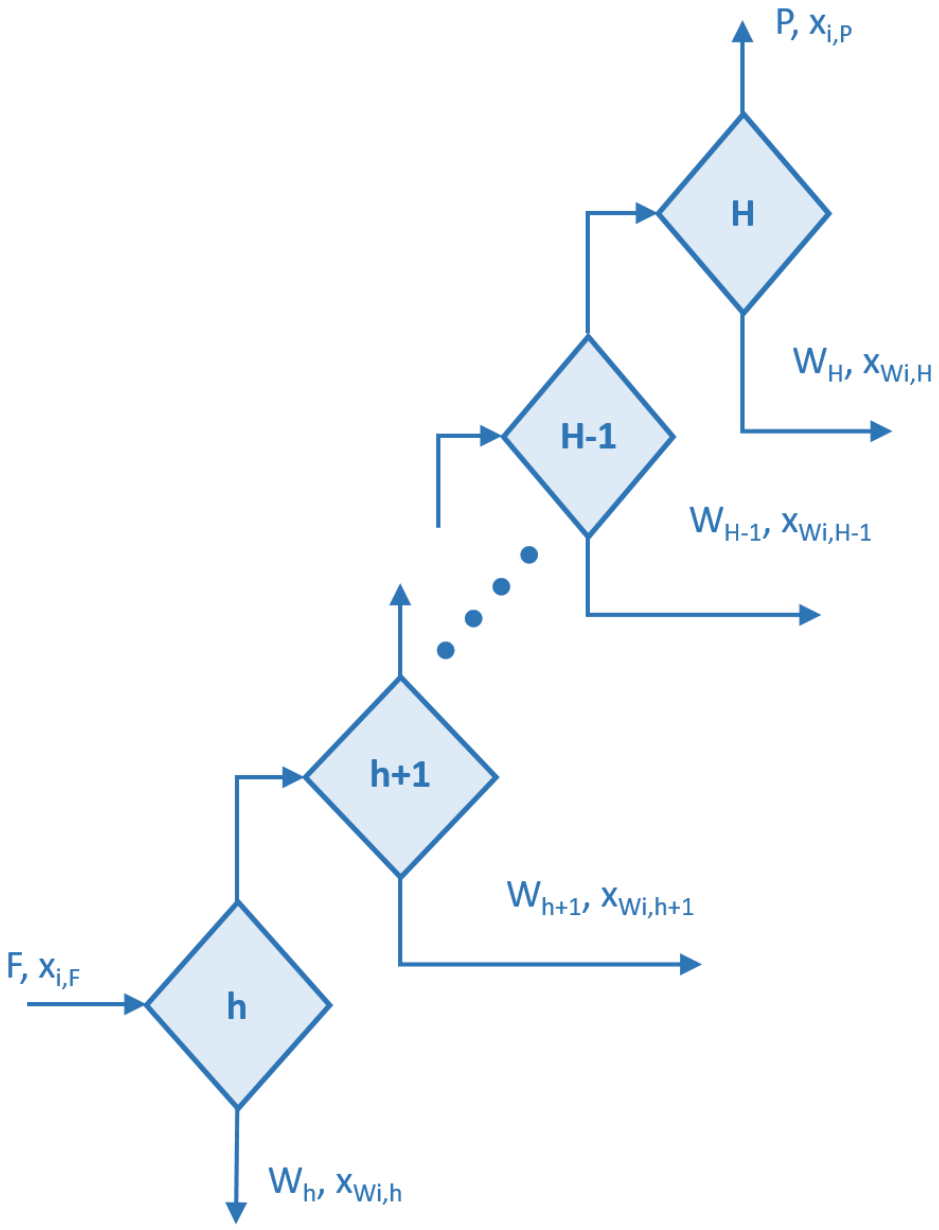

Figure 12. Cascade of cascades without waste recycle. The product stream from one cascade is directed to the feed of the next cascade. This is repeated until the desired product weight fraction is achieved in the top cascade. The waste streams are rejected.

The optimum key weight for the first cascade is the same result found as in the single cascade case with the low target weight fraction of 0.20. The mean separation factor resides at approximately one-third the range of the isotopes (M=128.0 amu). The remainder of the optimum key weights converge to the approximate weight fraction of the target isotope (M=125.0 amu) as the cascade product weight fraction increases. For reference, a linear fit has been provided in the figures. As can be seen from the linear fit, the optimum key weights generally increase linearly as the cascade product weight fraction increases. The deviations are a result of the discrete nature of the MARC (i.e., the number of stages must be an integer). The optimum key weights tend to fluctuate, back and forth, across the linear fit. In general, the deviations from the linear fit tend to increase as the separation factor increases. This does not appear to be the case in Figure 36, where the separation factor is equal to 1.3. In this case, the arbitrary values of the individual cascade target product weight fractions just happened to coincide with optimum key weight values for this separation factor.

Cascade of Cascades with Recycle

Figure 13 illustrates an example cascade of cascades with recycle. Recycle implies the waste stream (or product stream in the case of a light end component) from the cascade is redirected back to the feed in the next lower cascade (higher cascade). The product stream (or waste stream in the case of a heavy end component) from one cascade is still directed to the feed of the next cascade, as before. The only rejected waste stream is the waste (or product for heavy end components) of the bottom (top) cascade. The result is a conservation of feed material. This conservation might imply a reduced efficiency compared to the no-recycle case, analogous to the application of stripper stages in the single cascade case. However, this result was unfounded in the calculations as will be discussed later.

In these calculations, the cascade optimizations were performed iteratively. The waste stream from a higher cascade was combined with the feed of the lower cascade, and then the cascade was re-optimized. This calculation was performed throughout the cascade, then iterated

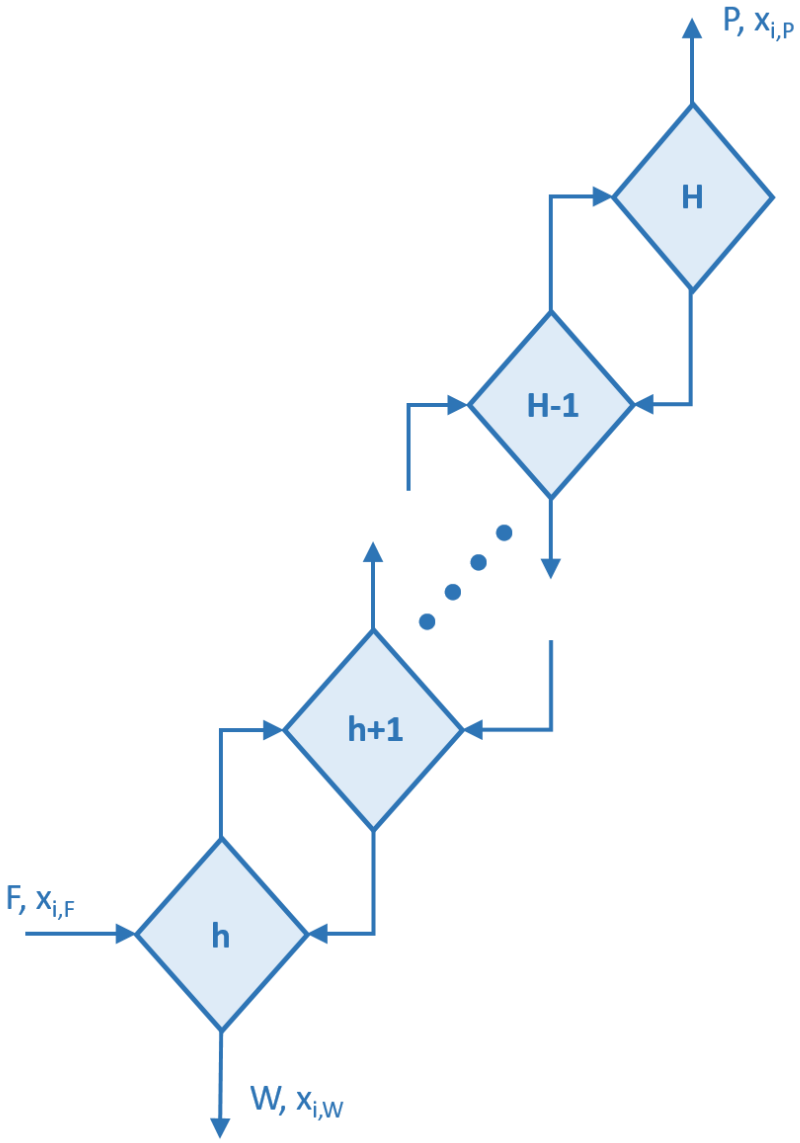

Figure 13. Cascade of cascades with waste recycle. Recycle implies the waste stream from the cascade is redirected back to the feed in the next lower cascade for a light end component. The product stream from one cascade is directed to the feed of the next higher cascade. The only rejected waste stream is from the bottom cascade.

until the convergence criterion was met. A mass balance was used as the convergence criterion. After the waste streams are combined with the previous cascades feed streams, the calculations were performed again until the mass of the cascade feed stream remained unchanged. Each cascade ultimately settled on an optimum key weight. Because of the number of independent variables available, the parametric calculations were performed in a number of logical methods to understand the impact of the various constraints.

First, an arbitrary number of cascades were chosen. The program chose the number of enricher stages needed for each cascade based on the simple average of the target product weight fraction. For instance, if six cascades were used and the target product weight fraction was chosen to be 0.70, each cascade target weight fraction was in increments of 0.1. Although this basis for splitting the cascades showed a consistent minimum amount of separative work in preliminary calculations, compared to varying the cascade target product weight fractions, the results required cascades of differing lengths. Differing cascade lengths would be consistent with the methodology chosen for the cascade of cascades without recycle. The results were also consistent with the previous results showing a linear relationship of the optimum key weight versus the cascade target weight fraction like those presented in Appendix C. The results did show opportunities for future optimization. For instance, the RTF routinely showed improvements over the other cascade of cascade methods chosen. The implication is that the recycle mode may be used as a necessity for conservation of feed material but does not have a directly negative correlation to cascade efficiency. Using recycle in general improves the cascade efficiency over the no-recycle case. No cases were found that were more efficient than the single cascade with optimum key weight. However, some cases approached the efficiency of the single optimized cascade. This result suggests that, in operations requiring a cascade of cascades, an optimized solution can be found with minimal detriment to the optimized single cascade. The next method used for analysis required the cascades within the cascade of cascades to be the same dimensions (i.e., the same number of enricher and stripper stages). This method was thought to be less arbitrary than the equivalent change in weight fraction method discussed above. The cascades analyzed here were comprised of only enricher stages to be consistent with previous calculation methods.

Figures 39-43 in Appendix D show some of the results of these calculations for various separation factors. The results presented are the optimum results for the minimum total number of enricher stages. A number of enrichers was chosen as the input to the code, the code then calculates the number of required cascades to achieve then target product weight fraction. After the number of cascades was chosen, the code then optimizes the key weight for each cascade. The calculations iterate until convergence using the same mass balance convergence criterion discussed previously.

Figures 39-43 show several interesting features. Most notably, the curves fitted to the data are quadratics. Although these are still simple curve fits, the fits are quite good. There is very little deviation of any of the points for any of the separation factors chosen. The minimum of the quadratic corresponds quite nicely with the optimum key weight for the first cascade. Although there is some variance, the optimum key weight for the first cascade is very near the minimum of the quadratic fit. Next, the range of the optimum key weights is quite similar. The optimum key weight for the first cascade falls into the narrow range of 129.4-130.0 amu in every case. This is noteworthy because the mean and median optimum key weight for the single optimized cascade case was less than 128.0 amu. This illustrates the effect of the recycle configuration to pull the optimum key weight away from the molecular weight of the targeted end component. This is nearly opposite of the effect of adding stripper stages. Although this might be a bit confusing at first inspection because of the similarity in conserving feed, the fact of having multiple cascades with different optimum key weights must be considered. The increased optimum key weight in the bottom cascade is an effect of having multiple cascades. The increased optimum key weight is even more interesting compared to previous results when considering the product weight fraction of the first cascade is significantly greater than 0.20 for every separation factor considered, approaching 0.30 in most cases. This is interesting because of the tendency of the optimum key weight to approach the molecular weight of the targeted end component at higher end component weight fractions. Once again, the effect of multiple cascades must be considered.

The effect of multiple cascades can also be seen in the optimum key weight of the top cascade. Those key weights for the methods and separation factors considered never fell below the 125.9 amu. So, the optimum key weight for the top cascade was also drawn away for the molecular weight of the targeted end component. This effect can be viewed in a practical manner. The waste streams of the cascades are concentrated in the undesirable (heavy, in this case) components, and this material in being mixed in with the feed. The net effect is pulling the optimum key weight away. In other words, the net feed has a skewed weight distribution toward the heavy end. This effect is significant for two reasons.

Firstly, this configuration allows significant mixing to occur, so this configuration is likely not optimum. This is especially true in that we are considering cases with no stripper stages. The matched abundances directed back into the feed stage are significantly different, because in most cases the waste stream skips over multiple enricher stages in the previous cascade to be directed into the feed. Secondly, this configuration is less efficient than the single cascade probably because this skewed waste stream must be processed through the entire previous cascade again, effectively acting like a stripper section. An opportunity for improving efficiency in the cascade of cascades with recycle configuration may be leveraged by adding stripper stages to the upper cascades to reduce mixing losses.

Table 2 compares some select results of the parametric study comparing the single optimized cascade with the two cascade-of-cascades configurations. In every case, the single optimized cascade is more efficient by the definition chosen here. For the lower separation factors, the cascade of cascades with recycle case is more efficient than the case with no recycle. However, for higher separations factors, the no recycle case is more efficient than the recycle case. It is unclear if this effect occurs because of the constraint on equal dimensional cascades in the recycle case. This constraint must be considered as a factor, because it is apparent when examining the difference in the product weight fractions, x_P. The target weight fractions were all set to the same conditional requirement in the computer code. They were set to 0.40, 0.70, and 0.90 for each separation factor. The actual achieved weight fractions are shown in Table 2. The weight fractions achieved are close, but always exceed the target by a little bit (with one distinct

Table 2. Comparison of Cascade Performance by Configuration. The table includes data for optimized single cascade, cascade of cascades with recycle, and cascade of cascades with no recycle for various separation factors and target product weight fractions. The cascade of cascades with no recycle uses arbitrary, individual cascade target product weight fractions. The cascade of cascades with recycle case uses cascades with equal lengths and was optimized to minimize the total number of enrichers. The single cascade with optimized key weight is more efficient than either of the cascade of cascades cases. The cascade of cascades with recycle has significant improvements in efficiency over the no-recycle case for long cascade cases.

α_o, Target X_P	Single cascade	C-of-C (recycle)	C-of-C (no recycle)	Single cascade	C-of-C (recycle)	C-of-C (no recycle)	Single cascade	C-of-C (recycle)	C-of-C (no recycle)	Single cascade	C-of-C (recycle)	C-of-C (no recycle)
	ΣL/P			P (g)			X_P			NE		
1.1, 0.90	1130.1	1.26E+05	N/A	6.59	0.09	N/A	0.9006	0.9082	N/A	51	84	N/A
1.1, 0.70	409.3	1.38E+04	7.04E+04	12.31	0.41	0.03	0.7006	0.7026	0.7007	26	40	27
1.1, 0.40	75.6	353.5	256.2	38.01	10.98	8.34	0.4001	0.4036	0.4001	10	16	12
1.2, 0.90	305.5	1.78E+04	7.07E+04	11.83	0.38	0.02	0.9002	0.9030	0.9000	26	48	27
1.2, 0.70	110.8	990.8	1765.7	18.23	6.24	0.64	0.7005	0.7102	0.7012	12	28	15
1.2, 0.40	20.5	65.0	40.1	62.35	69.51	26.88	0.4004	0.4150	0.4002	5	12	6
1.3, 0.90	146.3	3227.5	1.17E+04	15.07	2.35	0.15	0.9005	0.9090	0.9002	17	40	21
1.3, 0.70	52.4	396.3	447.8	23.47	16.65	3.86	0.7007	0.7046	0.7016	8	24	12
1.3, 0.40	9.0	37.3	22.1	65.71	113.99	72.28	0.4001	0.4004	0.4006	3	10	6
1.4, 0.90	88.6	1438.1	1617.1	18.22	6.46	0.42	0.9011	0.9275	0.9018	13	40	16
1.4, 0.70	31.0	247.2	112.1	27.29	30.23	5.98	0.7005	0.7244	0.7005	6	24	9
1.4, 0.40	6.7	31.6	8.6	113.50	141.19	61.68	0.4002	0.4036	0.4005	3	10	3
1.5, 0.90	60.5	959.2	751.7	18.87	9.57	1.08	0.9006	0.9121	0.9000	10	35	14
1.5, 0.70	20.9	195.0	71.1	32.67	41.91	11.17	0.7005	0.7206	0.7002	5	24	8
1.5, 0.40	3.7	28.1	7.0	101.02	168.72	93.94	0.4001	0.3948	0.4017	2	10	3

exception[11]). This excess in target weight fraction is caused by the discrete nature of the MARC and can be even more pronounced in the cascade-of-cascades calculations.

In Table 2, the comparison of the cascade of cascades appears to be significantly less efficient than the single optimized cascade case. As previously discussed, the limitations imposed for an equitable comparison may unnecessarily restrict the possibilities for the cascade-of-cascades configuration. Furthermore, it is important to understand how this algorithm works. The algorithm first optimizes each individual cascade within the cascade of cascades. This approach assumes that the results of the single optimized cascade, as shown in Figure 9, are valid for the individual cascade's product weight fractions. Once the individual cascades are optimized, the waste streams of the upper cascades are added to the feed streams of the lower cascades, and then the process is repeated. The iterations continue until the mass balance criterion is met. The effect is that the optimum key weights of the individual cascades converge for an optimized cascade solution.

An additional algorithm was developed in order to better accommodate the cascade of cascades configuration. This new algorithm removed the imposed limitations of equal length cascades. The new algorithm allows for defining the length of each individual cascade. This allows for minimizing mixing during recycle by better matching the abundance ratios from higher level cascade waste streams. In other words, the number of stripper stages of the next higher cascade can be chosen to match the number of enrichers in a cascade. Mixing will still occur because of the varying key weights between cascades, but the mixing can be minimized to improve performance. Because of the difficulty achieving convergence in the new algorithm, an alternative approach was used for optimizing the cascade. Instead of optimizing the individual

[11] The product weight fraction data point for the cascade-of-cascades case with recycle and a separation factor equal to 1.5 equals 0.3948. In this case, the input parameters were manually changed to exceed a target weight fraction of 0.39 versus 0.40. Because of the discrete nature of the MARC, the product weight fraction exceeded the target weight fraction of 0.40 substantially. The reduced target weight fraction was chosen to provide a more equitable comparison.

cascades first, a calculation for all available permutations of the available key weights to the 0.1 amu were used to optimize the entire cascade of cascades. The number of cascades were manually selected. Likewise, a manual parametric was performed for the number of cascades (*H*), the number of enrichers, and the number of strippers for each cascade. Because the process was quite laborious and the calculations consumed large amounts of processing time, only a relatively few cases were run. For cascades composed of three cascades, the calculations took approximately 25 seconds for each manually chosen set of inputs.[12] For cascades composed of four cascades, the calculations took over two hours, because the number of computer calculations increases exponentially with the number of cascades. Likewise, the number of manual permutations for the required inputs increases exponentially with the number of cascades. Some select results were chosen based on their favorable comparison to the single optimized cascade results and are shown on Table 3.

The results in Table 3 show that in most cases, an optimized cascade of cascades approaches the performance of the single optimized cascade. In a few cases, an optimized cascade of cascades improves the performance of the single optimized cascade. This result shows that MARC performance can be improved by varying the key weight. In those cases, the improvement is modest with less than a 10-percent improvement in efficiency. However, the results do show that the key weight should be varied to optimize a cascade of cascades. In general, the improvement seems to be better for larger separation factors and lower target enrichments. These are the cases that best simulate a single optimized cascade by limiting the number of stripper stages in the higher cascades. Because the tests were limited to cases with 2, 3, and 4 cascades, longer cascades were difficult to split into lengths that approximated a single optimized cascade. The need to match the number of stripper stages in the next cascade to the number of enrichers and the discrete nature of the MARC generally resulted in a large number of stages and greater internal flows. Also, reducing the number of stripper stages increased mixing losses resulting in a loss of efficiency.

[12] The calculations were performed on a desktop computer with a 64-bit operating system and an Intel® Core i5™-4590 processor. The calculations are well-suited for parallel processing for future work.

Table 3. Comparison of Optimized Cascade-of-Cascades Results to the Single Optimized Cascade. The table compares a selection of the optimized cascade-of-cascades results with the previously shown optimized single cascade results. In many cases, the results are comparable. In a few cases, varying the key weight by cascade improves performance over the single cascade case.

α_o, Target X_P	Single cascade	C-of-C (recycle)	Single cascade	C-of-C (recycle)	Single cascade	C-of-C (recycle)	Single cascade	C-of-C (recycle)	Single cascade	C-of-C (recycle)		
	ΣL/P		P (g)		X_P		X_W		NE		NS	H
1.1, 0.40	75.6	74.4	38.00	31.90	0.4001	0.3846	0.0881	0.0867	10	10	7	3
1.2, 0.40	20.5	20.9	62.35	51.13	0.4004	0.4091	0.0800	0.0806	5	5	3	2
1.3, 0.70	52.4	52.2	23.47	25.00	0.7007	0.6918	0.0656	0.0813	8	10	6	3
1.3, 0.40	9.0	9.8	65.71	76.80	0.4001	0.387	0.0789	0.0734	3	4	3	3
1.4, 0.90	88.6	88.8	18.22	15.66	0.9011	0.8906	0.0864	0.0827	13	14	10	3
1.4, 0.90	88.6	88.7	18.22	17.43	0.9011	0.9016	0.0864	0.0846	13	14	6	2
1.4, 0.70	31.0	32.7	27.29	28.94	0.7005	0.7005	0.0832	0.0775	6	8	6	3
1.4, 0.45	8.2	6.8	69.34	69.87	0.4585	0.4593	0.0733	0.0588	3	4	3	4
1.4, 0.45	7.9	6.8	74.80	69.87	0.4503	0.4593	0.0597	0.0588	3	4	3	4
1.4, 0.40	6.7	5.7	113.50	102.60	0.4002	0.3840	0.0616	0.0597	3	3	2	3
1.5, 0.90	60.5	60.2	18.87	18.35	0.9006	0.9012	0.0848	0.0820	10	11	5	2
1.5, 0.70	20.9	20.5	32.67	30.29	0.7005	0.7018	0.0797	0.0769	5	5	3	2
1.5, 0.70	20.9	20.7	32.67	34.09	0.7005	0.6875	0.0797	0.0701	5	6	4	3
1.5, 0.40	3.7	3.9	101.02	97.28	0.4001	0.4049	0.0663	0.0570	2	2	1	2

In the cases of low target enrichment, each cascade could be reduced in length effectively allowing a continuous change in the key weight. The total number of stages approximates those in a single optimized cascade thereby reducing the internal flow. This result might indicate the possibility of continuously varying the key weight across a long cascade as proposed by Zhang et al. [15]. However, to test this hypothesis, the cascade-of-cascades calculation would need to analyze many cascades each with the number of enrichers approaching one. Further analysis of the cascade-of-cascades' results below may indicate that continuously varying the key weight may not be an option.

In all the optimization cases found approximating or improving on the corresponding single optimized cascade, the key weight averaged across all cascades was less than 127.0 amu, which is less than a 2.0 amu mass difference from the target isotope. For approximately half of these results, the average key weight was 125.5 +/- 0.2, and these cases had a target weight fraction equal to or greater than 0.70. These results are consistent with the findings of de la Garza [27] showing that for a long cascade the optimum key weight would be 125.5 amu. As the target weight fractions decreased, the range of the cascade key weights increased. This result is comparable to the results found in the single optimized cascade results. In nearly every case, the optimum key weight for the lowest cascade was 125.1 amu, the lowest value allowed in the calculations. In the few cases where this value deviated, the value never reached the 125.5 amu and never exceeded the mean value of its particular case. The key weight of the lowest cascade was always the lowest value obtained for its particular case. This is the *opposite* result obtained from the previous cascade-of-cascades methodology.

Figure 14 shows exemplars of the relationship of optimum key weight versus cascade product weight fraction for two cascades composed of four individual cascades each. The results are conclusive in that a cascade-of-cascades must be optimized holistically for the final targeted product weight fraction and not by individual cascade. The optimum key weight for the lowest cascade tended to rise if only two cascades were being analyzed. This was especially true for higher targeted product concentrations. For higher targeted product concentrations, the range of key weights narrowed in general and approached the average of

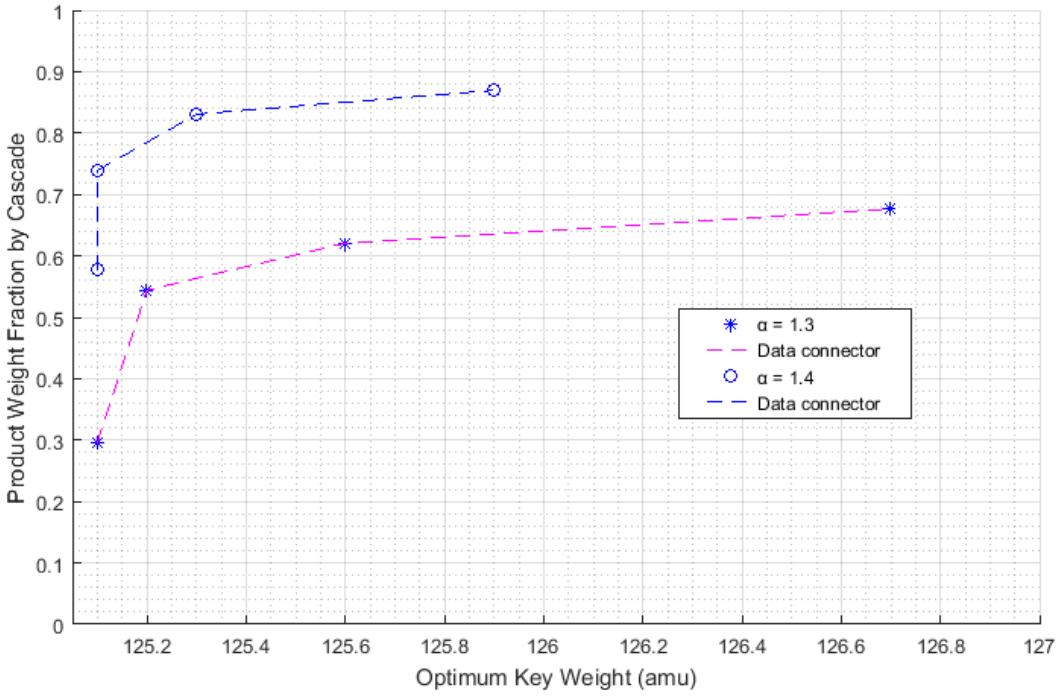

Figure 14. Optimum key weight versus product weight fraction by cascade in an optimized cascade of cascades with recycle. Two examples are shown; one for α = 1.3 and the other for α = 1.4. These cases were chosen as exemplars because they are optimized cascades that approximate or exceed the performance of a single optimized cascade. Also, these examples consist of cascades of four individual cascades showing the range of key weights. By having four data points each, the relationship in the change of the optimum key weight by cascade can be better observed.

125.5 amu. To meet this requirement, the key weight of the lowest cascade must necessarily rise when only two cascades are considered. The narrowing of the range of key weights for increased product weight fraction can be seen in Figure 14. The key weight of the second cascade varied depending on its relationship to the highest cascade. When more than three cascades were analyzed, the optimum key weight for the second cascade was either 125.1 or 125.2 amu. This effect can also be seen in Figure 14. When the second cascade was the highest cascade and the targeted product concentration was greater than or equal to 0.70, the optimum key was 125.5 +/- 0.2 amu. This explains the narrow range of key weights for the high targeted weight fraction cases. In the thirty optimization cases found, the optimized key weight of the second cascade exceeds 126.0 amu only three times, and exceeds 127.0 amu only once. For two of the cases exceeding 126.0 amu, the targeted product weight fraction was low (i.e., less than 0.50). These results are consistent with the findings for the single optimized cascade described earlier, where the key weights broadened at lower target weight fractions.

Finally, for the third cascade and higher, the maximum optimum key weight achieved was 128.8 amu, or a mass difference of 3.8 amu from the targeted isotope. For the cascades analyzed, when the targeted weight fraction was 0.85 or higher, the maximum optimum key weight achieved was 126.4 amu, or a mass difference of 1.4 amu. This confirms the narrow range of the optimum key weights for high targeted weight fractions. For the thirty cases analyzed, 75-percent of the optimum key weights in the third and higher cascades were less than 127.0 amu.

The Case for a Middle Component

As mentioned previously, the middle component case will build on the results of the end component. The middle component necessarily requires two cascades operated in a batch-wise process. The first cascade will be optimized to isolate the optimum amount of the end component into either the light product stream or the heavy waste stream. The next cascade will then feed the desired output of the first cascade, whether the product stream or the waste stream, and isolate the desired isotope. Because the practical considerations for the middle

component are broad in a real separations cascade, the analysis here will be necessarily limited. For example, in a real cascade to separate stable isotopes, the order of operations may be driven by other components, either as desirable and undesirable isotopes. If an isotope is particularly undesirable by an activated by-product perspective, the order of operations may be chosen specifically to avoid that isotope with less of a consideration for efficiency. Additionally, some elements may have multiple desirable isotopes. In these cases, multiple production streams may be considered, which changes the calculation of RTF with respect to product quantity. These considerations will be ignored here, and only the target isotope will be considered in the calculations.

Another factor complicating analysis of a middle component is the targeted weight fraction in the first cascade. The ability to reach high product weight fractions for a middle component is limited. In our fictitious material examined here, each of the components have equal initial feed weight fraction as before. The ability to obtain a high weight fraction is directly related to the sequential order of the targeted isotope and its relative distance from the end component. Because the analysis for final product weight fraction must consider the individual isotopes sequential order, too many permutations exist to adequately analyze all cases here. Therefore, the analysis here will be limited to the selection of the optimum key weight for the individual middle components in the first cascade only. The subsequent separation will be treated as an end component as has already been discussed.

For fictitious material of ten components, there are eight middle components. Four of those are heavy and four are light. Calculations have been performed for the heavy and the light components separately to confirm that their behavior is identical and is only affected by the individual component's relative distance from the end component. Only the results of the light component will be presented here for brevity, so only four middle components will be considered of our ten-component feed material. The components will be named the "second," "third," "fourth," and "fifth" components equating to their individual sequence from the light end component.

Second Component

For the second component (M=126), the optimum key weights range from 127.1 amu to 127.6 amu depending on the separation factor. The range of key weights versus the RTF are shown in Figure 15. The results are consistent with the results previously described in the end component calculations. Because the end component is being concentrated as well, the achievable weight fraction for the second component is quite restricted. For the number of enricher stages considered with no stripper stages, the achievable weight fraction for the second component ranges from 0.33 to 0.36. Not surprisingly, higher separation factors were able to achieve higher weight fractions. Because only relatively low weight fractions were achieved, the optimum key weights never fully approached the mass of the targeted component.

Third Component

For the third component (M=127), the optimum key weights range from 128.9 amu to 129.3 amu depending on the separation factor. The range of key weights versus the RTF are shown in Figure 16. The results are consistent with the results previously described. Because the end and second components are being concentrated as well, the achievable weight fraction for the third component is further restricted. For the number of enricher stages considered with no stripper stages, the achievable weight fraction for the third component ranges from 0.20 to 0.23. Again, higher separations factors were able to achieve higher weight fractions. Because only relatively low weight fractions were achieved, the optimum key weights never fully approached the mass of the targeted component. As the separation factors increased, the optimum key weights became smaller for the targeted light component.

Fourth Component

For the fourth component (M=128), the optimum key weights range from 130.2 amu to 131.1 amu depending on the separation factor. The range of key weights versus the RTF are shown in Figure 17. The results are consistent with the results previously described. Because

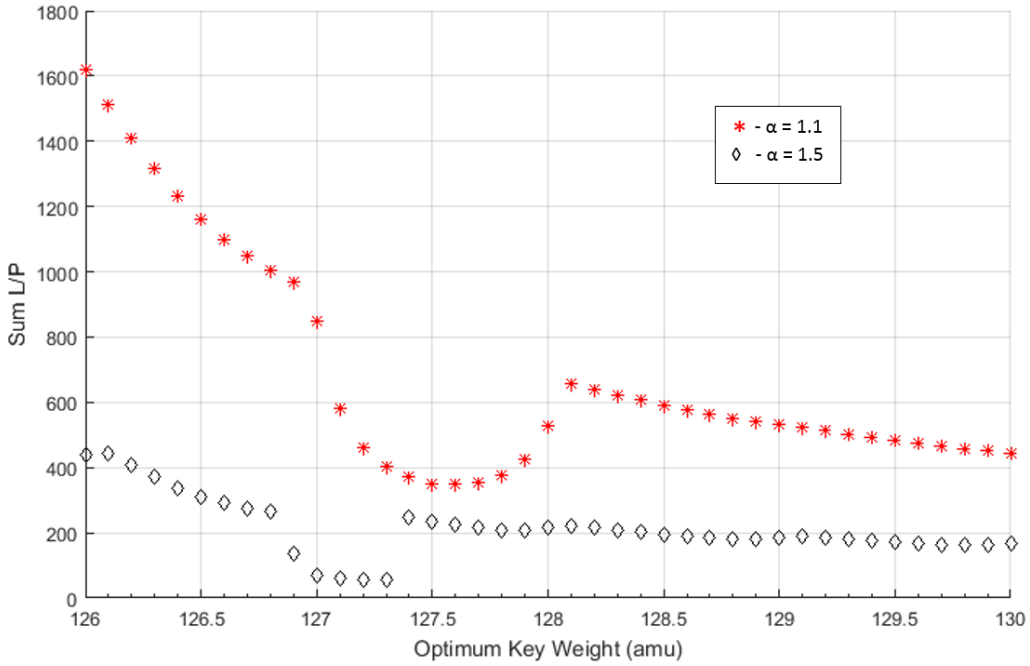

Figure 15. Optimum key weights for the second component. Two examples are shown; one for α = 1.1 and the other for α = 1.5. These two examples bracket the range of separation factors studied here, and illustrate the range of the effect on the optimum key weight as separation factor changes. As the separation factor increases, the optimum key weight shifts toward the second component, M=126. The dips in the curves represent a small subset of key weights that can reach the targeted weight fraction in a reduced number of stages.

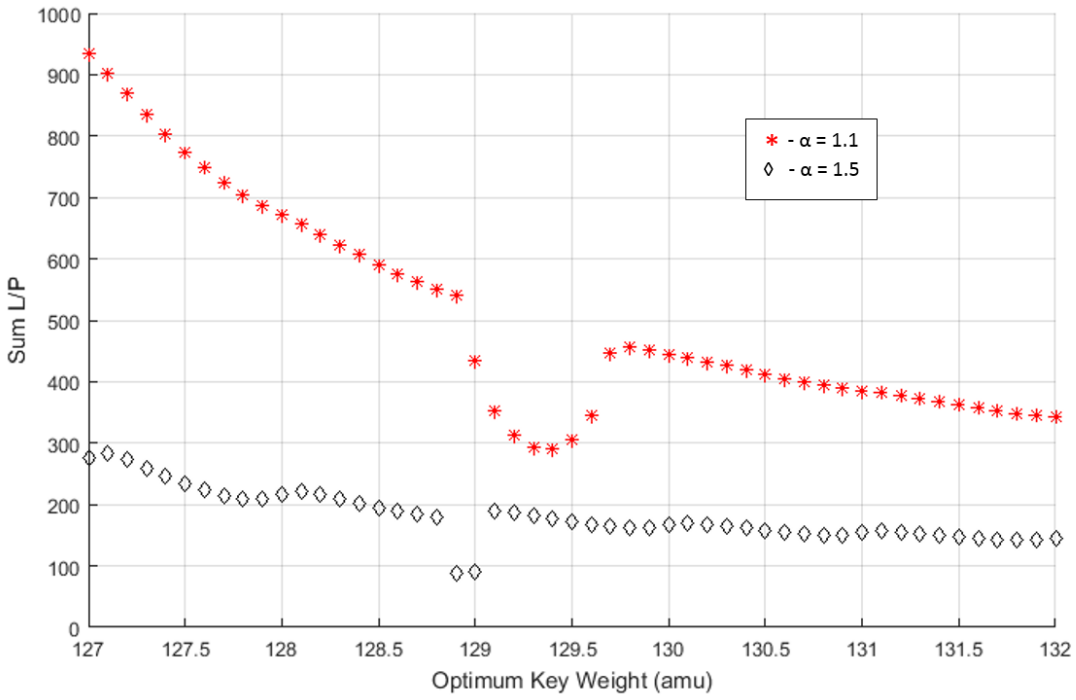

Figure 16. Optimum key weights for the third component. Two examples are shown; one for α = 1.1 and the other for α = 1.5. These two examples bracket the range of separation factors studied here, and illustrate the range of the effect on the optimum key weight as separation factor changes. As the separation factor increases, the optimum key weight shifts toward the third component, M=127. The dips in the curves represent a small subset of key weights that can reach the targeted weight fraction in a reduced number of stages.

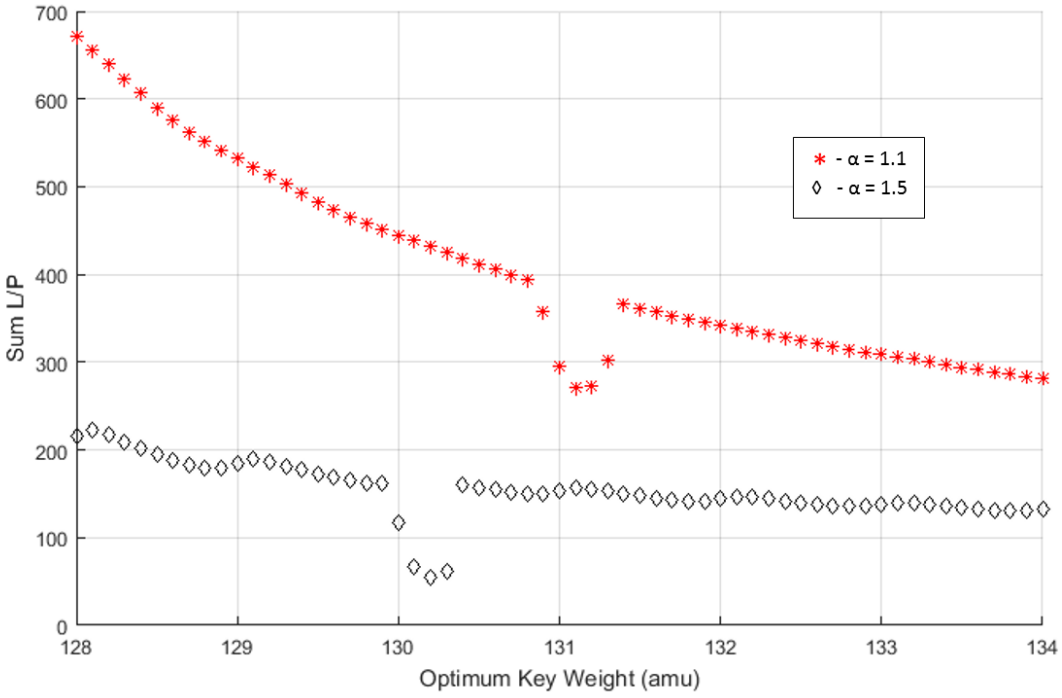

Figure 17. Optimum key weights for the fourth component. Two examples are shown; one for α = 1.1 and the other for α = 1.5. These two examples bracket the range of separation factors studied here, and illustrate the range of the effect on the optimum key weight as separation factor changes. As the separation factor increases, the optimum key weight shifts toward the fourth component, M=128. The dips in the curves represent a small subset of key weights that can reach the targeted weight fraction in a reduced number of stages.

the first separation factors increased, the optimum key weights became smaller for the targeted light component. Because three components are being concentrated, the achievable weight fraction is constrained. For the number of enricher stages considered with no stripper stages, the achievable weight fraction for the fourth component ranges from 0.15 to just shy of 0.17. Again, higher separation factors were able to achieve higher weight fractions. Because only relatively low weight fractions were achieved, the optimum key weights never fully approached the mass of the targeted component. As the separation factors increased, the optimum key weights became smaller for the targeted light component.

Fifth Component

For the fifth component (M=129), the optimum key weights range from 131.9 amu to 132.9 amu depending on the separation factor. The range of key weights versus the RTF are shown in Figure 18. The results are consistent with the results previously described. Because the fifth component is the extreme middle component, the achievable weight fraction is paltry. For the number of enricher stages considered with no stripper stages, the achievable weight fraction for the fifth component ranges from just shy of 0.12 to shy of 0.14. Again, higher separations factors were able to achieve higher weight fractions. Because only relatively low weight fractions were achieved, the optimum key weights were considerably heavier (in the case of a light fifth component) than the mass of the targeted component. As the separation factors increased, the optimum key weights became smaller for the targeted light component. As mentioned earlier regarding too many permutations to properly analyze all cases for the final product weight fraction (after the next cascade), the fifth component is a prime example. The feed weight fraction for the fifth component was 0.1. The product weight fraction failed to achieve 0.14 even in the case with the highest separation factor. The approach here would require many enrichers to obtain a pure product, 0.90 weight fraction or above. In this case, an alternative approach may be more attractive from an economic standpoint. A possible approach may be to separate other alternative products in a separate cascade first to condition the feed for better separation of the fifth component. Fortunately, the case of the fifth component as shown here, is a worst-case scenario. This scenario bounds all natural cases.

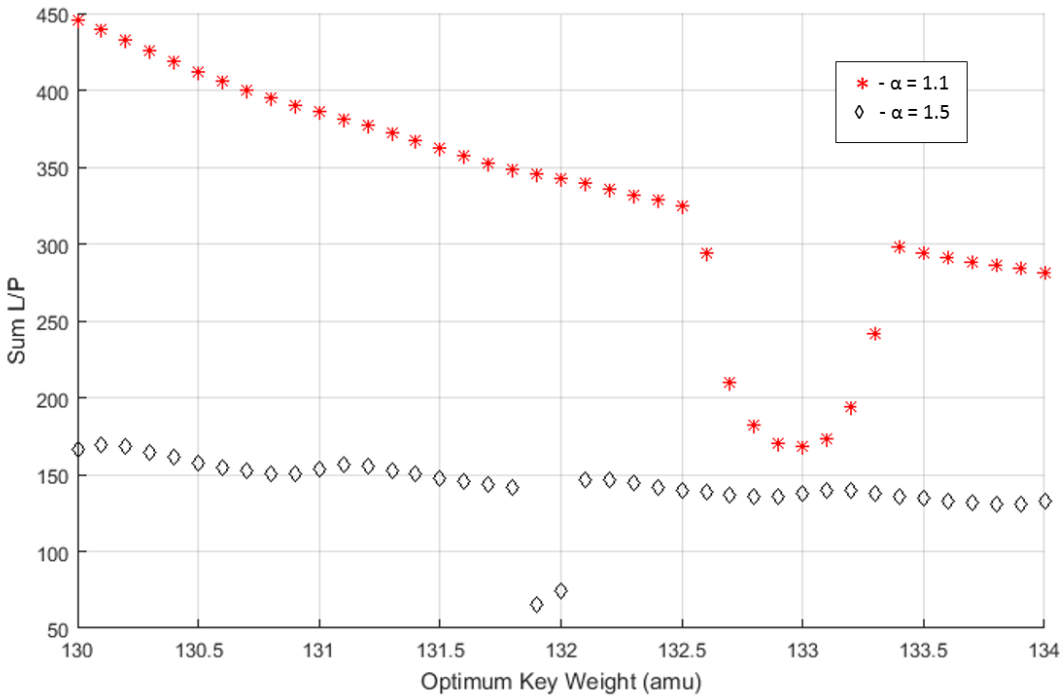

Figure 18. Optimum key weights for the fifth component. Two examples are shown; one for α = 1.1 and the other for α = 1.5. These two examples bracket the range of separation factors studied here, and illustrate the range of the effect on the optimum key weight as separation factor changes. As the separation factor increases, the optimum key weight shifts toward the fourth component, M=128. The dips in the curves represent a small subset of key weights that can reach the targeted weight fraction in a reduced number of stages.

CHAPTER 5: CONCLUSIONS AND RECOMMENDATIONS

Optimization Methodology

An optimization criterion commonly used in the literature was verified using a recently described multicomponent value function expanded to *n* components [54]. The comparison of the two calculations showed good agreement. The RTF criterion was used for the results and conclusions found here.

Single Optimized Cascade for an End Component with Constant Key Weight

Over 30 million cascade calculations were performed to obtain over 9000 optimized cascades corresponding to nearly 9000 useful data sets for analysis. In general, the results have shown that in a long cascade with a small separation factor, the optimum key weight approaches the target end-component molecular weight as the target end-component weight fraction is increased. These results here corroborated the results of Sulaberidze et al. [14], except the discrete stage-wise nature of the MARC calculations showed a large dependence of the optimum key weight on the separation factor. This dependence is difficult to predict because of that discrete nature, requiring cascades to be independently modeled.

For high target weight fractions, the optimum key weight approaches the midpoint between the end component and the nearest isotopic neighbor, reinforcing the results first described by de la Garza et al. [27]. However, this result appears to hold only for long cascades or a cascade with a constant key weight and high target weight fractions.

In general, the optimum key weight for isotope separation for a fixed key weight, single cascade varies with target weight fraction. For a feed material that is at least equally weighted or greater in the end component, the optimum key weight approaches the midpoint value of the mass of the end component and its nearest isotopic neighbor for target weight fractions of 0.70

or greater. For a low target weight fractions of 0.20 or less, the optimum key weight is expected to be roughly one-third the weighted average of the range of isotopes. For a feed material that is equally weighted across all isotopes (like the material studied here), the optimum key weight will just be roughly one-third the range of isotopic molecular weights. For example, in the material studied here, the optimum key weight for a low target weight fractions is approximately 128.0-128.5 amu. The range of isotopic molecular weights is 125.0 to 134.0 amu. One-third of that range would be approximately 128.3 amu.

For target weight fractions from 0.20 to 0.70, the optimum key weight varies as a quadratic from roughly one-third at 0.20 to the midpoint value between the end component and its nearest isotopic neighbor at 0.70. In general, the curvature of the quadratic is a function of the separation factor. The lower the separation factor, the more gradual the approach to the midpoint value between the end component and its nearest neighbor. A higher separation factor will approach that midpoint value steeper, initially, and then asymptotically.

In general, adding stripper stages pulls the optimum key weight closer to the midpoint value between the end component and its nearest neighbor at lower target weight fractions. Adding more stripper stages increases the effect.

Single Optimized Cascade for a Middle Component with Constant Key Weight

The optimum key weight for a middle component is limited to a very narrow range of key weights because of the competing effects of enriching the middle component with other components. All components lighter than the middle component are enriched to the detriment of the target component. The result is a practical limit on the target concentration. The optimum key weight varies with target concentration like the effect shown with the end component, except that this effect is much more pronounced. Furthermore, unlike the end component, the range of available key weights available to achieve the target weight fraction is quite narrow. The optimum key weights range from roughly one-fifth to four-fifths the range

of isotopic molecular weights. The optimum key weight depends not only on the isotopic sequence of the targeted component, but also the separation factor. Although not specifically tested, the optimum key weight likely depends on the initial isotopic weight distribution as was shown for the end component.

Cascade of Cascades

Cascade performance can be optimized by varying the key weight. This was shown for a cascade of cascades with recycle. The key weight was varied by cascade. Performance improved over the single optimized cascade with constant key weight when the number of stripper stages of the next higher cascade were matched with the number of enricher stages for the cascade being considered. This cascade scheme minimizes mixing losses within the cascade. Likewise, results indicate that performance improves as the number of enricher stages is reduced and approaching one. These results indicate the possibility of continuously varying the key weight across a long cascade as proposed by Zhang et al. [15].

The results of the cascade of cascades with recycle shows that the intuitive methodology for optimizing individual cascades for that cascade's product weight fraction is erroneous. This method is logical as it builds on the findings of Sulaberidze et al. [14] and Borisevich et al. [39]. However, the results here have shown that the variation in the key weight is the mirror *opposite* of that expected.

In a cascade of cascades, the lowest cascade's key weight will approach the mass number of the target isotope. In every case when targeting the lightest component (M=125.0 amu) in the fictitious material, the optimum key weight of the lowest cascade was 125.1 or 125.2 amu. In most cases where more than two cascades were analyzed, the optimum key was 125.1 amu, the lowest possible value used in the calculations. Similar results were found when the heavy component was targeted. These results can be viewed logically in that the lowest cascade has the highest internal flow.

The maximum, optimum key weight for the highest cascade is roughly one-third of the weighted range of isotopes, similar to the result for a low target weight fraction in the single optimized cascade with constant key weight. Likewise, this maximum generally applies to a low target weight fraction. As the target weight fraction increases, the range of optimum key weights for the cascades generally converge. In other words, the optimum key weight for the top cascade will converge toward the end component as the target weight fraction increases.

The optimum key weight for a cascade between the second and the last cascade will be roughly one-third of the mass difference of the target end component and the optimum key weight of the next higher cascade. As discussed previously, the cascades should be modeled independently because of the discrete nature of the MARC.

Future Work

Future work should modify the computer code to allow many more cascades. Each of these cascades could then consist of one enricher. This would allow a cascade of cascades to model a single cascade while varying the key weight continuously. This would determine whether cascade performance can be improved by varying the key weight continuously within a cascade. It is possible that any performance increase would be overcome by mixing losses introduced by varying the key weight too many times relative to the total number of enrichers.

Finally, the scope here was limited to one desired target isotope and a fictitious feed. The results should be extended to case studies for real isotope separations problems. Real feeds may have isotopic distributions that either enhance or diminish the results found here. Likewise, the real feed cases may have interesting and complicating problems like multiple products or undesirable isotopes to be considered.

BIBLIOGRAPHY

[1] "Compelling Research Opportunities Using Isotopes," NSAC Isotopes Subcommittee, https://science.energy.gov/np/nsac/reports/, April 23, 2009.

[2] J. Greenblatt, "Stable and Radioactive Isotopes," ITS-01, United States International Trade Commission, http://www.usitc.gov, June, 2009.

[3] M. Rivard et al., "The US National Isotope Program: Current Status and Strategy for Future Success," *Applied Radiation and Isotopes,* vol. 63, pp. 157-178, 2005.

[4] B. Egle, K. Hart and W. Aaron, "Stable Isotope Enrichment Capabilities at Oak Ridge National Laboratory," *Journal of Radioanalytical Nuclear Chemistry,* vol. 299, no. 2, pp. 995-999, 2014.

[5] A. Shubin et al., "Centrifugal Technology for Stable Isotope Separation at the Electrochemical Plant," in *Proceedings of the Fifth International Conference on Isotopes*, Brussels, Belgium, 2005.

[6] A. Pavlov and V. Borisevich, "Market of Stable Isotopes Produced by Gas Centrifuges: Status and Prospects," in *Proceedings of the Ninth International Workshop on Separation Phenomena in Liquids and Gases*, Beijing, 2006.

[7] A. Cheltsov, L. Sosnin and V. Khamylov, "Centrifugal Enrichment of Nickel Isotopes and Their Application to the Development of New Technologies," *Journal of Radioanalytical Nuclear Chemistry,* vol. 299, no. 2, pp. 981-987, 2014.

[8] "Meeting Isotope Needs and Capturing Opportunities for the Future: The 2015 Long Range Plan for the DOE-NP Isotope Program," NSAC Isotopes Subcommittee, https://science.energy.gov/np/nsac/reports/, July 20, 2015.

[9] E. von Halle, "Multicomponent Isotope Separation in Matched Abundance Ratio Cascades Composed of Stages with Large Separation Factors," in *Proceedings of the Seventh International Workshop on Separation Phenomena in Liquids and Gases*, Darmstadt, Germany, 1987.

[10] A. de la Garza, "A Generalization of the Matched Abundance-Ratio Cascade for Multicomponent Isotope Separation," *Chemical Engineering Science,* vol. 18, pp. 73-82, 1963.

[11] M. Zhou, X. Liang, W. Chen and Y.T.Ying, "Experimental Study of Multi-Component Separation by Gas Centrifuge," in *Proceedings of the Ninth International Workshop on Separation Phenomena in Liquids and Gases*, Beijing, 2006.

[12] H. Jiang, Z. Lei and F. Zhuge, "Basic Separative Power of Multi-Component Isotopes Separation in a Gas Centrifuge," in *Proceedings of the Tenth International Workshop on Separation Phenomena in Liquids and Gases*, Angros dos Reis, 2008.

[13] S. Zeng et al., "A Numerical Method of Cascade Analysis and Design for Multi-component Isotope Separation," *Chemical Engineering Research and Design,* vol. 92, pp. 2649-2658, 2014.

[14] G. Sulaberidze, V. Borisevich and Q. Xie, "Comparison of Optimal and Model Cascades for the Separation of Multicomponent Mixtures at Arbitrary Stage Enrichments," *Theoretical Foundations of Chemical Engineering,* vol. 42, no. 4, pp. 347-353, 2008.

[15] Y. Zhang et al., "Further Optimization of Q-Cascades," *Chemical Engineering Research and Design,* vol. 100, pp. 509-517, 2015.

[16] S. Zeng et al., "A Generalization of the Virtual Components Concept for Numerical Simulation of Multi-Component Isotope Separation in Cascades," *Chemical Engineering Science,* vol. 120, pp. 105-11, 2014.

[17] W. Roberts, "Gas Centrifugation of Research Isotopes," *Nuclear Instruments and Methods in Physics Research ,* vol. A282, pp. 271-276, 1989.

[18] A. Cheltsov and L. Sosnin, "Nuclear Engineering Stable Isotopes of Lead, Molybdenum, Nickel, and Methods for Their Production," in *Proceedings of the Ninth International Workshop on Separation Phenomena in Liquids and Gases*, Beijing, 2006.

[19] L. Sosnin and A. Tcheltsov, "Centrifugal Extraction of Highly Enriched Te-123 for the Production of I-123 at a Cyclotron," *Nuclear Instruments and Methods in Physics Research A,* vol. 438, pp. 14-19, 1999.

[20] A. Cheltsov et al., "Centrifugal Enrichment of Sulfur Isotopes," *Journal of Radioanalytical Nuclear Chemistry,* vol. 299, no. 2, pp. 989-993, 2014.

[21] V. Borisevich, A. Kurochkin and A. Tikhomirov, "Separation of Cadmium Isotopes by Gas Centrifuges: Theory and Practice," in *Proceedings of the Ninth International Workshop on Separation Phenomena in Liquids and Gases*, Beijing, 2006.

[22] J. Wu and F. Zhuge, "The Study of Multicomponent Separation of Xe Isotope by Centrifugal Method," in *Proceedings of the Fifth International Workshop on Separation Phenomena in Liquids and Gases*, Foz do Iguaçu, 1996.

[23] D. Li, Q. Xie, W. Li and H. Mou, "The Study of Cascade Characteristics for Si-28 Isotope Separation," in *Proceedings of the Tenth International Workshop on Separation Phenomena in Liquids and Gases,* Angra dos Reis, 2008.

[24] A. de la Garza, G. Garrett and J. Murphy, "Multicomponent Isotope Separation in Cascades," *Chemical Engineering Science,* vol. 15, pp. 188-209, 1961.

[25] S. Zeng et al., "The Q-Cascade Explanation," *Separation Science and Technology,* vol. 47, no. 11, pp. 1591-1595, 2012.

[26] Y. Zhang et al., "Further Optimization of Q-Cascades," *Chemical Engineering Research and Design,* vol. 100, pp. 509-517, 2015.

[27] A. de la Garza et al., "A Generalized Cascade for Multicomponent Isotope Separation," *Chemical Engineering Symposium Series,* vol. 61, no. 55, pp. 27-33, 1965.

[28] V. Palkin, "Optimization of a Cascade with Arbitrarily Specified Separation Coefficients of the Stages," *Atomic Energy,* vol. 82, no. 4, pp. 288-293, 1997.

[29] V. Palkin, "Multistream Cascades for Separation of Multicomponent Isotopic Mixtures," *Atomic Energy,* vol. 119, no. 2, pp. 125-131, 2015.

[30] D. Potapov, G. Sulaberidze and L. Kholpanov, "Designing a Rectangular Sectioned Cascade by Approximating the Separation Factor," *Theoretical Foundations of Chemical Engineering,* vol. 34, no. 2, pp. 129-133, 2000.

[31] C. Ying et al., "Analysis of Gas Centrifuge Cascade for Separation of Multicomponent Isotopes and Optimal Feed Position," *Separation Science and Technology,* vol. 32, no. 15, pp. 2467-2480, 1997.

[32] D. Olander, "Design of Ideal Cascades of Gas Centrifuges with Variable Separation Factors," *Nuclear Science and Engineering,* vol. 60, pp. 421-434, 1976.

[33] V. Palkin, "Determination of the Optimal Parameters of a Cascade of Gas Centrifuges," *Atomic Energy,* vol. 84, no. 3, pp. 190-195, 1998.

[34] V. Palkin, "Optimization of a Centrifuge Cascade for Separating a Multicomponent Mixture of Isotopes," *Atomic Energy,* vol. 115, no. 2, pp. 109-115, 2013.

[35] V. Palkin, "Centrifuge Number Optimization of a Cascade with One or Several Types of Steps," *Atomic Energy,* vol. 116, no. 3, pp. 206-212, 2014.

[36] A. Y. Smirnov, G. A. Sulaberidze and V. D. Borisevich, "Influence of Feed Flow Profile of Cascade Stages on the Mass Transfer of Intermediate Components," *Theoretical Foundations of Chemical Engineering,* vol. 44, no. 6, pp. 888-896, 2010.

[37] S. Zeng, et al., "Use of the Q-Cascade in Calculation and Optimization of Multi-Isotope Separation," *Chemical Engineering Science,* vol. 66, pp. 2997-3002, 2011.

[38] S. Zeng et al., "Enhancing the Performance of Q-Cascade for Separating Intermediate Components," *Journal of Physics: Conference Series,* vol. 751, no. 1, 2016.

[39] V. Borisevich, G. Sulaberidze and S. Zeng, "New Approach to Optimize Q-Cascades," *Chemical Engineering Science,* vol. 66, pp. 393-396, 2011.

[40] K. Cohen, *The Theory of Isotope Separation as Applied to the Large-Scale Production of U-235,* New York: McGraw-Hill Book Company, Inc., 1951, pp. 13-21.

[41] H. Wood, V. Borisevich and G. Sulaberidze, "On a Criterion Efficiency for Multi-Isoptope Mixtures Separation," *Separation Science and Technology,* vol. 34, no. 3, pp. 343-357, 1999.

[42] V. Palkin, "On the Value Function for Multi-Isotope Mixtures Separation," *Ars Separatoria Acta,* vol. 3, pp. 51-61, 2004.

[43] P. Louvet, "Survey of the Concepts of Value Function and Power Consumption of Separation Processes," in *Proceedings of the Tenth International Workshop on Separation Phenomena in Liquids and Gases*, Angros dos Reis, 2008.

[44] M. Benedict, T. Pigford and H. Levi, *Nuclear Chemical Engineering*, New York: McGraw-Hill Book Company, 1981, pp. 672-674, 693-701.

[45] V. Palkin, "Generalization of Smorodinskii's Solution for the Separation Potential of a Multicomponent Mixture of Isotopes," *Atomic Energy*, vol. 95, no. 5, pp. 786-793, 2003.

[46] I. Kolokol'tsov et al., "Value Function in Cascades for the Separation of a Multicomponent Isotope Mixture," *Atomic Energy*, vol. 29, no. 2, pp. 832-834, 1970.

[47] I. Yamamoto and A. Kanagawa, "Synthesis of Value Function for Multicomponent Isotope Separation," *Journal of Nuclear Science and Technology*, vol. 16, no. 1, pp. 43-48, 1979.

[48] Y. Lehrer-Ilamed, "On the Value Function for Multicomponent Isotope Separation," *Journal of Nuclear Energy*, vol. 23, pp. 559-567, 1969.

[49] V. Borisevich, G. Sulaberidze and H. Wood, "A Comparison of Two Efficiency Criteria for Separation of Multi-Isotope Mixtures," in *Proceedings of the Sixth International Workshop on Separation Phenomena in Liquids and Gases*, Nagoya, 1998.

[50] P. Gadkari and R. Govind, "Analytical Screening Criterion for Sequencing of Distillation Columns," *Computers and Chemical Engineering*, vol. 12, no. 12, pp. 1199-1213, 1988.

[51] A. Smirnov and G. Sulaberidze, "Comparison of Methods of Enriching Intermediate Components in Cascades with the Same Number of Separative Elements," *Atomic Energy*, vol. 117, no. 5, pp. 340-346, 2015.

[52] L. Wang, S. Zeng, D. Jiang and T. Song, "A Calculation Procedure for Designing Ideal Centrifugal Separation Cascades," *Separation Science and Technology*, vol. 43, pp. 3393-3416, 2008.

[53] G. Sulaberidze and V. Borisevich, "Cascades for Separation Of Multicomponent Isotope Mixtures," *Separation Science and Technology*, vol. 36, no. 8 and 9, pp. 1769-1817, 2001.

[54] C.D. Sulfredge and J.T. Slankas, Personal communication on November 4, 2016.

[55] T. Song, S. Zeng, G. Sulaberidze, V. Borisevich and Q. Xie, "Comparative Study of the Model and Optimum Cascades for Multicomponent Isotope Separation," *Separation Science and Technology*, vol. 45, pp. 2113-2118, 2010.

[56] S. Villani, *Isotope Separation*, American Nuclear Society, 1976, pp. 148-151.

APPENDICES

Table 4. Comparison of Calculated Results [27]. The values presented are the masses and weight fractions for each isotope of tungsten. The table compares the results published by de la Garza in 1965 (top portion of the table) with those calculated using the code developed here (middle portion of the table) for further verification. The differences in the results (bottom portion of the table) are consistent to within the significant figures provided.

	Cascade Stream	Mass	Isotope Weight Fraction				
			W-180	W-182	W-183	W-184	W-186
	Feed	1.00000	0.00140	0.26460	0.14400	0.30600	0.28400
Results from de la Garza 1965 paper	Product, 1	0.50716	0.00000	0.00089	0.02378	0.41773	0.55760
	Waste, 1	0.49285	0.00284	0.53597	0.26770	0.19103	0.00246
	Product, 2	0.21336	0.00000	0.00211	0.05630	0.93000	0.01159
	Waste, 2	0.29380	0.00000	0.00000	0.00017	0.04565	0.95418
Calculated Results	Product, 1	0.50708	0.00000	0.00089	0.02380	0.41764	0.55766
	Waste, 1	0.49292	0.00284	0.53589	0.26765	0.19115	0.00247
	Product, 2	0.21332	0.00000	0.00212	0.05634	0.92990	0.01163
	Waste, 2	0.29378	0.00000	0.00000	0.00017	0.04566	0.95416
Difference in Results	Product, 1	0.00007	0.00000	0.00000	-0.00002	0.00009	-0.00006
	Waste, 1	-0.00007	0.00000	0.00008	0.00005	-0.00012	-0.00001
	Product, 2	0.00003	0.00000	-0.00001	-0.00004	0.00010	-0.00004
	Waste, 2	0.00002	0.00000	0.00000	0.00000	-0.00001	0.00002

Table 5. Previously Published Results for Comparison [9]. This table directly restates the results published in 1987 by von Halle. The stages are numbered from the feed stage. E is for enricher. S is for stripper. The values presented are the product weight fractions for each isotope of tungsten at the indicated stage.

Stage Number	Stage Feed Isotope Weight Fraction				
	W-180	W-182	W-183	W-184	W-186
E-35	0.47313	0.52511	0.00174	0.00002	0.00000
E-34	0.43563	0.56232	0.00202	0.00003	0.00000
E-33	0.39883	0.59877	0.00236	0.00003	0.00000
E-32	0.36313	0.63408	0.00275	0.00004	0.00000
E-31	0.32887	0.66788	0.00320	0.00006	0.00000
E-30	0.29631	0.69989	0.00372	0.00008	0.00000
E-29	0.26569	0.72988	0.00433	0.00010	0.00000
E-28	0.23714	0.75769	0.00504	0.00013	0.00000
E-27	0.21076	0.78320	0.00587	0.00018	0.00000
E-26	0.18657	0.80637	0.00682	0.00023	0.00000
E-25	0.16456	0.82719	0.00793	0.00031	0.00000
E-24	0.14465	0.84570	0.00922	0.00042	0.00000
E-23	0.12676	0.86195	0.01072	0.00057	0.00000
E-22	0.11077	0.87602	0.01245	0.00076	0.00000
E-21	0.09654	0.88798	0.01446	0.00103	0.00000
E-20	0.08393	0.89790	0.01678	0.00139	0.00000
E-19	0.07281	0.90587	0.01946	0.00186	0.00000
E-18	0.06302	0.91191	0.02256	0.00251	0.00001
E-17	0.05443	0.91606	0.02613	0.00338	0.00002
E-16	0.04691	0.91829	0.03023	0.00454	0.00003
E-15	0.04035	0.91856	0.03494	0.00610	0.00005
E-14	0.03462	0.91677	0.04033	0.00818	0.00009
E-13	0.02964	0.91276	0.04648	0.01096	0.00017
E-12	0.02530	0.90629	0.05344	0.01466	0.00030
E-11	0.02153	0.89706	0.06130	0.01955	0.00055
E-10	0.01826	0.88467	0.07009	0.02600	0.00098
E-9	0.01541	0.86857	0.07982	0.03443	0.00176
E-8	0.01294	0.84811	0.09044	0.04537	0.00314

Table 5. Previously Published Results for Comparison (continued).

E-7	0.01079	0.82246	0.10179	0.05939	0.00556
E-6	0.00892	0.79061	0.11362	0.07709	0.00977
E-5	0.00729	0.75139	0.12540	0.09896	0.01696
E-4	0.00587	0.70355	0.13639	0.12517	0.02903
E-3	0.00463	0.64592	0.14547	0.15528	0.04871
E-2	0.00356	0.57784	0.15121	0.18773	0.07965
E-1	0.00265	0.49987	0.15201	0.21949	0.12598
S-14	0.00226	0.49567	0.15305	0.22170	0.12732
S-13	0.00192	0.49070	0.15418	0.22427	0.12893
S-12	0.00163	0.48483	0.15539	0.22729	0.13086
S-11	0.00138	0.47791	0.15667	0.23082	0.13321
S-10	0.00117	0.46976	0.15801	0.23496	0.13610
S-9	0.00098	0.46016	0.15934	0.23981	0.13970
S-8	0.00083	0.44888	0.16061	0.24545	0.14423
S-7	0.00069	0.43563	0.16172	0.25196	0.15001
S-6	0.00057	0.42007	0.16250	0.25938	0.15749
S-5	0.00047	0.40183	0.16274	0.26766	0.16730
S-4	0.00038	0.38054	0.16214	0.27664	0.18030
S-3	0.00031	0.35579	0.16034	0.28590	0.19767
S-2	0.00024	0.32728	0.15683	0.29473	0.22092
S-1	0.00019	0.29489	0.15111	0.30196	0.25186

Table 6. Calculated Results for Comparison [9]. Results calculated to replicate those by von Halle in 1987 for further code verification. The differences of these results and those from Table 5 in are presented in Table 7.

Stage Number	Stage Feed Isotope Weight Fraction				
	W-180	W-182	W-183	W-184	W-186
E-35	0.47313	0.52511	0.00174	0.00002	0.00000
E-34	0.43563	0.56232	0.00202	0.00003	0.00000
E-33	0.39883	0.59877	0.00236	0.00003	0.00000
E-32	0.36313	0.63408	0.00275	0.00004	0.00000
E-31	0.32887	0.66788	0.00320	0.00006	0.00000
E-30	0.29631	0.69989	0.00372	0.00008	0.00000
E-29	0.26569	0.72988	0.00433	0.00010	0.00000
E-28	0.23714	0.75769	0.00504	0.00013	0.00000
E-27	0.21076	0.78320	0.00587	0.00018	0.00000
E-26	0.18657	0.80637	0.00682	0.00023	0.00000
E-25	0.16456	0.82719	0.00793	0.00031	0.00000
E-24	0.14465	0.84570	0.00922	0.00042	0.00000
E-23	0.12676	0.86195	0.01072	0.00057	0.00000
E-22	0.11077	0.87602	0.01245	0.00076	0.00000
E-21	0.09654	0.88798	0.01446	0.00103	0.00000
E-20	0.08393	0.89790	0.01678	0.00138	0.00000
E-19	0.07281	0.90587	0.01946	0.00186	0.00000
E-18	0.06302	0.91191	0.02256	0.00251	0.00001
E-17	0.05443	0.91606	0.02613	0.00338	0.00002
E-16	0.04691	0.91829	0.03023	0.00454	0.00003
E-15	0.04035	0.91856	0.03494	0.00610	0.00005
E-14	0.03462	0.91677	0.04033	0.00818	0.00009
E-13	0.02964	0.91276	0.04648	0.01096	0.00017
E-12	0.02530	0.90629	0.05344	0.01466	0.00030
E-11	0.02153	0.89706	0.06130	0.01955	0.00055
E-10	0.01826	0.88467	0.07009	0.02600	0.00098
E-9	0.01541	0.86857	0.07982	0.03443	0.00176
E-8	0.01294	0.84811	0.09044	0.04537	0.00314

Table 6. Calculated Results for Comparison (continued).

E-7	0.01079	0.82246	0.10180	0.05939	0.00556
E-6	0.00892	0.79061	0.11362	0.07709	0.00977
E-5	0.00729	0.75139	0.12540	0.09896	0.01696
E-4	0.00587	0.70355	0.13639	0.12517	0.02903
E-3	0.00463	0.64592	0.14547	0.15528	0.04871
E-2	0.00356	0.57784	0.15121	0.18773	0.07965
E-1	0.00265	0.49987	0.15201	0.21949	0.12598
S-14	0.00226	0.49567	0.15305	0.22170	0.12732
S-13	0.00192	0.49070	0.15418	0.22427	0.12893
S-12	0.00163	0.48483	0.15539	0.22729	0.13086
S-11	0.00138	0.47791	0.15667	0.23082	0.13321
S-10	0.00117	0.46976	0.15801	0.23496	0.13610
S-9	0.00099	0.46016	0.15934	0.23981	0.13970
S-8	0.00083	0.44888	0.16062	0.24545	0.14423
S-7	0.00069	0.43563	0.16172	0.25196	0.15001
S-6	0.00057	0.42007	0.16250	0.25938	0.15749
S-5	0.00047	0.40183	0.16274	0.26766	0.16730
S-4	0.00038	0.38054	0.16215	0.27664	0.18030
S-3	0.00031	0.35579	0.16034	0.28590	0.19767
S-2	0.00024	0.32728	0.15683	0.29473	0.22092
S-1	0.00019	0.29489	0.15111	0.30196	0.25186

Table 7. Differences in Calculated and Published Results [9]. The table shows the differences in the results from Tables 5 and 6. The differences are mostly zero, except in only a few cases. In these cases, the differences are likely due to a rounding difference in the last digit.

Stage Number	Stage Feed Isotope Weight Fraction				
	W-180	W-182	W-183	W-184	W-186
E-35	0.00000	0.00000	0.00000	0.00000	0.00000
E-34	0.00000	0.00000	0.00000	0.00000	0.00000
E-33	0.00000	0.00000	0.00000	0.00000	0.00000
E-32	0.00000	0.00000	0.00000	0.00000	0.00000
E-31	0.00000	0.00000	0.00000	0.00000	0.00000
E-30	0.00000	0.00000	0.00000	0.00000	0.00000
E-29	0.00000	0.00000	0.00000	0.00000	0.00000
E-28	0.00000	0.00000	0.00000	0.00000	0.00000
E-27	0.00000	0.00000	0.00000	0.00000	0.00000
E-26	0.00000	0.00000	0.00000	0.00000	0.00000
E-25	0.00000	0.00000	0.00000	0.00000	0.00000
E-24	0.00000	0.00000	0.00000	0.00000	0.00000
E-23	0.00000	0.00000	0.00000	0.00000	0.00000
E-22	0.00000	0.00000	0.00000	0.00000	0.00000
E-21	0.00000	0.00000	0.00000	0.00000	0.00000
E-20	0.00000	0.00000	0.00000	0.00001	0.00000
E-19	0.00000	0.00000	0.00000	0.00000	0.00000
E-18	0.00000	0.00000	0.00000	0.00000	0.00000
E-17	0.00000	0.00000	0.00000	0.00000	0.00000
E-16	0.00000	0.00000	0.00000	0.00000	0.00000
E-15	0.00000	0.00000	0.00000	0.00000	0.00000
E-14	0.00000	0.00000	0.00000	0.00000	0.00000
E-13	0.00000	0.00000	0.00000	0.00000	0.00000
E-12	0.00000	0.00000	0.00000	0.00000	0.00000
E-11	0.00000	0.00000	0.00000	0.00000	0.00000
E-10	0.00000	0.00000	0.00000	0.00000	0.00000
E-9	0.00000	0.00000	0.00000	0.00000	0.00000
E-8	0.00000	0.00000	0.00000	0.00000	0.00000

Table 7. Differences in Calculated and Published Results (continued).

E-7	0.00000	0.00000	-0.00001	0.00000	0.00000
E-6	0.00000	0.00000	0.00000	0.00000	0.00000
E-5	0.00000	0.00000	0.00000	0.00000	0.00000
E-4	0.00000	0.00000	0.00000	0.00000	0.00000
E-3	0.00000	0.00000	0.00000	0.00000	0.00000
E-2	0.00000	0.00000	0.00000	0.00000	0.00000
E-1	0.00000	0.00000	0.00000	0.00000	0.00000
S-14	0.00000	0.00000	0.00000	0.00000	0.00000
S-13	0.00000	0.00000	0.00000	0.00000	0.00000
S-12	0.00000	0.00000	0.00000	0.00000	0.00000
S-11	0.00000	0.00000	0.00000	0.00000	0.00000
S-10	0.00000	0.00000	0.00000	0.00000	0.00000
S-9	-0.00001	0.00000	0.00000	0.00000	0.00000
S-8	0.00000	0.00000	-0.00001	0.00000	0.00000
S-7	0.00000	0.00000	0.00000	0.00000	0.00000
S-6	0.00000	0.00000	0.00000	0.00000	0.00000
S-5	0.00000	0.00000	0.00000	0.00000	0.00000
S-4	0.00000	0.00000	-0.00001	0.00000	0.00000
S-3	0.00000	0.00000	0.00000	0.00000	0.00000
S-2	0.00000	0.00000	0.00000	0.00000	0.00000
S-1	0.00000	0.00000	0.00000	0.00000	0.00000

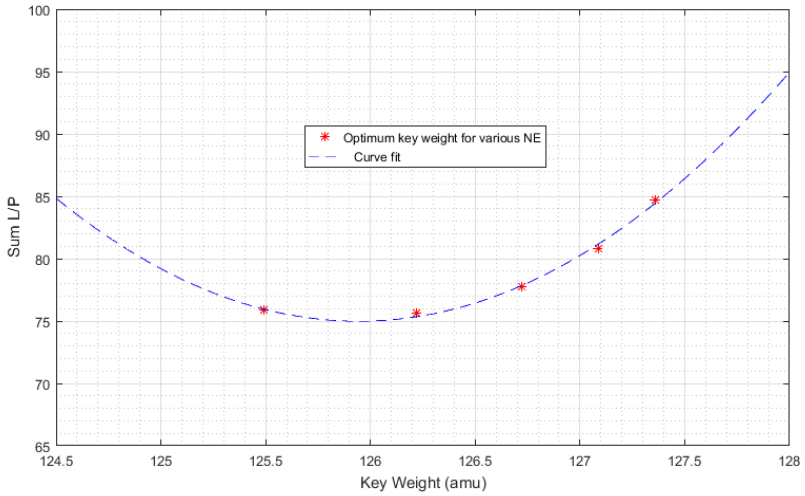

Figure 19. Optimum key weights for x_P = 0.4, α = 1.1.

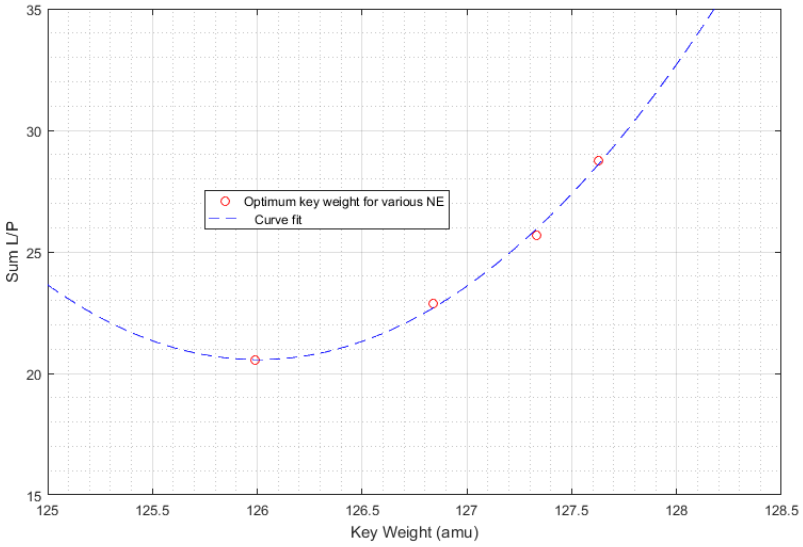

Figure 20. Optimum key weights for x_P = 0.4, α = 1.2.

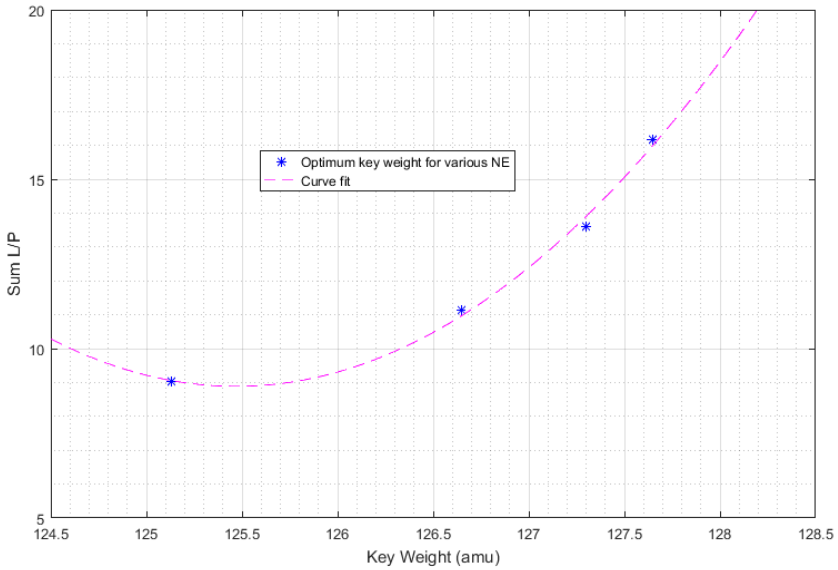

Figure 21. Optimum key weights for x_P = 0.4, α = 1.3.

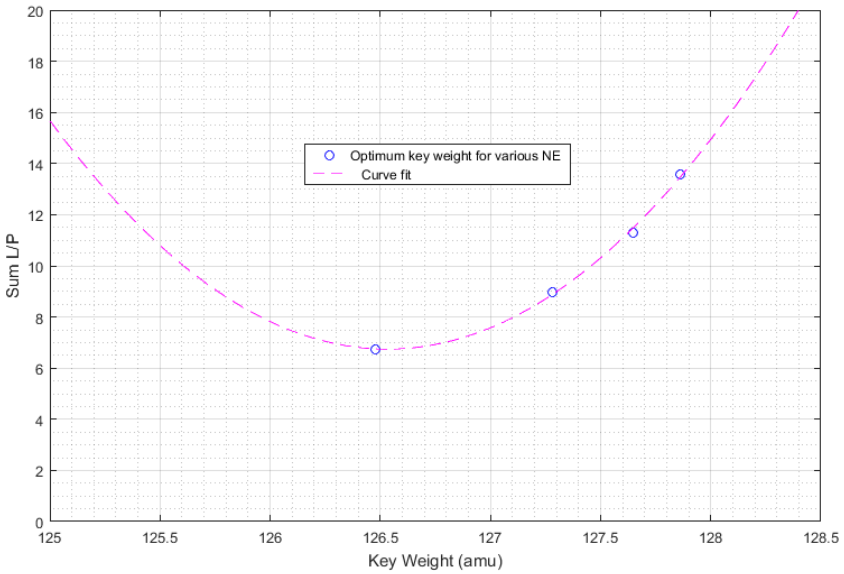

Figure 22. Optimum key weights for x_P = 0.4, α = 1.4.

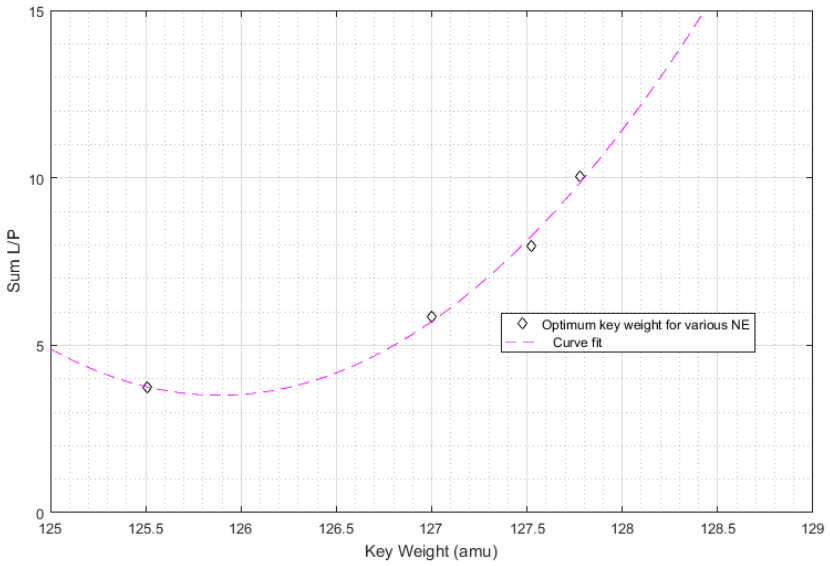

Figure 23. Optimum key weights for x_P = 0.4, α = 1.5.

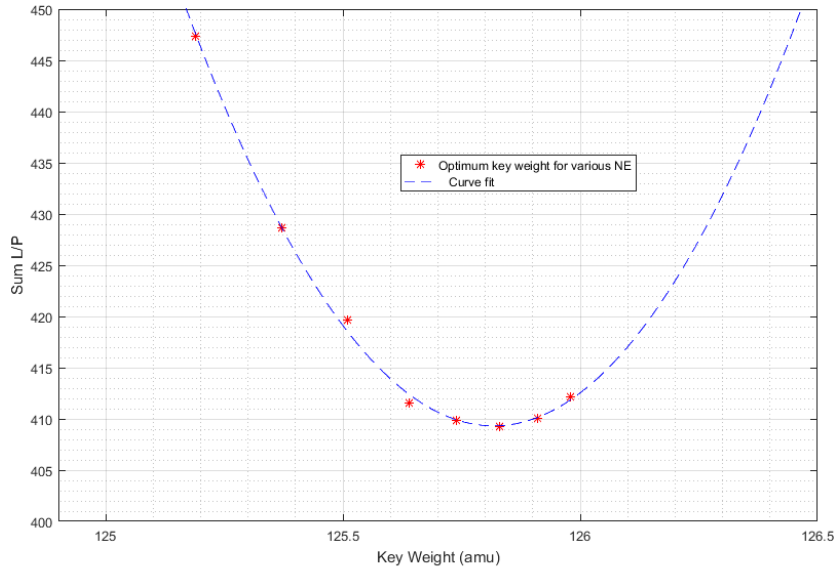

Figure 24. Optimum key weights for x_P = 0.7, α = 1.1.

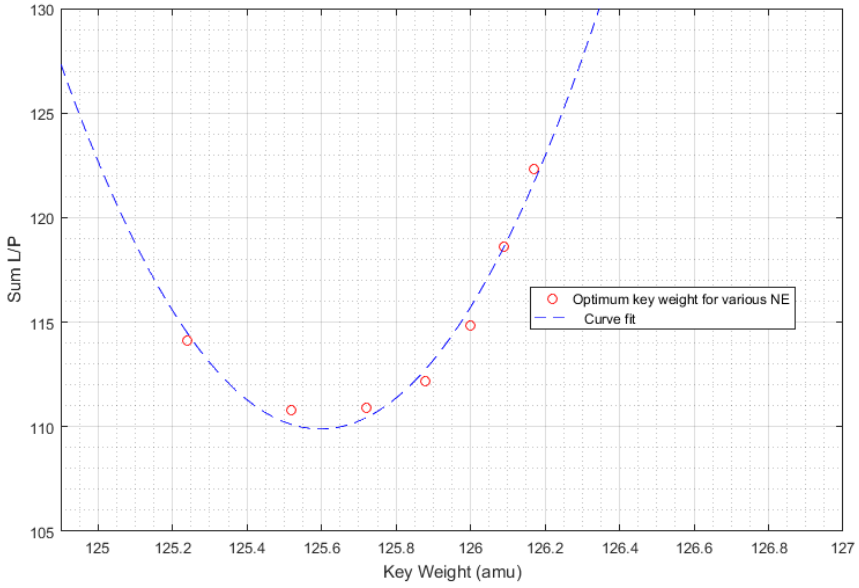

Figure 25. Optimum key weights for $x_P = 0.7$, $\alpha = 1.2$.

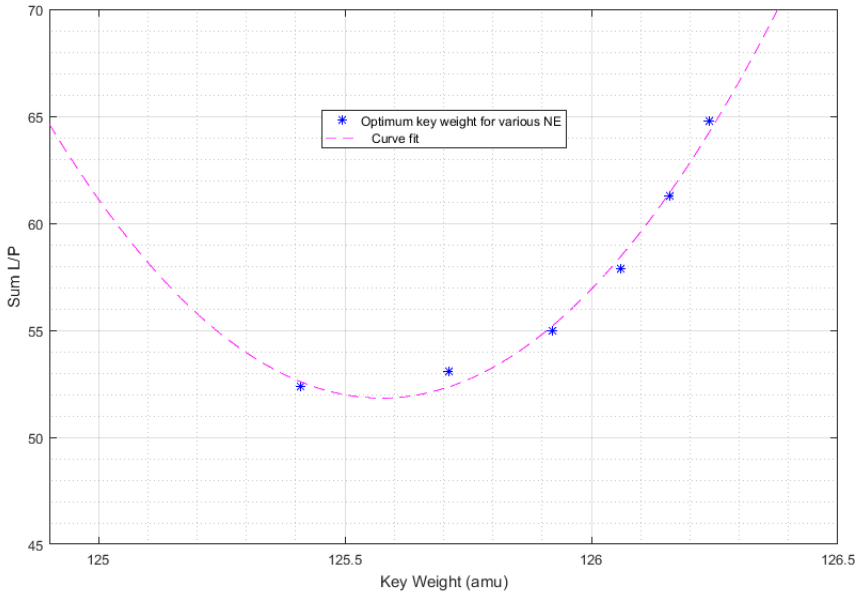

Figure 26. Optimum key weights for $x_P = 0.7$, $\alpha = 1.3$.

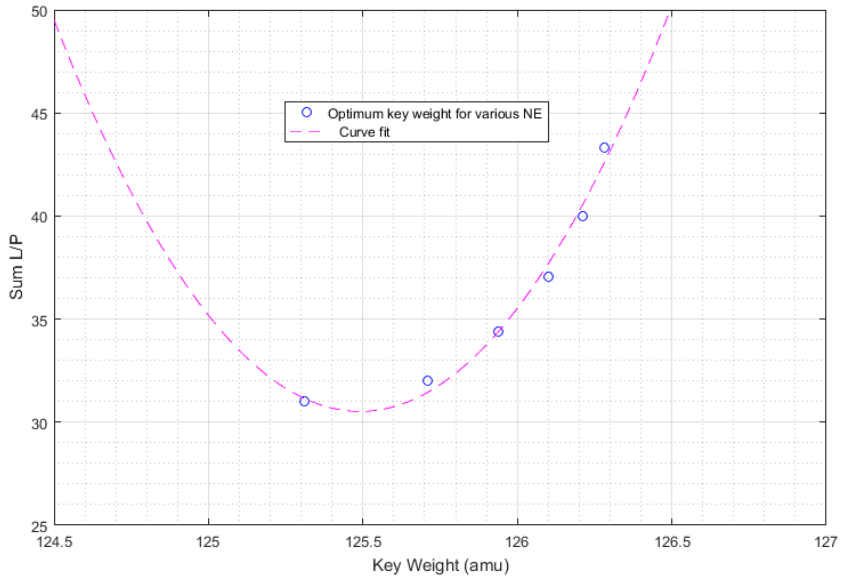

Figure 27. Optimum key weights for $x_P = 0.7$, $\alpha = 1.4$.

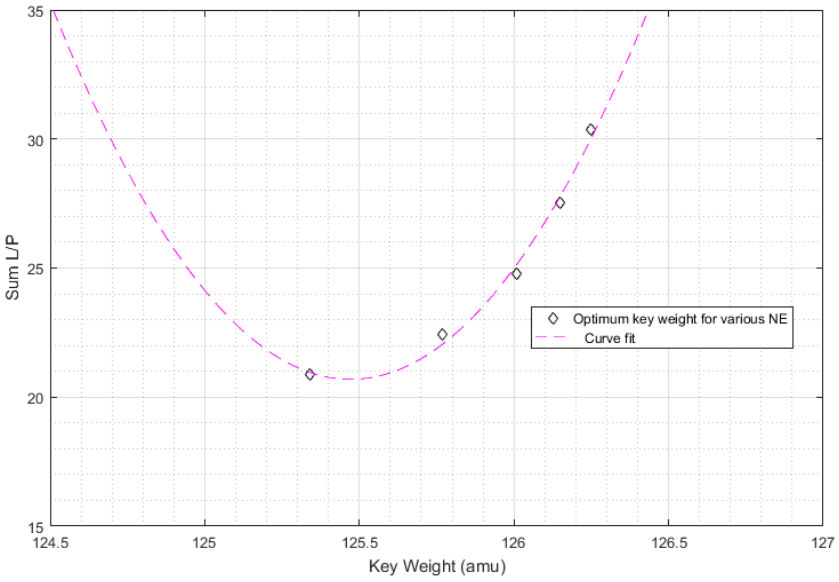

Figure 28. Optimum key weights for $x_P = 0.7$, $\alpha = 1.5$.

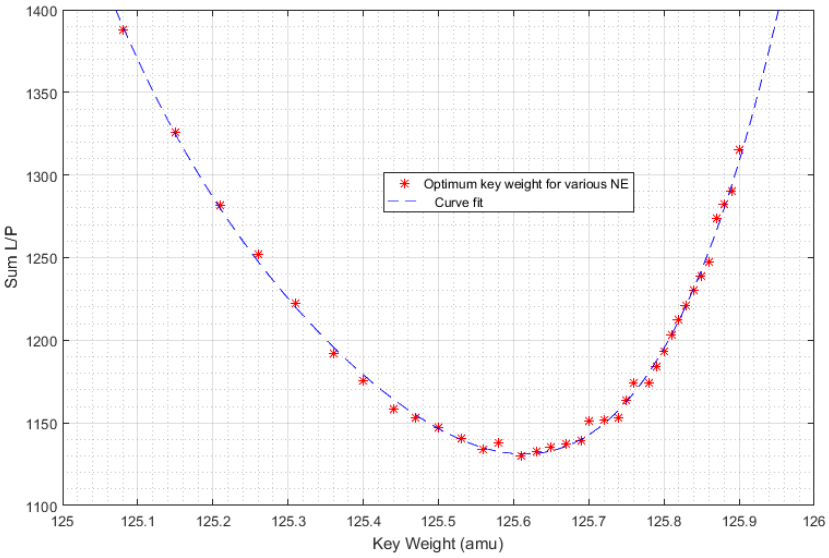

Figure 29. Optimum key weights for x_P = 0.9, α = 1.1.

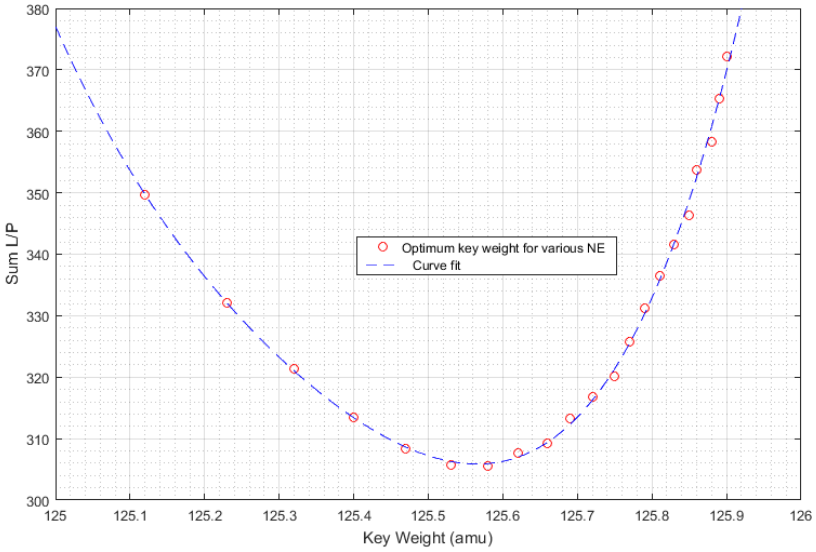

Figure 30. Optimum key weights for x_P = 0.9, α = 1.2.

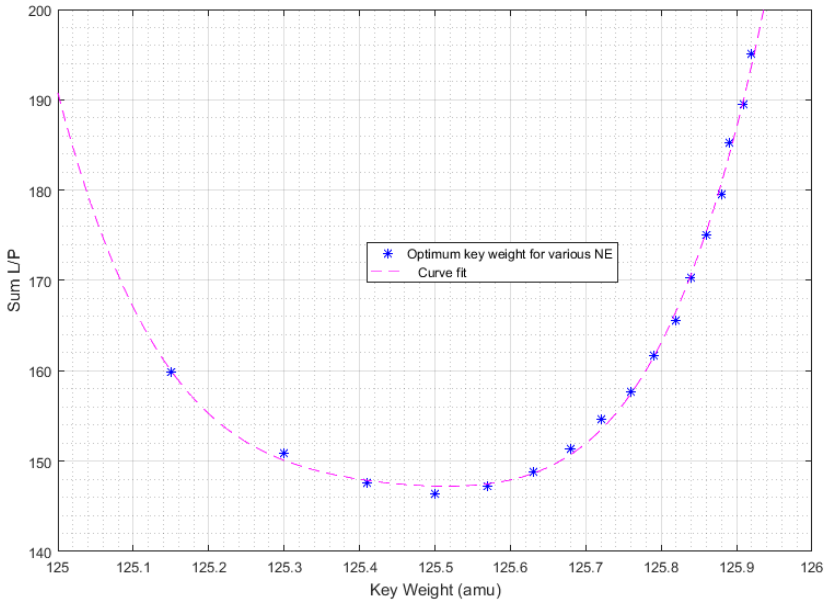

Figure 32. Optimum key weights for x_P = 0.9, α = 1.3.

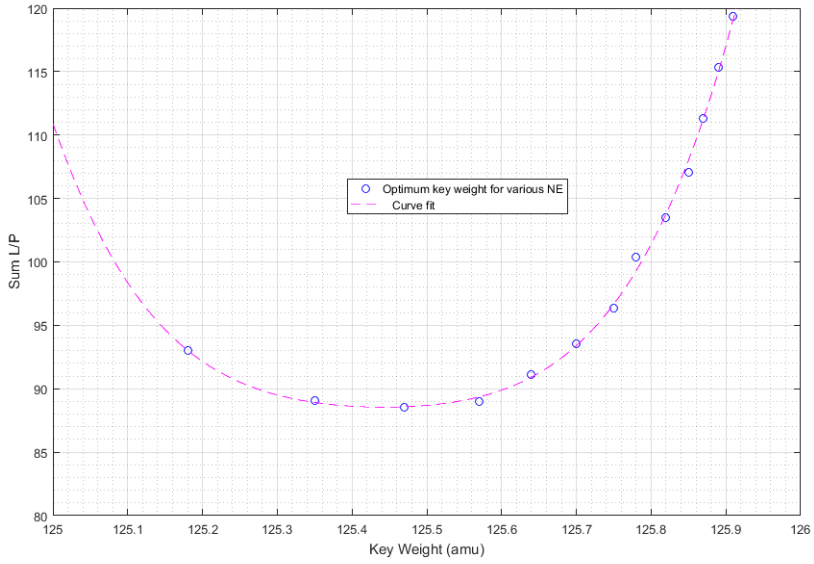

Figure 31. Optimum key weights for x_P = 0.9, α = 1.4.

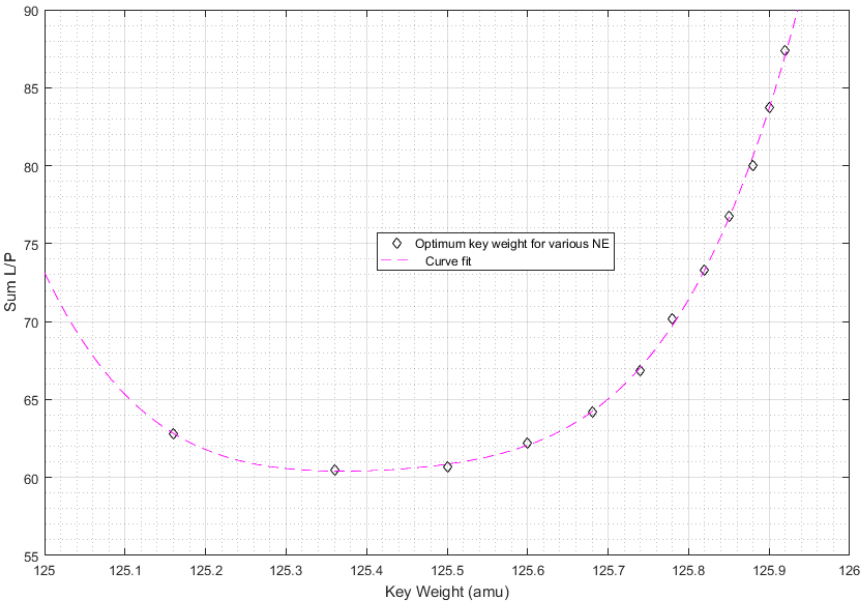

Figure 33. Optimum key weights for $x_P = 0.9$, $\alpha = 1.5$

APPENDIX C-OPTIMUM KEY WEIGHTS IN A CASCADE OF CASCADES WITHOUT RECYCLE

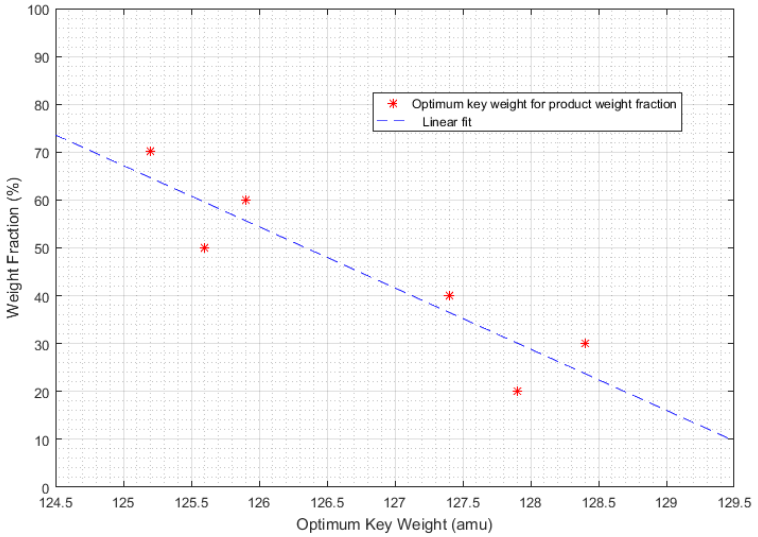

Figure 34. Optimum key weight versus cascade product weight fraction for cascade of six cascades with no recycle and $\alpha = 1.1$.

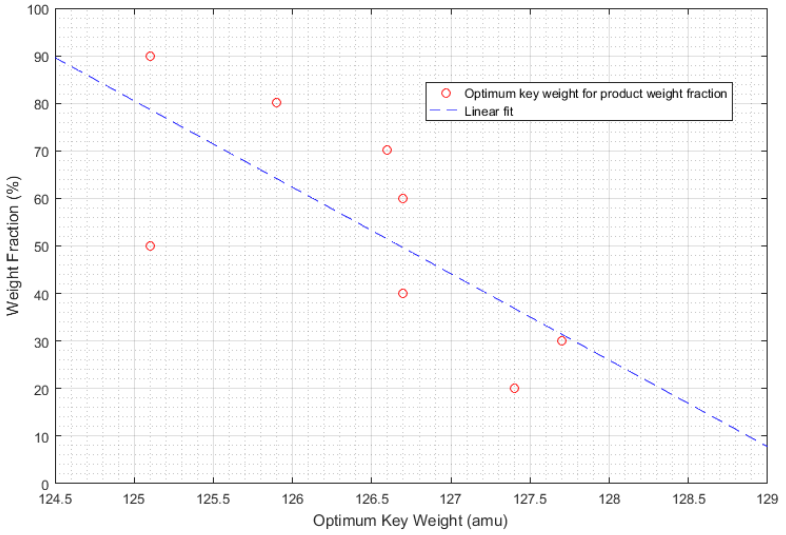

Figure 35. Optimum key weight versus cascade product weight fraction for cascade of eight cascades with no recycle and $\alpha = 1.2$.

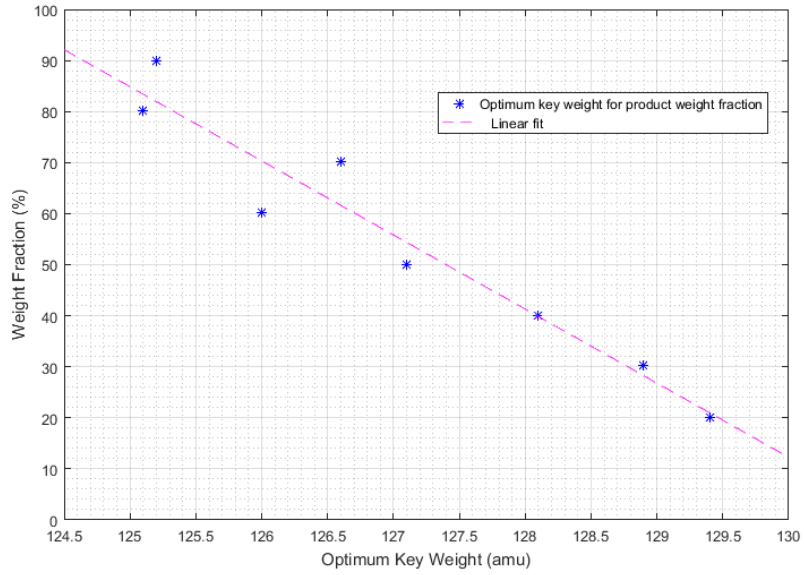

Figure 36. Optimum key weight versus cascade product weight fraction for cascade of eight cascades with no recycle and $\alpha = 1.3$.

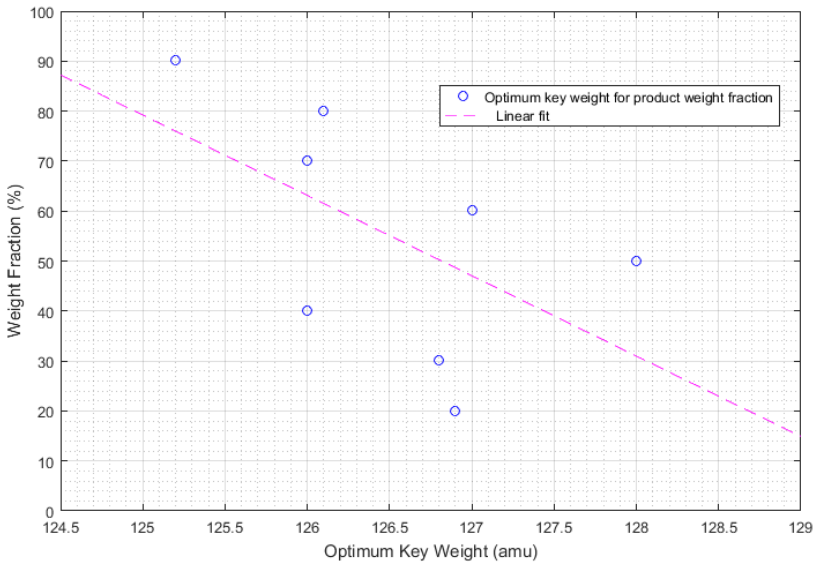

Figure 37. Optimum key weight versus cascade product weight fraction for cascade of eight cascades with no recycle and $\alpha = 1.4$.

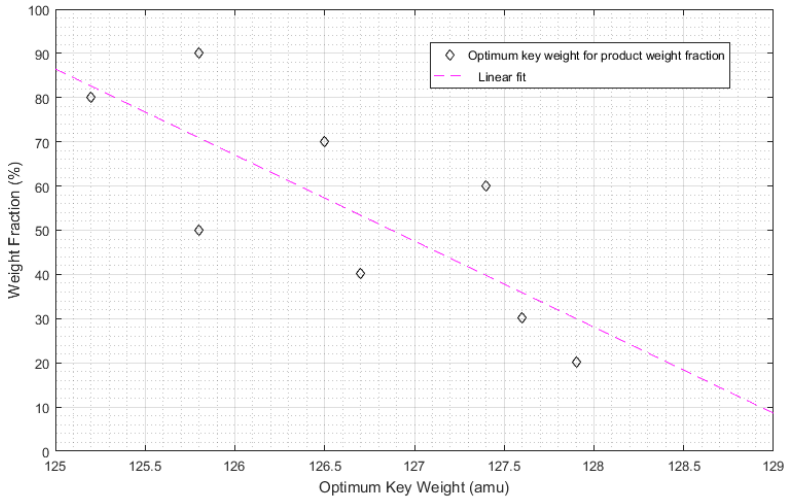

Figure 38. Optimum key weight versus cascade product weight fraction for cascade of nine cascades with no recycle and $\alpha = 1.5$.

APPENDIX D-OPTIMUM KEY WEIGHTS IN A CASCADE OF CASCADES WITH RECYCLE

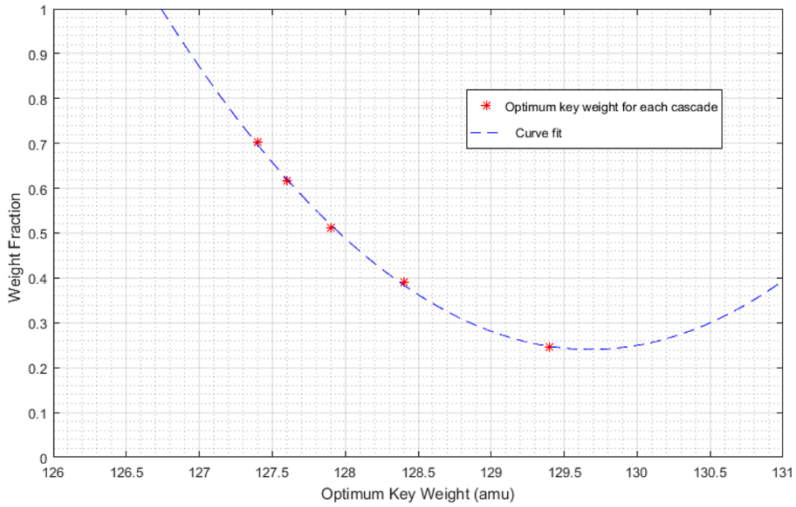

Figure 39. Optimum key weight versus cascade product weight fraction for cascade of cascades with recycle for $x_P = 0.7$ and $\alpha = 1.1$.

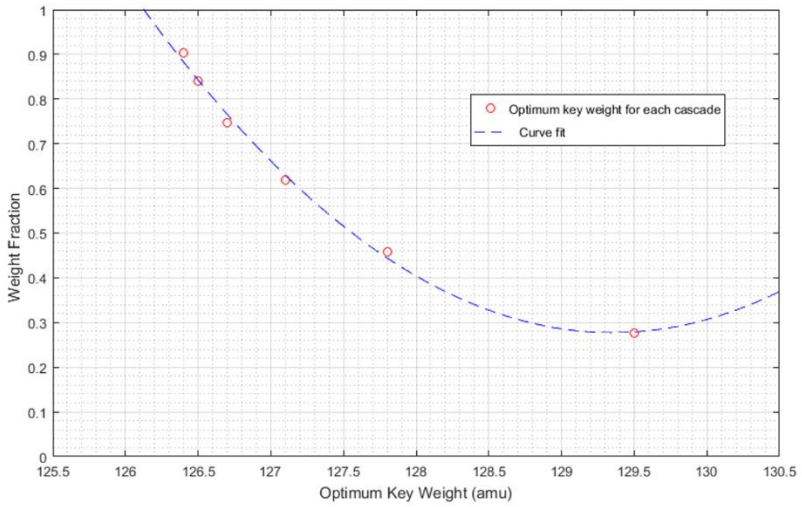

Figure 40. Optimum key weight versus cascade product weight fraction for cascade of cascades with recycle for $x_P = 0.9$ and $\alpha = 1.2$.

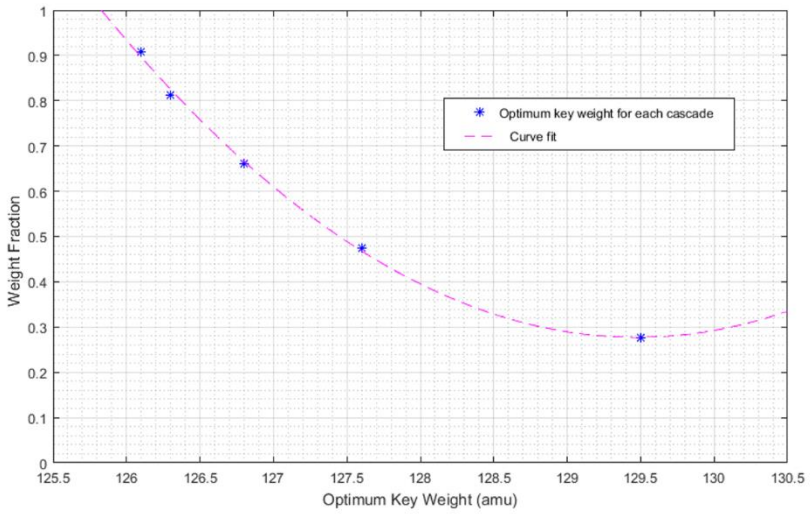

Figure 41. Optimum key weight versus cascade product weight fraction for cascade of cascades with recycle for $x_P = 0.9$ and $\alpha = 1.3$.

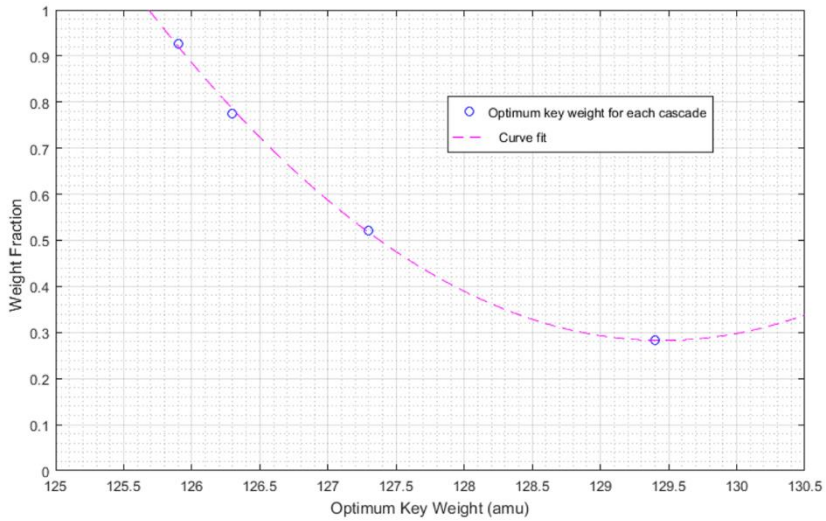

Figure 42. Optimum key weight versus cascade product weight fraction for cascade of cascades with recycle for $x_P = 0.9$ and $\alpha = 1.4$.

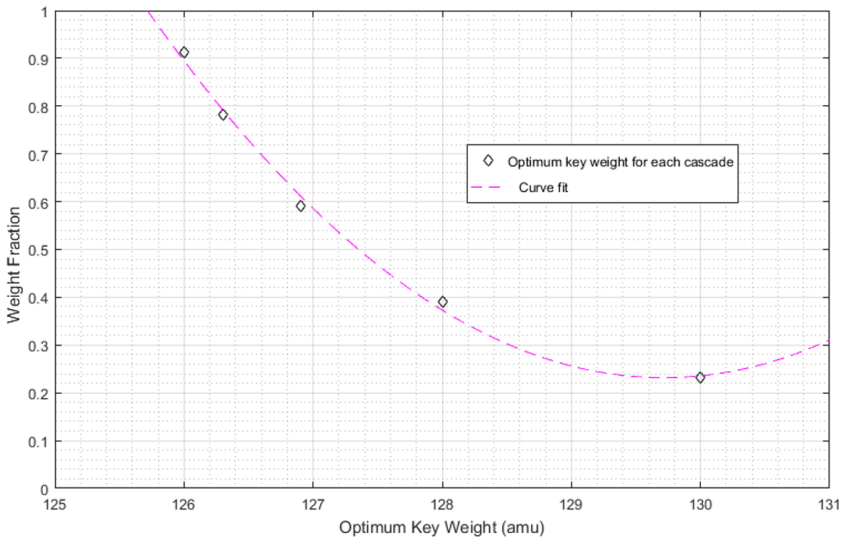

Figure 43. Optimum key weight versus cascade product weight fraction for cascade of cascades with recycle for $x_P = 0.9$ and $\alpha = 1.5$.

VITA

Richard Dale Harvey was born in Murfreesboro, Tennessee. He graduated from Smyrna High School in Smyrna, Tennessee, in 1987. Afterwards, he attended the University of Tennessee, Knoxville, as an engineering student before enlisting in the United States Navy in 1991. He served as a nuclear-qualified mechanical operator in the Navy until earning acceptance into the enlisted commissioning program. In December 1996, he graduated with a Bachelor of Science degree in nuclear engineering (magna cum laude) from Rensselaer Polytechnic Institute, while simultaneously earning his commission as an officer in the Navy.

Later, he was assigned to Vanderbilt University as a naval science instructor. He graduated from Vanderbilt with a Master of Science degree in mechanical engineering in the summer of 2005. Soon after leaving the Navy, he began working at Oak Ridge National Laboratory as a nuclear engineer. He is completing his doctoral degree in nuclear engineering at the University of Tennessee, nearly thirty academic years since the first quarter of his original attendance there.